

# **SKELETAL CELL EVOLUTION: COMPARING AN AMPHIBIAN MODEL TO EARLIER- AND LATER-DIVERGED VERTEBRATES**

A Thesis Submitted to the  
College of Graduate and Postdoctoral Studies  
in Partial Fulfillment of the Requirements  
for the degree of Master of Science  
in the Department of Anatomy, Physiology, and Pharmacology  
University of Saskatchewan  
Saskatoon

By

Jason Khoa Bui Nguyen

© Copyright Jason K. B. Nguyen, February 2021. All rights reserved.  
Unless otherwise noted, copyright of the material in this thesis belongs to the author

## **PERMISSION TO USE**

In presenting this thesis in partial fulfillment of the requirements for a Postgraduate degree from the University of Saskatchewan, I agree that the Libraries of this University may make it freely available for inspection. I further agree that permission for copying of this thesis in any manner, in whole or in part, for scholarly purposes may be granted by the professor or professors who supervised my thesis work or, in their absence, by the Head of the Department or the Dean of the College in which my thesis work was done. It is understood that any copying or publication or use of this thesis/dissertation or parts thereof for financial gain shall not be allowed without my written permission. It is also understood that due recognition shall be given to me and to the University of Saskatchewan in any scholarly use which may be made of any material in my thesis.

## **DISCLAIMER**

Reference in this thesis/dissertation to any specific commercial products, process, or service by trade name, trademark, manufacturer, or otherwise, does not constitute or imply its endorsement, recommendation, or favoring by the University of Saskatchewan. The views and opinions of the author expressed herein do not state or reflect those of the University of Saskatchewan and shall not be used for advertising or product endorsement purposes.

Requests for permission to copy or to make other use of material in this thesis in whole or part should be addressed to:

Head of the Department of Anatomy, Pharmacology, and Physiology  
107 Wiggins Road, University of Saskatchewan  
Saskatoon, Saskatchewan  
S7N 5E5 Canada

OR

Dean of the College of Graduate and Postdoctoral Studies  
University of Saskatchewan  
116 Thorvaldson Building, 110 Science Place  
Saskatoon, Saskatchewan  
S7N 5C9 Canada

## ABSTRACT

In principle, modern-day organisms retain many ancestral traits, some of which can be traced back quantitatively to approximate the order of evolutionary events. Within skeletal research, most studies have focused on more recently diverged vertebrate models, like mammals and birds, or on earlier-diverged fishes. This leaves a gap in the literature as the intermediately positioned amphibian model has been relatively under-explored. As such, amphibian skeletal cells might retain residual information that could account for any evolutionary differences observed between earlier- and later-diverged vertebrate clades. A comparative study of skeletal cell development across clades may reveal how bone and cartilage cells (osteoblasts and chondrocytes, respectively) have evolved over time. With few exceptions, many developmental features of bone and cartilage are currently understood to be fairly conserved among vertebrates. This includes the expression of certain skeletogenic genes that drive and characterize the different phases of skeletal cells as they develop. This thesis investigates and asks two specific questions regarding skeletal development. Is chondrogenic gene expression more common among osteoblasts, as recently discovered in frogs and fish, than previously thought? And is hypertrophy conserved within maturing amphibian chondrocytes as it is in earlier- and later-diverged vertebrates? Generally, we hypothesize that amphibian skeletal cells exhibit molecular and histological characteristics intermediate to those of other vertebrate models, given their position within phylogeny. Testing this hypothesis involved comparing osteoblasts and chondrocytes from skeletal elements in the amphibian frog homologous to those previously examined by the Eames lab in the mouse, chick, and gar. In the western clawed frog, *Xenopus tropicalis*, these elements were identified as the humerus (upper arm bone), medial angulosplenic (a dermal bone of the lower jaw), and ceratohyal (homologous to the hyoid bone of the larynx). Datasets from all four species were subjected to comparative analyses which were a combination of histology, RNA *in situ* hybridization, immunohistochemistry, and LCM-RNAseq (laser capture microdissection coupled with RNA sequencing). Preliminary bioinformatic analysis was also performed, but those results still require follow-up examination. Nonetheless, our data suggested amphibian skeletal cells have properties that did not conform to the phenotypic spectra as defined by other vertebrate models. Osteoblasts and hypertrophic chondrocytes of

amphibians appeared to express early chondrogenic markers at levels much higher or longer than were typically found in earlier- or later-diverged vertebrates, such as sex determining region Y-box 9 (*sox9*), collagen type II alpha 1 chain (*col2a1*), and possibly many other cartilage genes like Aggrecan (*acan*), sex determining region Y-box 5 (*sox5*), and sex determining region Y-box 9 (*sox6*), as well. To the best of our knowledge, these findings would be considered novel discoveries. Chondrogenic expression overall may have increased in skeletal cells of the amphibian lineage before decreasing in later-diverged tetrapods. This could somehow be related to the unusual hypertrophic development of amphibian head cartilages that was also revealed by this project; namely, the rapid hypertrophy of chondrocytes, which had not been previously characterized before, and the persistence of hypertrophic cartilage, a trait seemingly unique to frogs.

## ACKNOWLEDGEMENTS

First and foremost, I must offer my utmost gratitude to my supervisor and mentor, Dr. Brian Eames, for his guidance, patience, support, and for giving me the privilege of working with him and his team. It cannot be overstated how lucky I was to have him, and in particular, his first PhD student, Dr. Patsy Gómez Picos, show me the ropes throughout my Master's after having been away from academia for so long. I would like to thank my committee members, Drs. William Kulyk and Troy Harkness, who were my undergraduate professors almost 20 years ago, for their invaluable advice and feedback during my graduate training as well. I would also like to thank Dr. David Janz for agreeing to be my external examiner.

Next, I must acknowledge the rest of my lab mates and their incredible tolerance for putting up with me and all my silly questions day-in and day-out: Rafaela Grecco Machado, Oghenevwogaga (aka Joseph aka Gaga) Atake, Dr. Katie Ovens, Elham Koosha, Hamed Alizadeh, and former Eames lab members who have already moved on. I had never been part of such a hardworking group of people before. No motivation was ever needed, but it was easy to work hard when you saw others putting in the same kind of effort. Keep it up, guys!

Special acknowledgement must certainly go to Yiwen Liu for the work she had done previously on this project to make my life easier at the beginning, and to others who have had direct involvement in my training and/or assisting with my work: Dr. Adi Manek, Karen Yuen, Michelle Whalen, Albert Mark, Monica Salud, J-S Gauthier, and Dr. Arash Panahifar.

Lastly, I feel obliged to thank Brian again because you have challenged me in all the ways I hoped a teacher would. I hope we get to collaborate again in the future in any capacity, and that includes anyone else in this acknowledgement.

## DEDICATION

*In loving memory of my best friend, Crono. I will never forget the 20 years we spent together. If the past, present, and future are only an illusion, it means we are, have always, and will forevermore be linked in time. To my family for giving me the time and space I needed, and for supporting my decision to pursue this new path.*

## TABLE OF CONTENTS

<b>PERMISSION TO USE</b> .....	i
<b>DISCLAIMER</b> .....	ii
<b>ABSTRACT</b> .....	iii
<b>ACKNOWLEDGEMENTS</b> .....	v
<b>DEDICATION</b> .....	vi
<b>TABLE OF CONTENTS</b> .....	vii
<b>LIST OF TABLES</b> .....	xi
<b>LIST OF FIGURES</b> .....	xii
<b>LIST OF ABBREVIATIONS</b> .....	xiv
<b>CHAPTER 1: Introduction</b> .....	1
<b>CHAPTER 2: Background</b> .....	4
2.1 The evolution of skeletal cells .....	4
2.1.1 Significance of the amphibian model.....	5
2.1.2 <i>Xenopus tropicalis</i> and the Nieuwkoop and Faber staging system.....	5
2.1.3 Skeletal cell evolution can be reconstructed through comparative gene studies.....	7
2.2 An overview of skeletal cell development .....	8
2.2.1 Cartilage is a precursor for endochondral ossification .....	10
2.2.2 Cartilage matures during endochondral ossification .....	11
2.2.3 Endochondral ossification might reveal parts of skeletal evolution.....	12
2.3 The osteoblast hypothesis.....	13
2.4 The chondrocyte hypothesis .....	13
2.5 Evolution can be relevant to health research .....	14
<b>CHAPTER 3: Evolutionary repression of chondrogenic genes in the vertebrate osteoblast</b> .....	15
3.1 Abstract .....	15
3.2 Roll the clip, Jim: Phyletic constraint and skeletal cells .....	16
3.3 Osteoblasts suppressed chondrocyte genes during evolution.....	18
3.4 Using fingerprints to solve the hypothesis.....	21
3.5 Skeletal speculator.....	23
<b>CHAPTER 4: Chondrogenic expression in amphibian osteoblasts versus other vertebrates</b> .....	26
4.1 Abstract .....	26
4.2 Introduction.....	27

4.3 Materials and methods .....	29
4.3.1 Use of lab animals .....	29
4.3.2 Frog mating .....	29
4.3.3 Raising tadpoles to stages of interest .....	30
4.3.4 Fixation, processing, and sectioning for histology .....	31
4.3.5 Histology .....	32
4.3.6 Expression assays .....	33
4.3.7 Preliminary RNA-seq analyses .....	36
4.4 Results .....	37
4.4.1 Perichondral bone from the humerus and dermal bone of the lower jaw were identified and characterized through dissected whole-mount and section histology .....	37
4.4.2 The humerus has chondrogenic expression in layers inside and outside of perichondral bone .....	42
4.4.3 ISH and IHC show little to no chondrogenic expression in lower jaw osteoblasts .....	45
4.4.4 RNA-seq data confirmed chondrogenic expression in frog osteoblasts .....	47
4.4.5 Preliminary RNA-seq analysis suggests frog osteoblasts are highly chondrogenic .....	50
4.5 Discussion .....	52
4.5.1 Chondrogenic expression was specific to layers outside perichondral bone matrix .....	53
4.5.2 <i>sox9 in situ</i> expression is more prominent in perichondral than dermal bone .....	53
4.5.3 <i>col2a1</i> might have reduced expression in dermal bone, too .....	54
4.5.4 Expression assay results were insufficient to draw any definitive conclusions .....	56
4.5.5 The humerus and medial angulosplenic have little to no <i>col10a1</i> expression .....	56
4.5.6 Amphibian osteoblasts might be more chondrogenic than mouse, chick, and gar .....	57
4.5.7 Summary .....	61
<b>CHAPTER 5: Characterizing hypertrophy of amphibian cartilages .....</b>	<b>62</b>
5.1 Abstract .....	62
5.2 Introduction: Cartilage development and the hypertrophic cascade .....	64
5.2.1 Amphibian cartilage maturation has some differences versus other vertebrates .....	65
5.2.2 Higher precision ZO staging was used to track head cartilage development .....	68
5.3 Materials and methods .....	69
5.3.1 Use of lab animals .....	69
5.3.2 Frog mating .....	69
5.3.3 Raising tadpoles to stages of interest .....	69
5.3.4 Fixation, processing, and sectioning for histology .....	69

5.3.5 Histology.....	69
5.3.6 Expression assays.....	69
5.3.7 Preliminary RNA-seq analyses .....	70
5.4 Results.....	70
5.4.1 Stage NF57 of the humerus was determined to be consistent with previous datasets in the mouse and chick for analysis of immature and mature cartilage .....	70
5.4.2 Molecular data showed hypertrophy was mostly conserved in the humerus .....	72
5.4.3 Average normalized counts from RNA-seq revealed mature cartilage in the frog humerus had high expression of many immature cartilage markers .....	73
5.4.4 The frog ceratohyal undergoes rapid hypertrophy early and remains cartilaginous .....	75
5.4.5 Regulation of chondrogenic genes is not conserved in amphibian head cartilage .....	77
5.5 Discussion.....	79
5.5.1 Early chondrogenic markers are highly expressed in mature cartilage of frogs.....	80
5.5.2 <i>col10a1</i> did not appear to be a marker of hypertrophy in amphibians.....	81
5.5.3 Amphibian head cartilage is especially unique compared to other cartilages .....	82
5.5.4 Summary.....	83
<b>CHAPTER 6: Discussion, limitations, and future directions .....</b>	<b>85</b>
6.1 Discussion.....	85
6.1.1 Osteoblast evolution .....	86
6.1.2 Amphibian osteoblasts appeared to downregulate chondrogenic expression before maturing into osteocytes .....	87
6.1.3 Why did bone of later-diverged vertebrates lose chondrogenic expression? .....	88
6.1.4 Perichondral and intramembranous ossification are similar, but different .....	88
6.1.5 Where and how skeletal cells form could be clues into evolution .....	89
6.1.6 Chondrocyte hypertrophy .....	90
6.1.7 Amphibians have many unusual features during development compared to other vertebrates that generate more questions than answers about skeletal cell evolution .....	91
6.2 Limitations.....	91
6.2.1 Phyletic constraint is an unproven hypothesis .....	92
6.2.2 More species are needed for a robust evolutionary study .....	92
6.2.3 Vertebrate metamorphosis is unique to amphibians .....	93
6.2.4 Technical limitations .....	94
6.3 Future directions .....	96
6.3.1 Two frogs are better than one.....	96

6.3.2 Expression data of many important skeletogenic markers still need to be assayed .....	97
6.3.3 Hedgehog signaling may have a different role in amphibian skeletogenesis .....	99
6.3.4 Why are chondrogenic genes so highly expressed in amphibian skeletal cells? .....	101
6.3.5 Mature chondrocytes may share more genes with immature chondrocytes than osteoblasts in the amphibian .....	102
6.3.6 Thyroid hormone inhibition.....	102
6.3.7 Amphibian head cartilage could be a useful model for osteoarthritis.....	103
<b>APPENDIX A: Thyroid hormone inhibition .....</b>	<b>105</b>
A1.1 Thyroid hormone affects many aspects of skeletal development .....	105
T <sub>3</sub> is active even before the thyroid begins to function .....	106
T <sub>3</sub> competitors were required to inhibit binding of thyroid hormone to receptors .....	106
Rationale for the thyroid hormone inhibition experiment.....	107
A1.2 Materials and Methods.....	107
Use of lab animals.....	107
Frog mating .....	107
Exposure of tadpoles to thyroid hormone inhibitor .....	108
Fixation, processing, and sectioning for histology.....	108
Histology .....	108
Statistical analysis .....	109
A1.3 Preliminary results.....	109
A1.4 Discussion.....	111
<b>APPENDIX B: MicroCT and K-Edge Subtraction images .....</b>	<b>112</b>
<b>REFERENCES .....</b>	<b>113</b>

## LIST OF TABLES

### **CHAPTER 4: Chondrogenic expression in amphibian osteoblasts versus other vertebrates**

<b>Table 4.1</b>   Captured areas from skeletal tissues of stage NF57 tadpoles. ....	36
<b>Table 4.2</b>   Normalized counts of candidate skeletal genes in 3 different biological replicates for each skeletal cell type. ....	48
<b>Table 4.3</b>   Average normalized counts of candidate skeletal genes in frog skeletal cells. ....	50
<b>Table 4.4</b>   Heat map comparing chondrogenic ratios of osteoblasts in mouse, chick, gar, and frog. ....	51

### **CHAPTER 5: Characterizing hypertrophy of amphibian cartilage**

<b>Table 5.1</b>   Comparison of candidate cartilage gene counts in immature and mature chondrocytes of mouse, chick, gar, and frog. ....	75
<b>Table 5.2</b>   The similarities and differences between limb and head cartilage maturation in <i>Xenopus</i> . ...	83

## LIST OF FIGURES

### CHAPTER 2: Background

- Figure 2.1** | The Nieuwkoop and Faber staging system can be used to track *Xenopus tropicalis* development..... 7
- Figure 2.2** | Skeletal cells can be visualized with Safranin O/Fast Green and trichrome. .... 10

### CHAPTER 3: Evolutionary repression of chondrogenic genes in the vertebrate osteoblast

- Figure 3.1** | The relative location and molecular markers of major skeletal cell types during endochondral ossification. .... 18
- Figure 3.2** | A new(old) vertebrate model for skeletal development: *Xenopus tropicalis*. .... 20
- Figure 3.3** | Hypothetical evolution (and development?) of the osteoblast molecular fingerprint. .... 21
- Figure 3.4** | Comparing osteoblast molecular fingerprints across vertebrates to determine the levels of chondrogenic gene expression. .... 23

### CHAPTER 4: Chondrogenic expression in amphibian osteoblasts versus other vertebrates

- Figure 4.1** | Forelimb eruption occurs at stage NF58. .... 39
- Figure 4.2** | Whole-mount Alcian blue/Alizarin red staining shows ossification in the humerus and lower jaw. .... 40
- Figure 4.3** | Cartilage matures underneath perichondral bone before vascular invasion. .... 41
- Figure 4.4** | A developmental series with trichome pinpoints the exact moment of medial angulosplenic ossification. .... 41
- Figure 4.5** | *sox9* and *col2a1* are expressed on the inner and outer layers of perichondral bone. .... 43
- Figure 4.6** | *col10a1* is expressed in maxillary teeth of a stage NF59 tadpole. .... 45
- Figure 4.7** | Lower jaw osteoblasts of stage NF57 lack *sox9* expression, exhibit faint levels of *col2a1*, and have no Col2 protein expression. .... 46
- Figure 4.8** | Skeletal cells were laser captured from the lower jaw and humerus for RNA-seq. .... 47
- Figure 4.9** | Evolution of the osteoblast gene regulatory network. .... 60

### CHAPTER 5: Characterizing hypertrophy of amphibian cartilages

- Figure 5.1** | ZO staging subdivides NF stages of early larval development in *Xenopus tropicalis*. .... 68
- Figure 5.2** | Expression assays of the humerus mostly showed the expected patterns of the hypertrophic cascade. .... 72
- Figure 5.3** | Sub-staging early ceratohyal development revealed chondrocyte differentiation and hypertrophy. .... 76
- Figure 5.4** | From stages NF45 onwards, ceratohyal chondrocytes remained hypertrophic and never ossified. .... 76
- Figure 5.5** | Col2 immunostaining independently confirmed differentiation and hypertrophy of ceratohyal cartilage. .... 77

**Figure 5.6** | Analysis of the ceratohyal during hypertrophy showed gene regulation was not conserved. 78

**Figure 5.7** | Expression assays of *sox9*, *col2a1*, and *Col2* continued to be expressed at stage NF57 and *col10a1* was still negative. .... 79

**CHAPTER 6: Discussion, limitations, and future directions**

**Figure 6.1** | Preliminary RNA *in situ* hybridization assays of *runx2* show expression at stages NF33/34... 98

**APPENDIX A**

**Figure A1** | A simple schematic illustrates how thyroid hormone is biologically activated. .... 106

**Figure A2** | Experimental design of thyroid hormone inhibition experiment..... 108

**Figure A3** | Inhibiting thyroid hormone with TBBPA produced a global delay in development. .... 110

**APPENDIX B**

**Figure B1** | 3D images of stage NF57 and NF58 tadpoles during early metamorphosis. .... 112

## LIST OF ABBREVIATIONS

A	anterior
ANOVA	analysis of variance
<i>Acan</i>	Aggrecan
AP	alkaline phosphatase
As	angulosplenic
<i>Bglap</i>	bone gamma-carboxyglutamate protein (formerly <i>Osteocalcin</i> )
<i>Bgn</i>	Biglycan
C	cement gland
cDNA	complementary DNA
Ch	ceratohyal
ChIP-seq	chromatin immunoprecipitation sequencing
CLS	Canadian Light Source
cm	centimeter
Col1	collagen type I protein
Col10	collagen type X protein
<i>Col10a1</i>	collagen type X alpha 1 chain
<i>Col1a1</i>	collagen type I alpha 1 chain
<i>Col1a2</i>	collagen type I alpha 2 chain
Col2	collagen type II protein
<i>Col2a1</i>	collagen type II alpha 1 chain
<i>Col9a1</i>	collagen type IX alpha 1 chain
<i>Col9a2</i>	collagen type IX alpha 2 chain
<i>Col9a3</i>	collagen type IX alpha 3 chain
<i>Dcn</i>	decorin
DEPC	diethyl pyrocarbonate
ddH <sub>2</sub> O	double distilled water
dH <sub>2</sub> O	distilled water
D	dorsal
DIG	digoxigenin
dpf	days post-fertilization
DMSO	dimethyl sulfoxide
DNA	deoxyribonucleic acid
ECM	extracellular matrix
EDTA	ethylenediaminetetraacetic acid
<i>Epyc</i>	Epiphygan
EtOH	ethanol

<i>Fmod</i>	Fibromodulin
FP	frontoparietal
g	gram
<i>Gli1</i>	glioma-associated oncogene 1
GRN	gene regulatory network
h	humerus
H <sub>2</sub> O <sub>2</sub>	hydrogen peroxide
hCG	human chorionic gonadotropin
HCL	hydrochloric acid
hpf	hours post-fertilization
<i>Ibsp</i>	integrin binding sialoprotein
IHC	immunohistochemistry
<i>Ihh</i>	Indian hedgehog
IMM	immature chondrocyte
ISH	<i>in situ</i> hybridization
KOH	potassium hydroxide
L	left or liter
LCM	laser capture microdissection
MABT	maleic acid buffer with Tween20
mAs	medial angulosplenic
MAT	mature chondrocyte
<i>Matn1</i>	matrilin 1
MBS	Modified Barth's Saline
MgCl <sub>2</sub>	magnesium chloride
MgSO <sub>4</sub>	magnesium sulfate
Mk	Meckel's cartilage
ml	milliliter
mM	millimolar
mpf	minutes post-fertilization
mRNA	messenger RNA
Mya	million years ago
n	sample size
N	normality
NaCl	sodium chloride
Na <sub>2</sub> CO <sub>3</sub>	sodium carbonate
NaHCO <sub>3</sub>	sodium bicarbonate
NCBI	National Center for Biotechnology Information
NF	Nieuwkoop and Faber

NH3	thyroid hormone receptor antagonist
nM	nanomolar
NRC	National Research Council
OCT	optimal cutting temperature
OP	optic capsule
OST	osteoblast
P	posterior
PBS	phosphate-buffered saline
PBST	1X PBS with 0.5% Triton X-100
PCR	polymerase chain reaction
PFA	paraformaldehyde
<i>Ptch1</i>	protein patched homolog 1
PTHrP	parathyroid hormone-related protein
PS	parasphenoid
qPCR	quantitative polymerase chain reaction
R	right
RNA	ribonucleic acid
RNA-seq	RNA sequencing
RPM	revolutions per minute
RT-PCR	reverse transcription polymerase chain reaction
<i>Runx2</i>	runt-related transcription factor 2 (formerly <i>Cbfa1</i> )
Saf O	Safranin O
<i>Sox5</i>	sex determining region Y-box 5
<i>Sox6</i>	sex determining region Y-box 6
<i>Sox9</i>	sex determining region Y-box 9
<i>Sparc</i>	secreted protein acidic and rich in cysteine (formerly <i>Osteonectin</i> )
<i>Spp1</i>	secreted phosphoprotein 1 (formerly <i>Osteopontin</i> or <i>bone sialoprotein I</i> )
TBBPA	tetrabromobisphenol A
T <sub>3</sub>	triiodothyronine
T <sub>4</sub>	thyroxine
TH	thyroid hormone
Tri	trichrome
U/ml	units per milliliter
V	ventral
°C	Celsius
μl	microliter
μm	micrometer/micron

# CHAPTER 1

## Introduction

This chapter briefly summarizes the general organization of my thesis and provides an overview of the main objectives. It also acknowledges notable contributions made by those other than myself for each section. This thesis is comprised of six chapters. Chapters 2 and 3 serve as background, one of which was already published (Chapter 3), while others are manuscript-based (Chapters 4 and 5). The final chapter offers discussion, limitations, and future directions, and the enclosed Appendix details the results of a supplementary side project. Since all chapters inevitably contain some related background information, some of the same figures are referred back to in different chapters, although efforts were made to minimize this as much as possible.

Chapter 2 begins with a general overview of skeletal cell evolution, the significance of both the amphibian model and development in elucidating skeletal evolution, and a literature review of the current state of skeletal development. It concludes with the rationale behind my hypotheses for bone and cartilage evolution, respectively, and how each were tested. Chapter 3 reviews additional information that specifically sets the stage for an investigation into the evolution of the osteoblast, and has been published as a paper written with Dr. Eames for *The FEBS Journal* entitled, "Evolutionary repression of chondrogenic genes in the vertebrate osteoblast." This publication introduces the idea that the expression of genes that characterize cartilage (i.e., are chondrogenic) genes may have been lost during the evolution of the osteoblast and what steps are needed to uncover this possibility. It also showcases a high-resolution phase-contrast image that was scanned at the Canadian Light Source (CLS) by Jean-Sébastien Gauthier, an Artist-in-Residence member of the Eames lab.

Chapter 4 is a manuscript in preparation with Dr. Eames on osteoblast evolution and puts into practice many of the proposed experiments from our review paper in Chapter 3. It analyzes chondrogenic expression of the amphibian osteoblast and compares these results to other vertebrate models as described in the literature, as well as to unpublished datasets collected by past and present members of the Eames lab, to assess whether chondrogenic loss was a gradual

evolutionary event. Basic histology was used to identify osteoblasts within the humerus and lower jaw of the frog, and expression assays targeted cartilage genes and proteins within those bone regions. RNA *in situ* hybridization (RNA ISH) and immunohistochemistry (IHC) were relied upon for molecular studies. These allowed us to confirm the presence of some classic chondrogenic markers within amphibian bone as discovered previously in published results (Aldea et al., 2013; Bertin et al., 2014; Enault et al., 2015). LCM-RNAseq was also performed on lower jaw osteoblasts to provide a more quantitative assessment, although analyses of the RNA-seq data were limited. Existing RNA-seq datasets from the lower jaw of mouse, chick, and gar had already been available for comparison thanks to previous work done by Drs. Patsy Gómez Picos and Amir Ashique. Assistance in compiling the RNA-seq data, as well as some preliminary bioinformatical analysis, was performed by Dr. Katie Ovens. Some histological, RNA ISH, and IHC data on osteoblasts will be submitted for publication in collaboration with Dr. Sylvain Marcellini and his PhD student, Fret Cervantes, from the University of Concepción in Chile.

Chapter 5 is a third manuscript being co-authored with Dr. Eames on cartilage evolution and focuses on whether chondrocyte hypertrophy is conserved within the frog. Hypertrophy generally follows a very particular pattern during vertebrate development. To make these observations, the maturation of cartilages in the frog humerus and ceratohyal were characterized, compared to each other, and then to other vertebrates. Previous frog samples and work done by a former summer student, Yiwen Liu (who was supervised by Dr. Patsy Gómez Picos in 2015-16), were used to identify the relevant stages for studying the humerus and to narrow down when hypertrophy would occur within the ceratohyal. The analysis for this portion of the project depended mostly on histological and expression data, but some comparative RNA-seq analysis was performed as well to support any conclusions. Again, homologous datasets from the mouse, chick, and gar obtained by Drs. Patsy Gómez Picos and Amir Ashique were used for comparison, and Dr. Katie Ovens aided with handling of the RNA-seq data. Due to interesting findings in the ceratohyal, a side project involving thyroid hormone inhibition was carried out. Results for that experiment are still under investigation, however, and not directly related to the thesis objective, thus were limited to an appendix item. Although this side project has yet to be successfully replicated due to technical issues, important contributions were made by

collaborators from the National Museum of Natural History in France (Drs. Barbara Demeneix and Jean-Baptiste Fini) in providing us with a thyroid hormone competitor (NH-3), and from Michelle Whalen, our current lab manager for the Eames lab, who had assisted with multiple attempts at repeating this experiment.

Chapter 6 summarizes all results and conclusions, offers discussion points, speculations, and highlights any limitations that needed to be considered. Future directions are also proposed here. Aside from supplementary data and observations pertaining to the thyroid hormone inhibition experiment, the appendix also presents some 3D scans from PhD candidate, Oghenevwogaga (Joseph) Atake and Dr. Arash Panahifar that were meant to aid investigations into bone and thyroid, respectively.

## CHAPTER 2

### Background

*This chapter provides important concepts needed to understand this thesis that are only briefly touched upon or not covered at all in Chapter 3, which is a published review paper. Due to word limitations imposed by the journal to which that review was submitted, some concepts are introduced here first and any related details forthcoming in Chapter 3 will occasionally be referenced that either summarize or expand upon them further.*

#### **2.1 The evolution of skeletal cells**

Evolution is often thought of as an adaptive process, but constraint is just as foundational in shaping how life can evolve (S. J. Gould & Lewontin, 1979). As with many biological traits, skeletal cells have likely undergone millions of years of evolution, accumulating incremental changes along the way (Darwin, 1859). Over such large time scales, these subtle variations contributed to the derivation of novel skeletal traits among descendant clades (i.e., related groups of animals that have diverged from a common ancestor; Darwin, 1859; Steel & Penny, 2010; Theobald, 2010). In opposition to adaptation, constraint has also ensured that features defining a cell type (skeletal or otherwise) have been conserved and consistently passed on to future generations as well (Gould & Lewontin, 1979; Dietrich, 1998). The designation of a descendant species to a particular clade (e.g., Tetrapoda) means certain features were constrained upon them by their ancestors for them to be classified as such. For example, this is why most land vertebrates are tetrapods, or four-limbed, which includes many animals that have secondarily lost these limbs like whales and snakes (Schultze & Trueb, 1991; Clack, 2007, 2009). To some degree, features at the molecular level have also been conserved within extant animals (Dietrich, 1998), possibly chronicling how skeletal cells may have evolved in a particular clade as well. This allows us to probe what some shared ancestral features might have been and comparing the resultant differences could tell us what transpired as clades diverged over time. Uncovering these long-lasting connections is crucial for an evidence-based approach that aims to disentangle the evolution of skeletal cells. The limitations of this approach are outlined in Chapter 6, but these are currently the best available options for studying molecular evolution.

### **2.1.1 Significance of the amphibian model**

Most available data on the development of skeletal cells have been based on research in mouse and chick. Only recently has more emphasis been placed on fish and frog (Eames et al., 2012; Aldea et al., 2013; Bertin et al., 2014; Enault et al., 2015). As an amphibian, the last common ancestor of the frog is phylogenetically positioned between the respective common ancestors of earlier-diverged fish and later-diverged mammalian and avian models. Frogs can potentially provide valuable insight into the differences between these clades (Chapter 3 offers more details). The frog model is especially interesting given the amphibian clade also diverged around the time of a major evolutionary event, when aquatic vertebrates first began to transition onto land (Shubin, 2002; Clack, 2012; Wood & Nakamura, 2018). This seismic shift in habitat not only resulted in gross morphological changes to skeletal structures, but influenced changes at the molecular level as well. Incidentally, the life cycle of the frog (particularly metamorphosis) embodies the dramatic transformations needed for survival on land, seemingly recapitulating the progression of vertebrate evolution (Haeckel, 1866; Schaeffer, 1941; Gray, 1968; Edwards, 1977). While recapitulation theory has been largely overturned in favor of heterochrony (i.e., changes in developmental timing) as the primary force behind evolutionary change (Gould, 1977; McNamara, 1986; Hall, 2003), it remains an influential hypothesis within evolutionary developmental biology. Either way, current amphibians remain the most accessible intermediates for interrogating any developmental and genetic differences that exist between skeletal cells of earlier-diverged fish and later-diverged mammalian/avian models.

### **2.1.2 *Xenopus tropicalis* and the Nieuwkoop and Faber staging system**

The genome of the western clawed frog, *Xenopus tropicalis*, has a high degree of conservation with humans, making it a viable model system for biomolecular and medical research (Miura et al., 2008; Hellsten et al., 2010; Grainger, 2012; Blum & Ott, 2019). Classified as a fully aquatic tetrapod, *X. tropicalis* is an amphibian that undergoes metamorphosis to form limbs and lungs. This gives it the ability to survive on land for an appreciable amount of time when necessary (De Villiers & Measey, 2017). *X. tropicalis* was the frog model chosen here to represent the amphibian clade, but the limitations of its use are thoroughly detailed in Chapter 6. This frog species very closely resembles its more widely used cousin, *Xenopus laevis* (Yanai et al., 2011), but offers some

notable conveniences over *X. laevis*: quicker generation times, relatively smaller size, and a simpler genome (Beck & Slack, 2001; Grainger, 2012). As such, many studies between the two species are considered interchangeable, including developmental stages (Nieuwkoop & Faber, 1994), gene sequences (Miura et al., 2008; Yanai et al., 2011), and various lab techniques (Khokha et al., 2002). Thus, to stage and track the development of *X. tropicalis*, the “Normal Table of *Xenopus laevis*,” originally published in 1956 by Nieuwkoop and Faber (reprinted in 1994), was used as a reference. *X. tropicalis* offers some significant observational advantages over other classical vertebrates due to its external development, large embryonic size from the onset of fertilization, and transparent skin up until the later larval stages (Beck & Slack, 2001; Grainger, 2012).

Very briefly, the Nieuwkoop and Faber system is comprised of 66 stages (Fig. 2.1; Nieuwkoop & Faber, 1994), beginning from stage NF1, when the egg is fertilized (zygote), to stage NF66, with the emergence of an adult frog approximately six to eight weeks later (Khokha et al., 2002). Stages in between detail the embryonic (NF1 to NF27) and larval phases (NF28 to NF57), concluding with metamorphosis (NF57-66) as the tadpole transforms from an immature froglet into a four-limbed, adult frog (Kawahara et al., 1991; Nieuwkoop & Faber, 1994; Jupp et al., 2015). Beyond the adult stage (NF66+) is primarily physical growth, sexual maturity, and finally senescence. The stages investigated in this thesis were almost exclusively concentrated on the early larval and early metamorphic stages (i.e., early-to-mid NF40s and mid-to-late NF50s). These stages were when skeletal development began and when relevant skeletal cell types and processes were widely available for a comparative study with existing datasets.

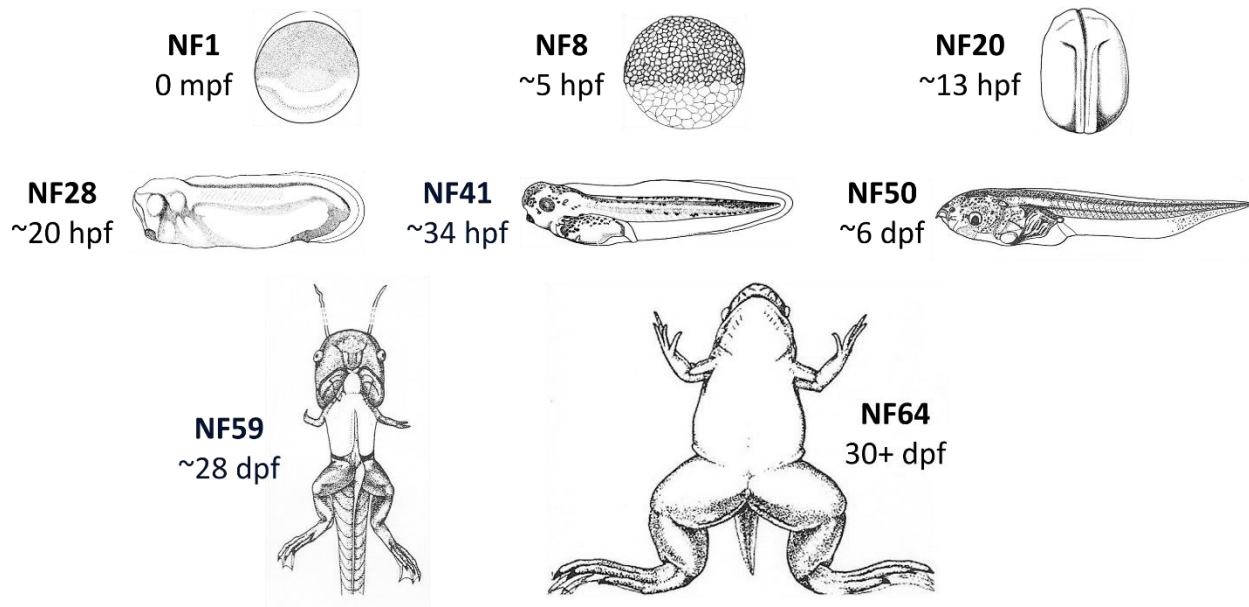


**Figure 2.1| The Nieuwkoop and Faber staging system can be used to track *Xenopus tropicalis* development.** These are some illustrations taken directly from the “Normal Table of *Xenopus laevis*” (1994). The selected images provide an idea of the embryonic phases (NF1 to NF27), early larval phases (NF28 to NF44), late larval phases (NF45 to NF57), metamorphic climax (NF58-62), and subsequent completion of metamorphosis (NF63-66) as the larval tadpole transforms into an adult frog. The developmental times have been modified to reflect the rate of *Xenopus tropicalis* growth raised at 27-28 °C. Abbreviations: dpf=days post-fertilization; hpf=hours post-fertilization; mpf=minutes post-fertilization. (Credit: Nieuwkoop & Faber, 1994).

### 2.1.3 Skeletal cell evolution can be reconstructed through comparative gene studies

Fundamentally speaking, evolutionary transitions can be explained by developmental processes that, in turn, were driven by gene expression (Li & Graur, 1991; Carroll et al., 2001; Carroll, 2008). At the very crux of skeletal cell evolution is the fact that the genes responsible for regulating skeletal development (skeletogenesis) had themselves evolved over time (Dobzhansky, 1937). This could have been attributed to multiple genetic factors like duplication events, recombination, and random mutations, all of which often affect chromosomal DNA, and thus, were capable of modifying skeletogenic genes and their regulatory elements (Li & Graur, 1991; Carroll et al., 2001; Stone & Wray, 2001; Wittkopp & Kalay, 2012; Lan & Pritchard, 2016; Signor & Nuzhdin, 2018). These natural occurrences likely influenced gene expression and gradually steered new generations of skeletal cells along divergent developmental pathways relative to those followed by their predecessors (Khaitovich et al., 2006; Blekhman et al., 2008). Differences in development could then account for the skeletal variations among phylogenetic clades,

thereby making comparative development an invaluable trove of information (Bedford & Hartl, 2009; Dunn et al., 2013). It is conceivable that recapitulation of phylogeny (evolution) might be directly ascertainable from observations of ontogeny (development) alone, although this idea has notable detractors and remains controversial (Haeckel, 1866; de Beer, 1930; Gould, 1977, 2002). More empirically, however, studying skeletal development within a model system elucidates the most current state of skeletal evolution within that lineage, and might also provide input into the ancestral traits constrained upon it.

Phylogenetic relationships are built based on the similarities and differences between clades. Therefore, it should be feasible to reconstruct evolution at the cellular level by employing similar tactics. When comparing skeletal cells—whether against each other or across clades—a high degree of similarity between cell populations means many of their properties were likely constrained (i.e., resistant to change) during the course of their evolution. Heavy constraint is associated with a high level of gene conservation. This can be further correlated with the development of shared skeletal traits when sampling descendant clades for comparative analysis. On the other hand, phylogenetic differences typically arise when less constrained genes have the freedom to vary. Herein lies the evidence for decoding how skeletal cells may have evolved. Ideally, with enough representative data, the order in which model vertebrates were positioned within phylogeny should map out how skeletal development and the expression of their corresponding skeletogenic genes may (or may not) have evolved over time (Nguyen & Eames, 2020). The methodology for making this comparison is detailed in Chapter 3.

## **2.2 An overview of skeletal cell development**

Skeletogenesis begins with the condensation (i.e., aggregation) of mesenchymal stem cells and their expression of the regulatory genes necessary to develop into either chondrocytes or osteoblasts (Eames et al., 2003, 2004; Eames & Helms, 2004). This describes cartilage formation (chondrogenesis) in a nutshell as mesenchymal precursors can differentiate directly into chondrocytes. However, vertebrate bone development (ossification or osteogenesis) can follow two main pathways. Like chondrocytes, osteoblasts are capable of forming directly from mesenchyme as well via intramembranous ossification. Alternatively, endochondral ossification is an indirect route, whereby osteoblasts are introduced following the maturation of a cartilage

template. Maturing chondrocytes differ morphologically and molecularly from immature chondrocytes in terms of size and gene expression. Interestingly, very few genes distinguish mature chondrocytes from osteoblasts and the literature is rife with examples of chondrocytes transdifferentiating into osteoblasts, both from its immature and mature forms (Moskalewski & Malejczyk, 1989; Thesingh et al., 1991; Lefebvre et al., 1995; Vortkamp et al., 1996; Inada et al., 1999; Neuhold et al., 2001; Zaragoza et al., 2006; Abzhanov et al., 2007; Mak et al., 2008; Hammond & Schulte-Merker, 2009; Sophia Fox et al., 2009; Eames et al., 2012; Huycke et al., 2012; Nishimura et al., 2012; Weng & Su, 2013; Ono et al., 2014; Zhou et al., 2014; Decker et al., 2015; Wang et al., 2017; Aghajanian & Mohan, 2018; Giovannone et al., 2019). This exemplifies the common developmental origins (and potential evolutionary connections) shared between these two cell types (Nakahara et al., 1990; Wagner & Lynch, 2010; Gómez-Picos & Eames, 2015; Nguyen & Eames, 2020). During development, the vast majority of skeletal cells available for study exist as chondrocytes and osteoblasts, which is why skeletal research often target these two cell types in particular. We are mostly focused on endochondral ossification as this process produces all the skeletal cell types of interest: resting and proliferating (immature) chondrocytes; prehypertrophic and hypertrophic (mature) chondrocytes; and osteoblasts (Fig. 2.2). Regardless of how bone forms, osteoblasts secrete a bone-specific matrix containing tightly wound collagen fibers like Col1 (collagen type I protein) that can be seen with Aniline blue through trichrome staining (Fig. 2.2C; Eames et al., 2003, 2004; Eames & Helms, 2004; Gentili & Cancedda, 2009). Once osteoblasts are completely surrounded by bone matrix, they are known as osteocytes (Erlebacher et al., 1995). In terms of gene expression, there are notable differences that exist between osteoblasts of earlier- and later-diverged vertebrate clades, which will be covered in Chapter 3. As for cartilage, the development and morphology of immature and mature chondrocytes can be visualized through Safranin O (Saf O), a red stain which binds to the sulfated proteoglycans characteristic of cartilage ECM (extracellular matrix) (Fig. 2.2A,B; Eames et al., 2003, 2004; Eames & Helms, 2004; Gentili & Cancedda, 2009).

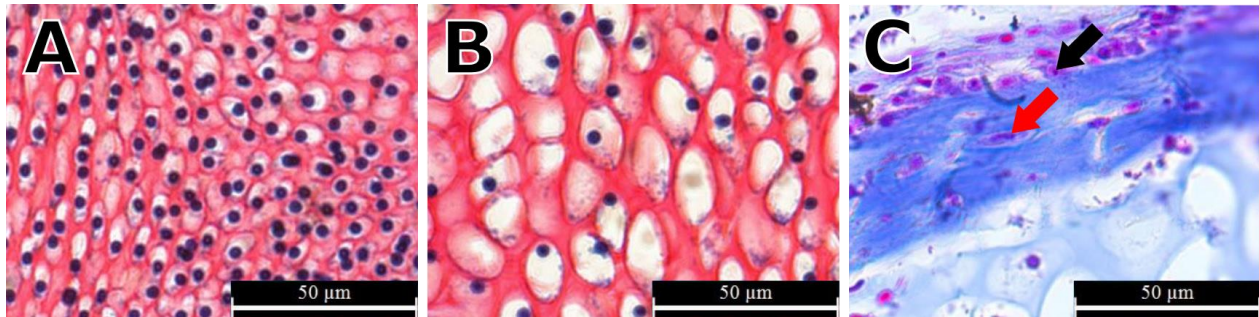


**Figure 2.2 | Skeletal cells can be visualized with Safranin O/Fast Green and trichrome.** Safranin O (red color) stains the sulfated proteoglycans found in the extracellular matrix of [A] resting and proliferating (immature) chondrocytes, as well as [B] prehypertrophic and hypertrophic (mature) chondrocytes. [C] An osteoblast is indicated by the black arrow. Osteoblasts secrete ECM containing tightly wound collagen fibers (Col1) which stain with Aniline blue from trichrome. Once completely surrounded by bone matrix, osteoblasts become osteocytes, as shown by the red arrow.

### 2.2.1 Cartilage is a precursor for endochondral ossification

The commitment of mesenchymal condensations to become prechondroblasts and their subsequent development into chondrocytes are driven primarily by the transcription factor, Sox9 (Akiyama et al., 2002; Mori-Akiyama et al., 2003). This is why Sox9 is considered the master regulator of chondrogenesis (Lefebvre & de Crombrughe, 1998; Bi et al., 1999). Sox9 directly mediates the expression of at least two key indicators denoting that cells have differentiated into chondrocytes: the secretion of sulfated proteoglycans (especially Aggrecan; Lefebvre et al., 2001) into cartilage ECM by chondroblasts (Fig. 2.2A,B; Tew et al., 2008; Daniels et al., 2019); and the presence of extracellular Col2 (collagen type II protein), which is encoded by the *Col2a1* gene (Bell et al., 1997; Lefebvre et al., 1997; Bi et al., 1999). Epiphycan (*Epyc*), Decorin (*Dcn*), Biglycan (*Bgn*), and Fibromodulin (*Fmod*) are also proteoglycans that characterize cartilage, with *Dcn*, *Bgn*, and *Fmod* sharing significant homology with one another (Roughley & Lee, 1994; Johnson et al., 1997; Gómez-Picos & Eames, 2015). Two other important transcription factors needed for chondrocyte differentiation, Sox5 and Sox6, are driven by Sox9 as well (Akiyama et al., 2002). Similarly, *Col9a1* (collagen type IX alpha 1 chain), *Col9a2* (collagen type IX alpha 2 chain), *Col9a3* (collagen type IX alpha 3 chain), and *Matn1* (matrilin 1) are important markers of immature chondrocytes under Sox9 control (Lefebvre et al., 2001; Zhang et al., 2003; Nicolae et al., 2007; Nagy et al., 2011; Henry et al., 2012; Liu et al., 2018).

### 2.2.2 Cartilage matures during endochondral ossification

After chondrogenesis, cartilage maturation is the next necessary step for endochondral ossification to proceed. All long bones (e.g., the humerus) and some head skeletal elements (e.g., the ceratohyal) are examples of (endo)chondral bones in most vertebrates. In contrast, most bones of the craniofacial skeleton are intramembranous (or dermal), which include bones of the lower jaw (e.g., medial angulosplenial in frog). Regardless, all ossification modes rely on *Runx2* (runt-related transcription factor 2, formerly *Cbfa1*) expression at some point (Ducy & Zhang, 1997; Komori et al., 1997; Otto et al., 1997). *Runx2* is best known as the main transcription factor of osteogenesis and is responsible for activating another key transcription factor downstream called *Sp7* (commonly referred to as *osterix*) that is important for osteoblast differentiation (Ducy & Zhang, 1997; Komori et al., 1997; Otto et al., 1997; Nishio et al., 2006; Komori, 2011)—although a homolog to *Sp7* is not present in most bird species and does not appear to be required for osteoblasts to form in zebrafish (Kague et al., 2016; Yu et al., 2017). While *Runx2* can induce mesenchymal condensations to differentiate directly into osteoblasts (i.e., intramembranous ossification), another major role of *Runx2* involves initiating and guiding cartilage through maturation in preparation for endochondral ossification (Kim et al., 1999; Yoshida et al., 2004; Mackie et al., 2008). The maturation of cartilage is dependent on the coordinated actions of *Sox9* downregulation and *Runx2* upregulation (Eames et al., 2003, 2004; Eames & Helms, 2004; Zhou et al., 2006). The stages of cartilage maturation are hypertrophy (an increase in cell size), mineralization (deposition of calcium phosphates, namely hydroxyapatite), and apoptosis (degradation through programmed cell death) (Kronenberg, 2003; Mackie et al., 2008; Long & Ornitz, 2013). Using the humerus as an example, maturation typically begins deep within the middle of the cartilage model—in this case, the diaphysis—and coincides with perichondral ossification of the bone collar (Kronenberg, 2003; Mackie et al., 2008; Long & Ornitz, 2013). Perichondral bone formation is initiated by the differentiation of osteoblasts from mesenchymal cells located inside the perichondrium, just superficial to the region of maturing chondrocytes (Egawa et al., 2014). As the first group of mature chondrocytes terminally differentiate and die, blood vessels penetrate through perichondral bone and into apoptotic cartilage, bringing in red blood cells, chondroclasts, osteoclasts, and osteoblasts (Kronenberg, 2003; Mackie et al., 2008;

Long & Ornitz, 2013). This is how trabecular bone is formed during endochondral ossification; perichondrial mesenchymal cells are introduced via vascular invasion and subsequently differentiate into osteoblasts (Egawa et al., 2014; Ono et al., 2014). Altogether, these events create the primary ossification center responsible for remodeling cartilage into chondral bone (Kronenberg, 2003; Mackie et al., 2008; Long & Ornitz, 2013). Secondary ossification centers later invade the epiphyses (Mackie et al., 2008). From here, cartilage maturation, perichondral, and endochondral ossification all progress outwards bilaterally from the diaphysis, eventually outpacing chondrocyte proliferation at the growth plates (metaphyses), then fuse with bone from the epiphyses (Mackie et al., 2008). These ossification sites work in tandem to ossify the entirety of the humerus, save for the articular surfaces, which persist into adulthood as immature and mature (hyaline) cartilage (Gray & Williams, 1989; Leboy et al., 1988; Eames et al., 2003, 2004; Eames & Helms, 2004; Yang et al., 2014; Zhou et al., 2014; Hinton et al., 2017; Aghajanian & Mohan, 2018).

### **2.2.3 Endochondral ossification might reveal parts of skeletal evolution**

The sequential steps needed to form chondral bone (i.e., from immature to mature chondrocytes to osteoblasts) often draw parallels to the respective evolutionary appearances of immature cartilage and bone (~530 vs ~500 Mya; Mallatt & Chen, 2003; Rychel et al., 2006; Gómez-Picos & Eames, 2015). As a consequence, it has been speculated whether this might yet be another example of ontogeny recapitulating phylogeny (Haeckel, 1866; de Beer, 1930; Gould, 2002), where the order of cartilage and bone during development might have been influenced by the order of their evolution. Since endochondral ossification must have been shaped by an evolutionary precedent, it is possible there are remnants of this ancestry contained within the process itself. Information might also be derived from studying how conserved endochondral ossification, or portions of its development are, among clades. Given that chondrogenic downregulation is needed for chondral bone to form, might this somehow be connected to the lack of cartilage gene expression in osteoblasts of later-diverged vertebrates (Nguyen & Eames, 2020)? As it currently stands, endochondral development appears to be fairly consistent across vertebrate clades, such as mammals, birds, and fish (Eames et al., 2004, 2011, 2012; Eames & Helms, 2004; Long & Ornitz, 2013). However, endochondral ossification has been described as

being delayed in the amphibian limb (Moriishi et al., 2005; Miura et al., 2008; Egawa et al., 2014), and in particular the head, where arrested development is common to most frogs (Porter & Vial, 1974; Thomson, 1986). What could be responsible for these unusual phenotypes? What is the expression profile of well-established skeletal genes during amphibian bone development? Since the progression of endochondral ossification in amphibians is not well-understood compared to other models, especially with regard to chondrocyte hypertrophy, these inquiries with respect to bone and cartilage development guided the subject matter under investigation in this thesis.

### **2.3 The osteoblast hypothesis**

The latest evidence suggests there is a clear molecular difference between osteoblasts of earlier- and later-diverged vertebrates in terms of chondrogenic expression: bone of fish and frog express cartilage genes, whereas mouse and chick do not (Eames et al., 2012; Aldea et al., 2013; Bertin et al., 2014; Enault et al., 2015). Chapter 3 covers this in more detail, but given that chondrogenic markers are generally defined by research in the later-diverged mouse and chick, this led to the hypothesis that chondrogenic gene expression became repressed during the evolution of the osteoblast (Nguyen & Eames, 2020). One of the objectives of this thesis was to verify whether amphibian osteoblasts were chondrogenic and at what level compared to other vertebrate models. In order to achieve this, histology, RNA *in situ* hybridization, immunohistochemistry, and LCM-RNAseq were performed, then compared against similar datasets in mouse, chick, and gar. These results are presented in Chapter 4.

### **2.4 The chondrocyte hypothesis**

The specific aspect of cartilage development being targeted here for comparative study was chondrocyte hypertrophy and whether this process was conserved in amphibians. Hypertrophy is an obvious morphological indicator of cartilage maturation given that chondrocytes increase dramatically in size, but hypertrophy also has associated changes in gene expression. For instance, *Sox9* and *Col2a1* levels usually drop as chondrocytes begin to mature, whereas prehypertrophic and hypertrophic markers like *Ihh* (Indian hedgehog) and *Col10a1* (collagen type X alpha 1 chain) normally increase (Eames et al., 2003; Mackie et al., 2008; Long & Ornitz, 2013). Since hypertrophy appears to be highly conserved (Eames et al., 2004, 2011, 2012; Eames &

Helms, 2004; Long & Ornitz, 2013), we hypothesized that amphibian cartilages underwent a standard hypertrophic cascade, both histologically and molecularly. This was tested by analyzing limb and head cartilages of *Xenopus tropicalis*, and comparing those results to homologous datasets from other vertebrate models. The investigation into conservation of chondrocyte hypertrophy is presented in Chapter 5.

## **2.5 Evolution can be relevant to health research**

Genetic factors more than likely contribute to most, if not all major diseases afflicting society today (Khoury, 2014). Gene mutations are responsible for the abnormal function and/or production of proteins underlying diseases like Huntington's, cystic fibrosis, progeria, some cancers, and many more (Verkerk et al., 1991; De Sandre-Giovannoli et al., 2003; Ratjen & Döring, 2003; Bates et al., 2015; Nielsen et al., 2016). Even for conditions where the full mechanism is currently unknown or multifactorial (e.g., Alzheimer's, multiple sclerosis, osteoarthritis, etc.), chances are high that dysfunctional genes have some role to play once these pathologies are understood at the molecular level (Burns & Iliffe, 2009; Nakahara et al., 2012; Glyn-Jones et al., 2015).

Since genes drive development, which has inextricable ties to evolution, gaining a deeper insight into one area naturally uncovers some information about the other (Baer, 1828; Dobzhansky, 1937; Carroll, 2005; Abzhanov, 2013; Cardoso-Moreira et al., 2019). Knowledge about normal development is critical for identifying and subsequently targeting the causes of disease (Shriver, 2001; Magrun, 2011). While observational studies can be made to reveal the progression of development (e.g., the stages of endochondral ossification and its regulation), oftentimes that cannot explain how or why processes came to be that way. This is where evolutionary studies can help broaden perspectives and approaches towards health issues. For instance, the frog appears to have a hypertrophic phenotype that would be considered aberrant in other species (Thomson, 1986), making the amphibian a potentially intriguing model for osteoarthritic disease (Bayles, 1950; Dreier, 2010). Why did this development come to be normal for amphibians and not others? Could the amphibian offer some bit of information that is lacking or not easily derived from traditional models? What genes are at play? More specifics and discussion points pertaining to this will be raised in Chapters 5 and 6.

## CHAPTER 3

### Evolutionary repression of chondrogenic genes in the vertebrate osteoblast

Nguyen, J. K. B., & Eames, B. F. (2020). *Evolutionary repression of chondrogenic genes in the vertebrate osteoblast. The FEBS Journal. Blackwell Publishing Ltd.*

<https://doi.org/10.1111/febs.15228>

#### 3.1 Abstract

Gene expression in extant animals might reveal how skeletal cells have evolved over the past 500 million years. The cells that make up cartilage (chondrocytes) and bone (osteoblasts) express many of the same genes, but they also have important molecular differences that allow us to distinguish them as separate cell types. For example, traditional studies of later-diverged vertebrates, like mouse and chick, defined the genes *Col2a1* and *Sox9* as cartilage-specific. However, recent studies have shown that osteoblasts of earlier-diverged vertebrates, such as frog, gar, and zebrafish, express these “chondrogenic” markers. In this review, we examine the resulting hypothesis that chondrogenic gene expression became repressed in osteoblasts over evolutionary time. The amphibian is an under-explored skeletal model that is uniquely positioned to address this hypothesis, especially given that it diverged when life transitioned from water to land. Given the relationship between phylogeny and ontogeny, a novel discovery for skeletal cell evolution might bolster our understanding of skeletal cell development.

### **3.2 Roll the clip, Jim: Phyletic constraint and skeletal cells**

In cosmology, researchers observe distant light and leftover radiation from the Big Bang in an attempt to piece together the origins of the early universe. Evolutionary biologists take a similar approach by categorizing traits of living things, hoping to recreate the story of how life on Earth may have unfolded. Traditionally, bone and some cartilages were obvious targets for evolutionary study, because mineralization made them more likely to be retained in the fossil record (H. Gray & Williams, 1989). Digging deeper into the evolutionary relationship of skeletal cells, however, a molecular fossil record of sorts can be unearthed from living animal models. To a great extent, this is possible due to phyletic constraint, which asserts that there are limitations on available evolutionary pathways in a given group of animals (i.e., a phylogenetic clade; Gould & Lewontin, 1979). As a result, each clade might retain some features that represent ancestral features of the last common ancestor with their sister clade. Accordingly, since amphibians diverged ~375 million years ago (Mya) from the last common ancestor of all tetrapods, they might exhibit better ancestral vertebrate features than mammals, who diverged from the last common ancestor of all amniotes more recently, ~310 Mya (Clack, 2007; Wheeler & Brändli, 2009). Therefore, we might learn more about the traits of ancestral vertebrates by studying earlier-diverged clades. In principle, phyletic constraint would leave enduring imprints that link living animals with the ancestors of their clade, specifically capturing in time features of an ancestral tetrapod, for example, in modern frogs. Combining phyletic constraint with advancements in high-throughput molecular techniques, it is feasible to quantitate the possible evolutionary history of skeletal cells in an unbiased, systemic fashion. Let's play back the tape of skeletal cell evolution by comparing gene expression in various living animals.

The standard list of genes expressed in cartilage and bone came from studies in mouse and chick, two land animals that share a relatively-recent common ancestor (~310 Mya; Wheeler & Brändli, 2009), compared to the evolutionary appearance of bone (~500 Mya; Janvier, 1996). The cells that make up cartilage and bone are chondrocytes and osteoblasts, respectively (Fig. 3.1). Generally, the transcription factors Sox9 and Runx2 drive formation of chondrocytes and osteoblasts, respectively (Eames et al., 2003, 2004). In many contexts, it is useful to subdivide cartilage into two distinct forms: immature cartilage, made up of resting and proliferating

chondrocytes (Fig. 3.1A); and mature cartilage, comprised of prehypertrophic and hypertrophic chondrocytes (Fig. 3.1B; Eames et al., 2003, 2004; Eames & Helms, 2004). Immature cartilage is characterized by high levels of “typical” cartilage genes, such as *Sox9*, *Col2a1*, and *Aggrecan* (Fig. 3.1A; Sandell et al., 1994; Ng et al., 1997; Smits et al., 2001). While immature cartilage can be found throughout adults (e.g., the middle zone of articular cartilage; Gray & Williams, 1989), it often undergoes a series of maturation events (turning into mature cartilage) during the embryonic process of bone formation known as endochondral ossification (Eames et al., 2003, 2004; Eames & Helms, 2004; Mackie et al., 2008). Mature cartilage is marked by *Ihh* and *Col10a1* expression (Fig. 3.1B), and its formation actually requires a coordinated downregulation of *Sox9* and upregulation of *Runx2* (Schmid & Linsenmayer, 1985; Leboy et al., 1988; Koyama et al., 1996; Enomoto et al., 2000; Eames et al., 2003, 2004; Eames & Helms, 2004; Mackie et al., 2008). Mature cartilage also can be found throughout adults (e.g., deep and calcified zones of articular cartilage; (Leboy et al., 1988; Eames et al., 2003, 2004; Eames & Helms, 2004), but most mature cartilage is degraded during endochondral ossification (Hatori et al., 1995; Eames et al., 2003, 2004; Eames & Helms, 2004). Since mature chondrocytes can express most known “bone” genes, including *Runx2*, *Spp1* (secreted phosphoprotein 1, formerly called *Osteopontin*), and *Bglap* (bone gamma-carboxyglutamate protein, formerly called *Osteocalcin*), only *Col1a1* (collagen type I alpha 1 chain) and *Col1a2* (collagen type I alpha 2 chain) are considered defining markers to discriminate osteoblasts from chondrocytes (Fig. 3.1C; Karsenty & Park, 1995; Ducy & Zhang, 1997). Further illustrating the similarities between gene expression in mature chondrocytes and osteoblasts, some mature chondrocytes actually transdifferentiate into osteoblasts (Moskalewski & Malejczyk, 1989; Thesingh et al., 1991; Hammond & Schulte-Merker, 2009; Zhou et al., 2014; Giovannone et al., 2019). On the other hand, *Col10a1* expression indeed distinguishes mature chondrocytes from osteoblasts in mouse and chick (Schmid & Linsenmayer, 1985; Leboy et al., 1988; Koyama et al., 1996; Eames et al., 2003, 2004; Eames & Helms, 2004; Mackie et al., 2008).

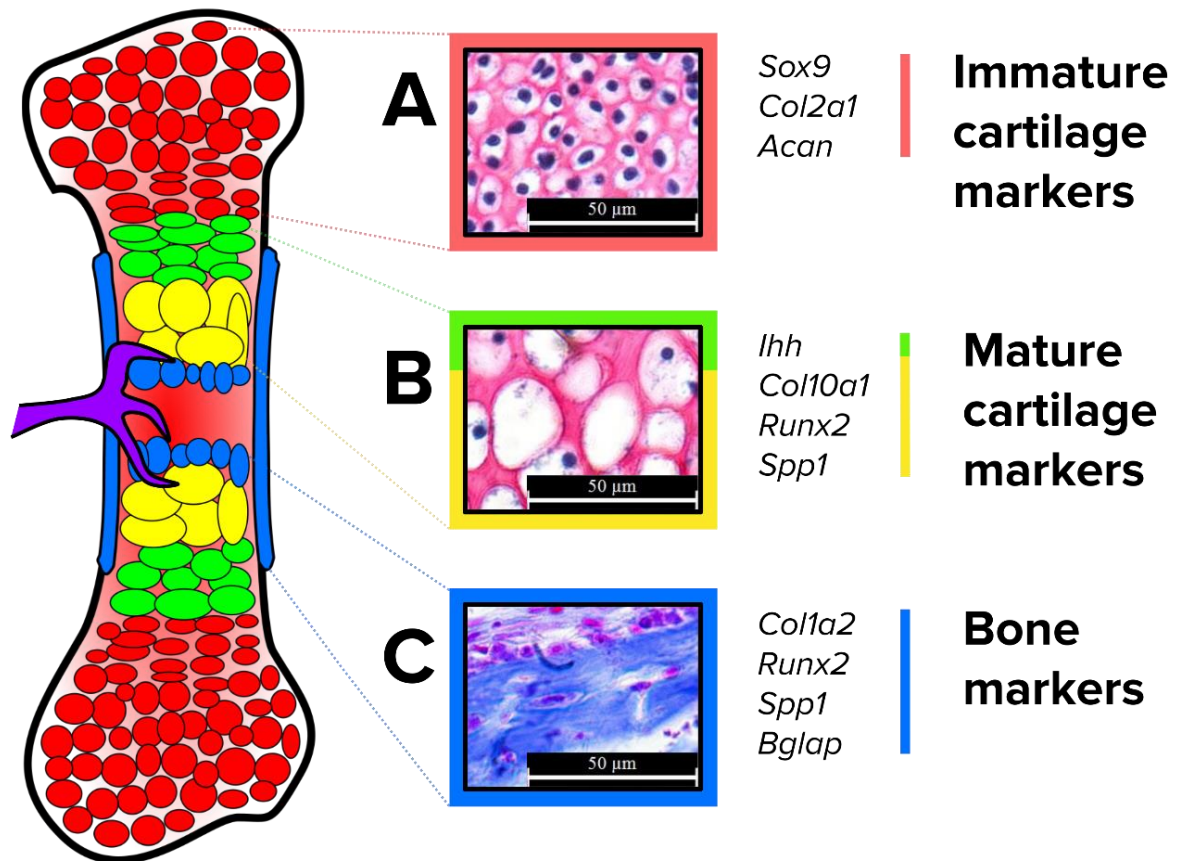


**Figure 3.1 | The relative location and molecular markers of major skeletal cell types during endochondral ossification.** A schematic of a frog humerus illustrates where **[A]** resting and proliferating chondrocytes (red cells) are found in immature cartilage, relative to **[B]** prehypertrophic (green cells) and hypertrophic chondrocytes (yellow cells) of mature cartilage. The increase in cell size of maturing chondrocytes is made very apparent through Safranin O staining of sulfated proteoglycans in the cartilaginous extracellular matrix on tissue sections of a larval *Xenopus tropicalis* humerus **[A vs. B]**. **[C]** Osteoblasts (blue cells), located near invading vasculature (purple), secrete tightly wound collagen fibers into the bony extracellular matrix (e.g., blue perichondral bone), visualized with Aniline blue in Trichrome staining.

### 3.3 Osteoblasts suppressed chondrocyte genes during evolution

Recent studies have revealed that osteoblasts of earlier-diverged clades, like bony fishes and amphibians, express molecular markers normally associated with cartilage of later-diverged clades, such as mammals and birds (Eames et al., 2012; Aldea et al., 2013; Bertin et al., 2014; Enault et al., 2015). A big surprise came when extremely high levels of *col10a1* expression (again, THE definitive marker of mature chondrocytes in chick and mouse) were demonstrated in osteoblasts of both zebrafish and gar (Eames et al., 2012). Perhaps given the overlap in gene expression among mature chondrocytes and osteoblasts of chick and mouse, such a result was a

relatively subtle variation among animal clades. However, even immature chondrocyte genes are expressed in osteoblasts of fish and frog. Low-to-moderate osteoblast expression of *col2a1*, which is usually only highly expressed in immature chondrocytes of chick and mouse, was demonstrated in zebrafish, gar, and even the western clawed frog, *Xenopus tropicalis* (Fig. 3.2; Eames et al., 2012; Aldea et al., 2013; Bertin et al., 2014; Enault et al., 2015). As far back as 1988, often-overlooked papers described Col2 protein in fish bone (Benjamin, 1988, 1989; Benjamin & Ralphs, 1991). Although most studies show near background *Col2a1* levels in bone of mouse and chick (e.g., Eames & Helms, 2004), one study even showed relatively high *Col2a1* expression levels (Abzhanov et al., 2007). Col2 protein production in chick bones was not demonstrated, however, suggesting that evolutionary mechanisms of post-transcriptional regulation might also be at play. These unexpected data point out that any traditional understanding of the evolutionary relationship between the chondrocyte and osteoblast is based upon a biased and incomplete molecular description of osteoblasts, since the vast majority of existing studies have focussed primarily on amniotes (e.g., mammals and birds). Therefore, any meaningful discussion about skeletal cell evolution needs to include all of the major vertebrate classes (Fig. 3.3), and despite some recent work, amphibians remain over-looked (Hanken & Gross, 2005; Gross & Hanken, 2005, 2008; Moriishi et al., 2005; Kerney et al., 2007; Miura et al., 2008; Rose, 2009; Wheeler & Brändli, 2009; Kerney, Hall, et al., 2010; Kerney, Wassersug, et al., 2010; Agüero et al., 2012; Kerney et al., 2012; Aldea et al., 2013; Bertin et al., 2014; Rose, 2014; Enault et al., 2015; Rose et al., 2015; Tussellino et al., 2016; Deniz et al., 2017; Porro & Richards, 2017).

Since frogs and fish shared a common ancestor further back in evolutionary time than land animals, and phyletic constraint might preserve ancestral features, these data lead to the hypothesis that chondrocyte genes became repressed during evolution of the osteoblast (Fig. 3.3A). As a less parsimonious, alternative argument, bony fish and frogs could have independently converged on increased chondrogenic expression in bone. Amphibians diverged from a common ancestor with mammals and birds approximately 375 Mya (Clack, 2007; Wheeler & Brändli, 2009). Given that most research is carried out on zebrafish, chick, and mouse, the intermediately positioned frog provides a critical weigh station along any vertebrate evolutionary trajectory.

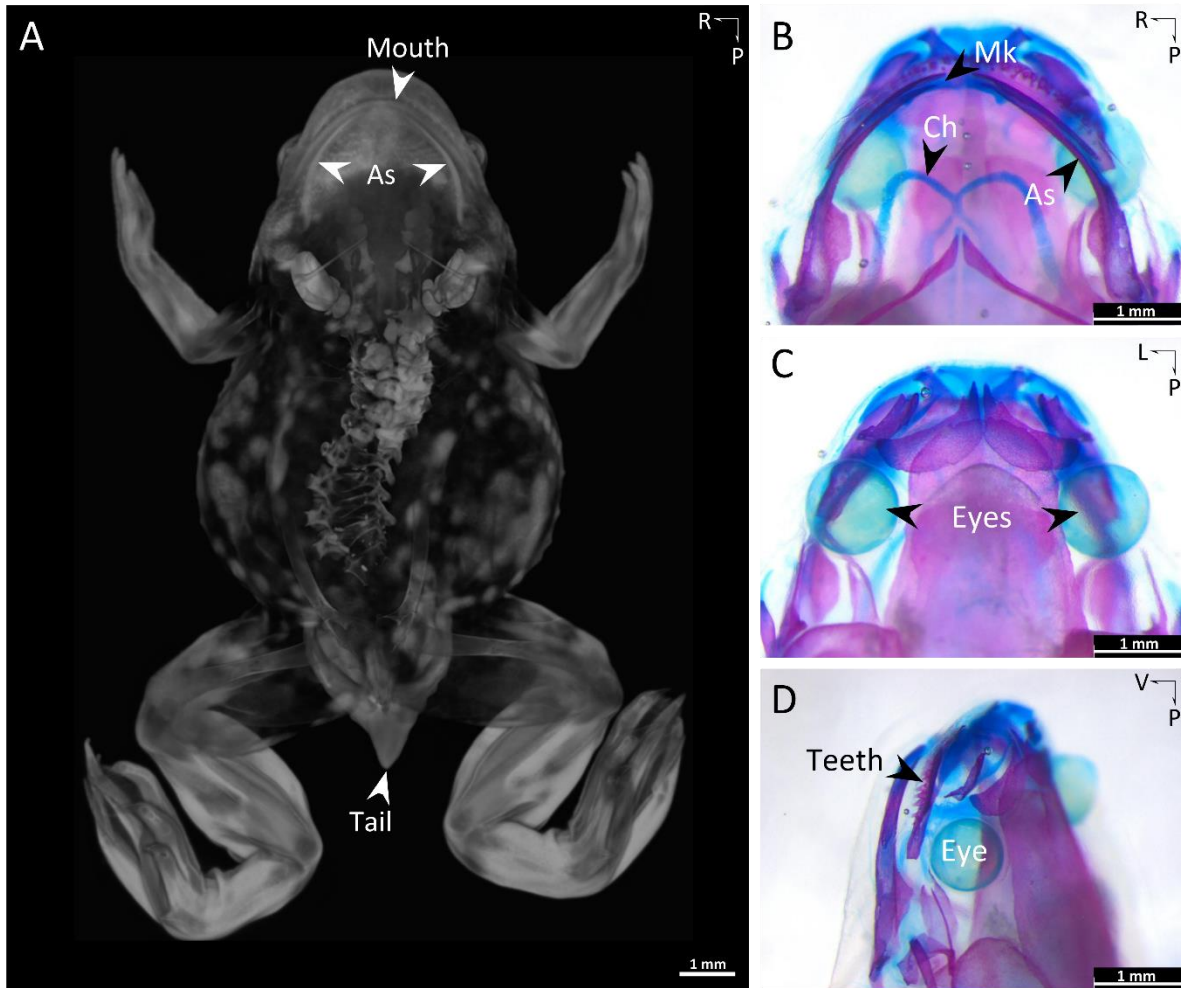


**Figure 3.2 | A new(old) vertebrate model for skeletal development: *Xenopus tropicalis*.** [A] A ventral view of a stage NF64 *X. tropicalis* froglet stained with phosphotungstic acid (PTA) contrast agent and scanned at the Canadian Light Source, the only synchrotron in Canada, using phase-contrast imaging (Olubamiji et al., 2016, 2017). [B] Ventral, [C] dorsal, and [D] lateral views of the craniofacial skeletal structures of a freshly metamorphosed, stage NF66 adult frog made visible through whole-mount Alcian Blue/Alizarin Red staining, where the blue indicates cartilage and red signifies calcified bone. Having diverged during a transitional period in evolution, the frog displays characteristics of both aquatic and terrestrial vertebrates, potentially making it a critical resource for understanding how evolutionary patterns in skeletal development may have arisen. Abbreviations: As=angulosplenic; Ch=ceratohyal; L=left; Mk=Meckel's cartilage; P=posterior; R=right; V=ventral. (Fig. 3.2A credit: J-S Gauthier).

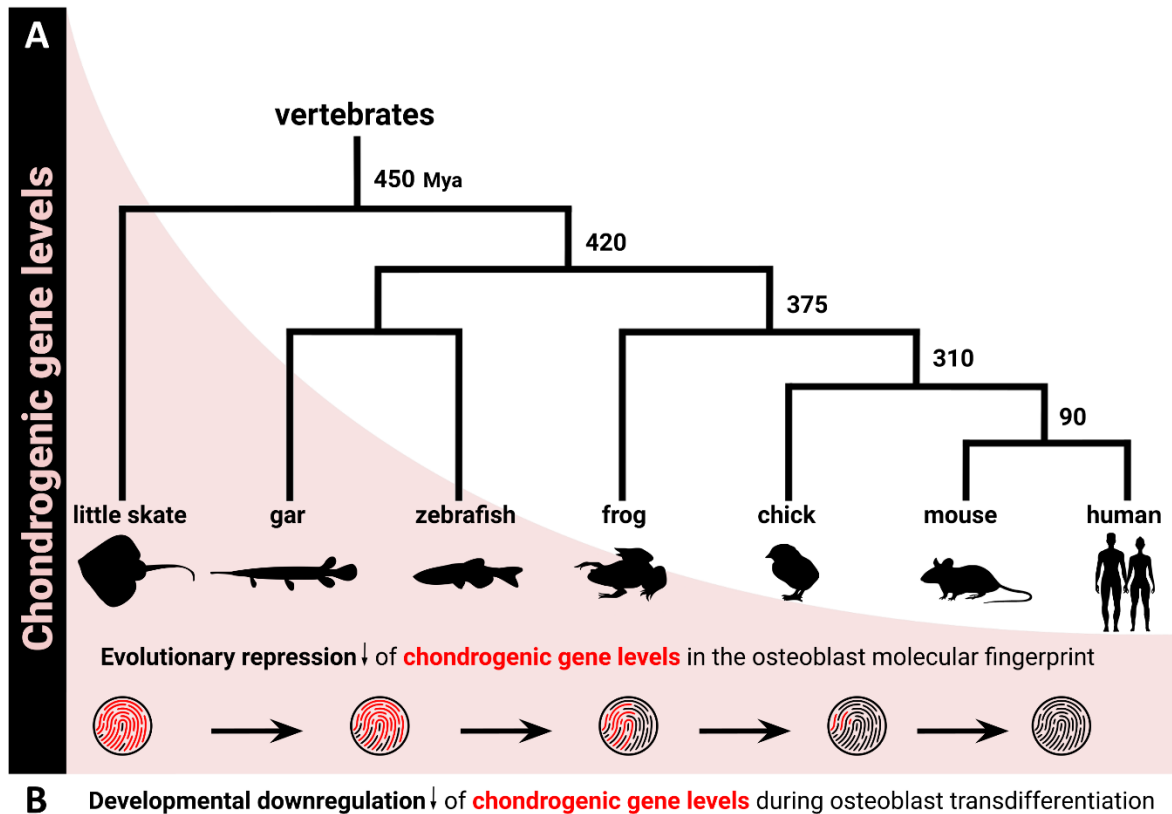


**Figure 3.3 | Hypothetical evolution (and development?) of the osteoblast molecular fingerprint. [A]** Molecular fingerprints can be compared across cell types and/or species to determine chondrogenic gene levels of osteoblasts. Comparing species, chondrogenic gene expression in osteoblasts of earlier-diverged vertebrates are relatively high compared to land vertebrates (Eames et al., 2012), suggesting that the vertebrate osteoblast may have evolved to become less chondrogenic. The frog osteoblast might have levels of chondrogenic genes that are somewhere in between osteoblasts of other aquatic vertebrates and land tetrapods, possibly revealing a gradual repression of this trait over evolutionary time. **[B]** Perhaps confirming further that ontogeny recapitulates phylogeny, a comparable chondrogenic downregulation is observed during the developmental process of endochondral ossification, when some maturing chondrocytes transdifferentiate into osteoblasts.

### 3.4 Using fingerprints to solve the hypothesis

High-throughput RNA sequencing (RNA-seq) is the unbiased and quantitative method of choice for generating the comprehensive transcriptomic data needed to assess the levels of chondrocyte gene expression in osteoblasts (Wang et al., 2009; Nagalakshmi et al., 2010). Rather creatively, the transcriptome of a specific cell type of interest has been termed its molecular fingerprint (Arendt, 2008). Similar to other traits, molecular fingerprints likely evolve through adaptation and constraint, but comparing molecular fingerprints is a novel approach for unraveling the

evolution of cell types (Gould & Lewontin, 1979; Arendt, 2008; Arendt et al., 2016). To evaluate the relationships among cell types, molecular fingerprints can be compared among different cell types in a given species (e.g., chondrocyte vs. osteoblast in mouse) or a given cell type in different species (e.g., osteoblasts in mouse vs. frog; Fig. 3.3). These analyses reveal not only qualitative data about what genes are included in each molecular fingerprint, but also quantitative data on the relative expression levels of genes expressed in both cell types. The latter aspect is critical in evaluating levels of chondrocyte gene expression during osteoblast evolution.

To test our osteoblast evolution hypothesis, several benchmarks might be used to determine how the osteoblast molecular fingerprint can be considered more or less chondrogenic (Fig. 3.4):

- A. What percentage of genes from the osteoblast molecular fingerprint are considered classical chondrogenic markers (from the published chick and mouse literature)? How do these percentages vary across vertebrate clades?
- B. What percentage of genes are shared between the osteoblast and chondrocyte molecular fingerprints within a vertebrate clade (immature and mature chondrocytes considered both separately and together)? How do these percentages vary across vertebrate clades?
- C. Of shared genes between the osteoblast and chondrocyte, what are the relative levels of chondrocyte gene expression in the osteoblast? How do these levels vary across vertebrate clades?

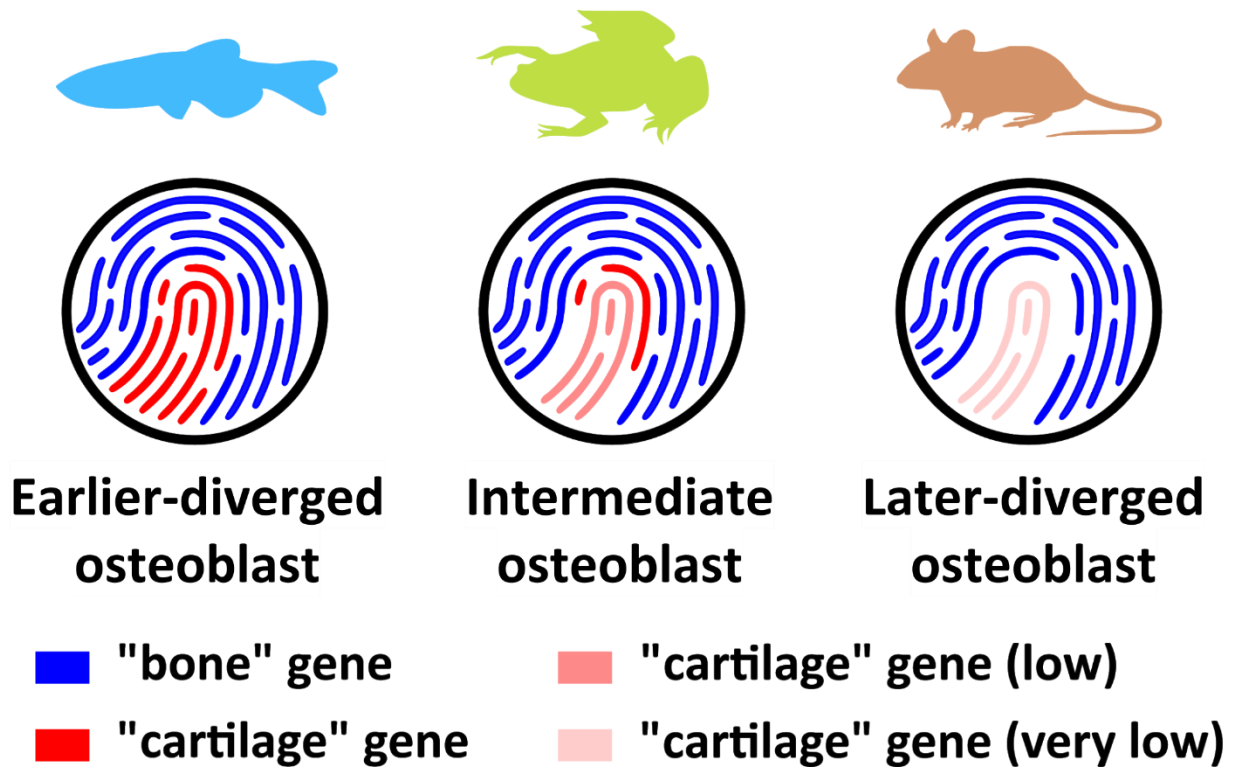


**Figure 3.4| Comparing osteoblast molecular fingerprints across vertebrates to determine the levels of chondrogenic gene expression.** Recent studies show that osteoblasts of earlier-diverged, aquatic clades express genes that are normally associated with cartilage (red) (Eames et al., 2012; Aldea et al., 2013; Bertin et al., 2014; Enault et al., 2015). In contrast, later-diverged osteoblasts express primarily “bone” genes (blue), thereby displaying little to no chondrogenic expression. RNA-seq of chondrocytes and osteoblasts in each vertebrate clade can reveal two important parameters to test the hypothesis that a gradual repression of chondrogenic genes occurred during evolution of the vertebrate osteoblast. First, an unbiased list of the number of “cartilage” genes expressed in osteoblasts across vertebrates would be generated. Second, the levels of expression of any “cartilage” genes common to all osteoblast fingerprints would be determined (lighter shades of red).

### 3.5 Skeletal speculator

We conclude with a few further speculations. Two possible scenarios are consistent with the published data showing chondrocyte gene expression in osteoblasts of earlier-diverged vertebrates. First, repression of chondrocyte genes in osteoblasts might have occurred specifically in the ancestor to chick and mouse, perhaps related to adjustment to life in a strictly terrestrial environment. Second, this process might have been somewhat gradual during evolution of vertebrates. As amphibians, frogs are nicely positioned to resolve among these two possibilities. For example, if the frog osteoblast fingerprint were to present a chondrogenic level

that falls somewhere between that of other established models, it would support the emergence of a gradual repressive pattern (Fig. 3.3A). Of course, the more animals analyzed, the better. For example, do cartilaginous fishes express even more chondrocyte genes in their bones than bony fishes (yes, we and others argue that living sharks and skates make bone; Allen et al., 2007; Atake et al., 2019)?

Expanding the relevance of this hypothesis, we suggest that an overlap in chondrocyte and osteoblast gene expression in earlier-diverged vertebrates provides insight into the evolutionary origins of the osteoblast. The fossil record clearly demonstrates that cartilage preceded bone, and chondrocytes and osteoblasts have similar functional and molecular features (Mallatt & Chen, 2003; Rychel et al., 2006; Gómez-Picos & Eames, 2015). These observations led us to hypothesize that the osteoblast evolved from the chondrocyte (Gómez-Picos & Eames, 2015). Embryonically, both chondrocytes and osteoblasts develop from common progenitor cells—a nontrivial matter when establishing evolutionary connections between cell types (Nakahara et al., 1990; Wagner & Lynch, 2010). In fact, the idea that the first osteoblast evolved from a chondrocyte would be consistent with the fact that osteoblasts of earlier-diverged vertebrates express many chondrocyte genes.

Finally, we pay homage to Haeckel, de Beer, and others who noted the many similarities between development (ontogeny) and evolution (phylogeny; Haeckel, 1866; de Beer, 1930; Gould, 2002). During endochondral ossification in mouse and zebrafish, at least a few of the cells that differentiate into immature chondrocytes and transition to mature chondrocytes, eventually transdifferentiate into osteoblasts (Moskalewski & Malejczyk, 1989; Thesingh et al., 1991; Hammond & Schulte-Merker, 2009; Zhou et al., 2014; Giovannone et al., 2019). Does this recapitulate phylogeny? Interestingly, these developmental transitions involve the progressive downregulation of “typical” cartilage genes, such as *Sox9* and *Col2a1* (Fig. 3.3B; Schmid & Linsenmayer, 1985; Koyama et al., 1996; Enomoto et al., 2000; Eames et al., 2003, 2004; Eames & Helms, 2004; Mackie et al., 2008; Cole, 2011). Is this further insight into the evolution of the osteoblast? It would be fascinating to look at whether the changes to *Sox9* binding loci during this developmental transition mirror those during evolution of the osteoblast (Fig. 3.3A). Nevertheless, skeletal cell evolution has been a longstanding topic of contention among

researchers. Fortunately, comparing the molecular mechanisms underlying skeletal cell differentiation among extant vertebrate clades might provide us with the very clues needed to unravel the history of chondrocytes and osteoblasts.

## CHAPTER 4

### Chondrogenic expression in amphibian osteoblasts versus other vertebrates

*Nguyen, J. K. B., Gómez-Picos, P., Liu, Y., Ovens, K., and Eames, B. F.*

#### 4.1 Abstract

*Sox9*, *Col2a1*, and *Col10a1* are traditionally referred to as genes that characterize cartilage because research performed on mouse and chick models defined them as such. However, it was recently discovered that bone of earlier-diverged vertebrate models like zebrafish, gar, and *Xenopus* frogs also featured these markers. Considering the order in which these clades diverged relative to one another, this suggested chondrogenic expression might have been a primitive trait of osteoblasts that was lost during vertebrate evolution. We hypothesized that this chondrogenic loss was an incremental process as the vertebrate osteoblast evolved over time. Since amphibians diverged after fish but before land animals, the frog osteoblast would need to exhibit a level of chondrogenic expression somewhere in between these earlier- and later-diverged clades in order to support this. To test the hypothesis, histological and molecular assays were conducted to gauge the level of chondrogenic expression in amphibian osteoblasts from the humerus and lower jaw, then compared to other vertebrate models. Laser capture microdissection coupled with RNA sequencing was also performed on lower jaw osteoblasts for a limited comparative study. It was found that amphibian osteoblasts expressed many chondrocyte genes (like *col2a1*, *acan*, *sox5*, *sox6*, and more) at levels much higher than expected. Through comparison of amphibian data to published literature, it was also discovered that perichondral osteoblasts may have stronger expression of chondrocyte genes than dermal osteoblasts. If these findings are validated, it would seem chondrogenic repression was not as gradual as previously postulated during evolution. These results are still preliminary and require more thorough bioinformatical support, but it appeared amphibian bone was more chondrogenic than even earlier-diverged fish. This could mean chondrogenic expression actually increased in the amphibian lineage before disappearing in later-diverged land tetrapods.

## 4.2 Introduction

Bony limbs likely aided in the diversification of terrestrial life thanks to the added support bone offers against the extra stresses of living on land (Shubin et al., 2004; Volkmann & Baluška, 2006). Generally speaking, bone cells (osteoblasts) can either form directly without cartilage (intramembranous ossification), or be introduced indirectly via a cartilage template (endochondral ossification). As skeletal tissues, both cartilage and bone offer structural support and share many properties, including a tremendous overlap in gene expression, which suggests a possible common ancestry (Gómez-Picos & Eames, 2015; Nguyen & Eames, 2020). Of course each skeletal type has defining markers as well, but these were classically derived from research performed primarily in mouse and chick (Schmid & Linsenmayer, 1985; Leboy et al., 1988; Linsenmayer et al., 1991; Sandell et al., 1994; Vortkamp et al., 1996; Bi et al., 1999). For instance, *Sox9* and *Col2a1* are currently understood to be typical markers of resting and proliferating chondrocytes found in immature cartilage, whereas *Col1a1* and *Col1a2* differentiate osteoblasts from chondrocytes (Sandell et al., 1994; Karsenty & Park, 1995; Ducky & Zhang, 1997; Ng et al., 1997; Smits et al., 2001). Furthermore, *Col10a1* distinguishes hypertrophic chondrocytes of mature cartilage from immature cartilage (Linsenmayer et al., 1991; Poole, 1991). The latest reports have demonstrated higher than anticipated expression of *sox9*, *col2a1*, and *col10a1* in osteoblasts of zebrafish, gar, and frogs, clades which diverged from a last common ancestor earlier than mouse and chick (Eames et al., 2012; Aldea et al., 2013; Bertin et al., 2014; Enault et al., 2015). We sought to quantitate how chondrogenic earlier-diverged osteoblasts were versus later-diverged osteoblasts by comparing the molecular profiles of these vertebrate models.

A comparative study such as this relies on phyletic constraint, a limitation that generally dictates how certain traits can evolve within future generations, including at the molecular level (Gould & Lewontin, 1979; Arendt, 2008; Nguyen & Eames, 2020). Extant animals are assigned to particular clades partly based on the very traits constrained upon them by their ancestors, meaning they must retain some ancestral information. These parameters still allow for specific adaptations to take place and it appears an ancestral feature (i.e., chondrogenic expression) may have been lost during the evolution of the vertebrate osteoblast (Eames et al., 2012; Aldea et al., 2013; Bertin et al., 2014; Enault et al., 2015; Nguyen & Eames, 2020). When did chondrogenic

expression in osteoblasts (begin to) disappear? What other classical markers associated with cartilage were present in bone of earlier-diverged clades—particularly immature cartilage markers, given very few genes distinguish maturing cartilage from bone (Lefebvre et al., 1995; Sophia Fox et al., 2009; Decker et al., 2015; Wang et al., 2017)? At what levels are these genes being expressed in one clade relative to another? These details can address whether evolutionary repression of chondrogenic genes occurred in the vertebrate osteoblast and possibly even the rate at which this might have progressed. The amphibian is ideal for this investigation given its position within phylogeny, having diverged during an intermediate period between clades that either exhibit this trait or lack it altogether (Wheeler & Brändli, 2009; Eames et al., 2012; Aldea et al., 2013; Long & Ornitz, 2013; Bertin et al., 2014; Enault et al., 2015). Based on these observations, we hypothesize that the amphibian osteoblast has a chondrogenic level that is intermediate to earlier- and later-diverged vertebrates.

To test this hypothesis, the set of genes that make the frog osteoblast unique (i.e., its molecular fingerprint; Arendt, 2008), and the level to which these genes constitute chondrogenic expression, are compared against published and unpublished data from mouse, chick, and gar. To implement this comparative transcriptomic approach, the criteria for determining levels of chondrogenic expression across clades were detailed previously in Chapter 3, although only a limited analysis could be performed here due to time constraints. Regardless, the following steps were involved:

1. Identification of skeletal elements homologous to those previously analyzed in mouse, chick, and gar through whole-mount histology, i.e., the humerus (a chondral bone of the upper limb) and the medial angulosplenic (an intramembranous/dermal bone of the lower jaw).
2. Characterization of these elements using section histology to determine the stages and regions from which the appropriate skeletal cells would be analyzed, i.e., immature and mature chondrocytes from the humerus and osteoblasts from the medial angulosplenic.
3. Expression assays to confirm and semi-quantitate the presence of chondrogenic markers (e.g., RNA *in situ* hybridization and immunohistochemistry).

4. Isolation of the cells of interest with laser capture microdissection in order to avoid any cross contamination with unwanted cell types for RNA-seq. Extraction of RNA from those captured cells, then amplification and purification for Illumina sequencing. And finally, a preliminary analysis relying on normalized counts of candidate cartilage genes from the raw RNA-seq data.

It was found that amphibian osteoblasts do express many prominent chondrocyte genes and perhaps at levels higher than both earlier- and later-diverged vertebrates. Follow-up analyses are required in order to confirm these findings, but preliminary results suggest chondrogenic expression may have ramped up in the amphibian clade before dissipating to negligible levels in mammals and birds. This was an unexpected but novel discovery, and does not support the hypothesis that amphibian osteoblasts have an intermediate level of chondrogenic expression compared to other vertebrate models.

## **4.3 Materials and methods**

### **4.3.1 Use of lab animals**

Wild type adult male and female *Xenopus tropicalis* frogs were purchased from Xenopus 1 ([www.xenopus1.com](http://www.xenopus1.com)), housed in the Health Sciences Building vivarium, and cared for by the Animal Care & Research Support (ACRS) unit, formerly known as Lab Animal Services Unit (LASU). The protocols used for this research were approved by the University Animal Care Committee Animal Research Ethics Board (UACC AREB) at the University of Saskatchewan (Animal Use Protocol; AUP# 20130092).

### **4.3.2 Frog mating**

While previous matings had been performed before by Yiwen Liu and Dr. Patsy Gómez Picos, I was able to update and optimize our protocol to better suit the facilities and equipment available to us for frog husbandry. This involved making use of and combining techniques from other labs that have significant expertise working with *Xenopus* frogs (Sive et al., 2000; Khokha et al., 2002; Showell & Conlon, 2009). All husbandry and experimental procedures were maintained at an ambient water temperature of around 27-28 °C and room lighting was automated on a daily 12h:12h light-dark cycle. To mate frogs, females with prominent cloacas and bellies were paired

with males that had dark nuptial pads (aides with grip during mating; Willaert et al., 2013), whenever possible. Chorulon human chorionic gonadotropin (hCG) hormone was requisitioned from the Veterinary Medical Centre on campus at the University of Saskatchewan. Injections were administered with 30-gauge needles and directed into the dorsal lymph sac, a region just underneath the skin, anterior to the cloaca. The day before pairing, each frog was primed with a dose of 100 ul of hCG at 100 U/ml that had been diluted with ddH<sub>2</sub>O. After 20-24 hours, each frog was subsequently boosted with 200 ul of hCG at 1000 U/ml (stock concentration of Chorulon), then left undisturbed in a partially closed container filled with system water to a height of 8 cm. The container was placed in a 27-28 °C waterbath and covered to provide privacy and to keep the frogs from escaping. The male would mount the female shortly after the boost injections and amplexus would last anywhere from 2 to 9 hours (sometimes longer). Once mating was complete, eggs were sorted through and any dead or unfertilized eggs were discarded.

#### **4.3.3 Raising tadpoles to stages of interest**

Whenever stages of interest were reached, 0.02% tricaine was used to anesthetize specimens for staging. Less than 24 hours after fertilization, embryos hatched into tadpole larvae (NF24-27) and those exhibiting movement around NF28-32 were transitioned gradually to 0.1X MBS (Modified Barth's Saline) media. First, system water was replaced with 25% 0.1X MBS, then changed in a graded fashion every 30-60 mins to 50%, 75%, and finally to 100% 0.1X MBS. This transition was to avoid any edema that would result if larvae were transferred to a high salt solution too soon. Once tadpoles began to swim freely by NF41-43, they were transferred to nursery tanks and daily feedings were initiated when their embryonic yolk sacs were near depletion (~NF45). Early feeds consisted of Sera Micron powder (16 g mixed with 1 L system water) where 10 ml was added for every 20-50 tadpoles, twice a day. The amount of feed was increased by 10 ml per week, but adjusted accordingly depending on the mortality and morbidity rate. Excess food was periodically cleaned from nurseries and after two weeks, feedings were supplemented with crushed Frog & Tadpole pellets (¾ powder, ¼ pellets). Feeds were eventually modified to ½ powder, ½ pellets during the week of visible forelimb growth (~NF55 to NF58) until the very beginning of metamorphic climax (~NF59), at which point feeding was no longer required. In instances where food ran out, a home-made recipe kindly provided to us by Dr. Zachery Belak was used as a

substitute (by weight: 1 part spirulina powder; 1 part dried small shrimp; and 1 part dried yolk from a hard-boiled egg). Metamorphosing tadpoles obtained all their energy from the resorbing tail during this distressful period until metamorphosis was complete at NF66 (Denver, 2010), so sterile flotation devices were added to the habitat to prevent drowning (<https://medicine.yale.edu/lab/khokha/>).

#### **4.3.4 Fixation, processing, and sectioning for histology**

Tricaine at a concentration of 0.2% was used to euthanize samples. Tissues were fixed with 4% PFA, added at a volume of at least 10-20 times the size of the tadpole(s) collected. Fixed samples were left on a rocker overnight at 4 °C, then washed twice with 1X PBS for 15 mins each. For long-term storage of tissues, samples were dehydrated in ethanol series buffered with PBS (EtOH/1X PBS) for 15 mins each, rocking at room temperature, from 25% to 50% to 75% to 100% EtOH, then stored at -20 °C. Stored samples were rehydrated in reverse order for use in downstream experiments. Occasionally, samples were used directly after overnight fixation and 1X PBS washes.

Paraffin tissue processing, embedding, and microtome sectioning were performed here at the Histology Core Facility located on 1<sup>st</sup> floor. Processing was automated via a tissue processor through a series of chemical changes by dehydrating and clearing, and then embedded in paraffin wax. Samples prepared for cryostat sectioning were done directly in our cluster on the 3<sup>rd</sup> floor in B330. Both frozen and paraffin sections were collected at 7 µm thicknesses on glass slides (Fisherbrand™ Superfrost™ Plus Microscope Slides) for section histology. Longitudinal sections were obtained from the humerus (stage NF57) and coronal sections were obtained from the lower jaw (stages NF51 to NF57). Prior to cryosectioning, sample tissues were placed into cryomolds (Tissue-Tek; Sakura Finetek USA, Torrance, CA) with OCT (optimal cutting temperature) embedding medium (Tissue-Tek; Sakura Finetek USA, Torrance, CA), and submerged in a beaker containing isopentane. Tissues were snap frozen with liquid nitrogen, then cryosectioned or kept in -80 °C storage. Cryoblocks stored at -80 °C were warmed to -20 °C in the cryostat before sectioning and frozen sections were left to dry at room temperature. Paraffin sections were left to dry overnight in a 37 °C incubator.

### **4.3.5 Histology**

#### **Whole mount Alcian blue/Alizarin red acid-free staining**

For 2-3 day old tadpoles (e.g., stages NF47 and earlier), whole mount staining was performed as described previously (Eames et al., 2011). However, for larger tadpoles (NF48 and older), some modifications were made (e.g., increased incubation times and concentrations of certain reagents, and extra washes to de-stain or remove excess reagents; Van Eeden et al., 1996; Walker & Kimmel, 2006). All steps were nutated at room temperature, unless stated otherwise.

Larger samples were fixed overnight at 4 °C in 4% PFA/1X PBS (or rehydrated from -20 °C storage if already fixed), washed twice in 1X PBS for 15 mins each, then 100 mM Tris pH 7.5/10 mM MgCl<sub>2</sub> for 20 mins, stained with 0.04% Alcian blue/100 mM Tris pH 7.5/10 mM MgCl<sub>2</sub>/80% EtOH overnight, washed in 100% EtOH to de-stain for at least 24 hrs (twice, if necessary), taken through graded EtOH series for at least 1 hour each (80% EtOH/100 mM Tris pH 7.5/10 mM MgCl<sub>2</sub>; 50% EtOH/100 mM Tris pH 7.5/10 mM MgCl<sub>2</sub>; 25% EtOH/100 mM Tris pH 7.5/10 mM MgCl<sub>2</sub>), washed three times with dH<sub>2</sub>O for at least 2 hours each, left in trypsin for several hours or in the cold room overnight (until soft tissues were visibly digested), rinsed briefly in dH<sub>2</sub>O, stained with 0.02% Alizarin red/0.5% KOH for 4 hours, bleached in 0.06% H<sub>2</sub>O<sub>2</sub>/0.5% KOH overnight, and de-stained in series with 25% glycerol/0.5% KOH; 50% glycerol/0.5% KOH; 75% glycerol/0.5% KOH for at least 24 hrs each, then stored in 100% glycerol.

#### **Safranin O and trichrome section histology**

Safranin O/Fast green staining on paraffin and frozen sections were performed as previously described with slight modifications (McManus & Mowry, 1960). Paraffin sections were deparaffinized in xylene for 5 mins, then dehydrated in series (100% EtOH for 5 mins; 95% EtOH for 3 mins; 70% EtOH for 2 mins), whereas frozen sections were dehydrated in 70% EtOH only. Sections were stained with Weigert's iron hematoxylin for 5 mins, washed with tap water for 2-3 mins, stained with 0.02% Fast green (CI 42053) for 30 secs, de-stained with 0.5% Safranin O (CI 50240) for 30-45 mins, then dehydrated with 95% EtOH and 100% EtOH for 12 dips each, and xylene for 5 mins before mounting the slide for imaging.

Trichrome stained sections were deparaffinized and/or dehydrated in a similar manner as above, but rinsed with dH<sub>2</sub>O for 3 mins prior to staining with Milligan's trichrome for 5 mins, dH<sub>2</sub>O for 1 min, 1% acid fuchsin stained for 30s, dH<sub>2</sub>O for 30 secs, 1% phosphomolybdic acid stained for 2 mins, 2% orange g/1% phosphomolybdic acid stained for 30 secs, dH<sub>2</sub>O for 1 min, de-stained with 1% acetic acid for 2 mins, stained with 1% Aniline blue/0.2% acetic acid, 1% acetic acid for 3 mins, then dehydrated in ethanol series (70%; 95%; 95%; 100%; 100%) to xylene before mounting for imaging.

### **4.3.6 Expression assays**

#### **RNA *in situ* hybridization**

Plasmids containing the *Xenopus* genes were kindly provided to us from various labs: *sox9* (Spokony, 2002), *col2a1* (Kerney, Hall, et al., 2010), and *col10a1* (Aldea et al., 2013). These were chemically transformed into calcium-competent *E. coli* bacterial cells (OneShot, Invitrogen), selected for with ampicillin, and cultured overnight in liquid medium, then plasmid DNA was extracted and purified to produce minipreps. Minipreps were DNA sequenced and blasted on NCBI online to ensure the genes were correct, then linearized accordingly to produce the proper sense and anti-sense probes, which were transcribed *in vitro*, and labeled with digoxigenin (DIG) for chromogenic RNA ISH. In addition, a *col10a1* anti-sense probe was also hydrolyzed following a Cold Spring Harbor Protocol (Ferrandiz & Sessions, 2008; with some modifications) to improve probe entry through the cellular membrane. Hydrolysis was done by incubating the probe with twice the volume of RNase-free hydrolysis buffer (40 mM NaHCO<sub>3</sub>/60 nM Na<sub>2</sub>CO<sub>3</sub>) at 58 °C for about 10 mins, before stopping the reaction, re-precipitating the hydrolyzed probe, and dissolving again with 0.1% DEPC for use in RNA ISH.

RNA ISH was carried out on tissue sections as previously described (Strähle et al., 1994; Jowett & Yan, 1996; Eames et al., 2011), with modifications, on stage NF57 of the humerus and lower jaw. All solutions were prepared with DEPC to preserve RNA until the actual hybridization reaction and all incubation steps longer than 1 hour were performed in a humidity chamber with the appropriate buffer.

On day 1, paraffin sections were deparaffinized and rehydrated in graded fashion to 70% EtOH/0.1% DEPC, then baked at 58 °C for at least 1 hour (frozen sections were only baked for 10-30 mins). Slides were fixed in 4% PFA/1X PBS/0.1% DEPC for 20 mins, rinsed in 1X PBS/0.1% DEPC for 5 mins, incubated in 0.2 N HCl/0.1% DEPC at room temp for 10 mins, rinsed twice in 1X PBS/0.1% DEPC for 5 mins each, permeabilized with proteinase K/1X PBS/0.1% DEPC (3 ug/ml for paraffin; 1 ug/ml for frozen) at 37 °C for 15 mins, rinsed in 1X PBS/0.1% DEPC for 5 mins, post-fixed in 4% PFA/0.1% DEPC for 15 mins, rinsed in 1X PBS/0.1% DEPC for 2 mins, then pre-hybridized in hybridization buffer for at least 3 hrs at 58 °C to denature and unravel RNA. RNA probes were then prepared at a concentration of at least 1 ng/ul in hybridization buffer, denatured for 5 mins at 70 °C, then left on ice to prevent reannealing, and loaded onto sections to hybridize overnight at 58 °C.

On day 2, unbound probes were washed away at 58 °C in washing solution for 15 mins once, and 30 mins twice, then 1X MABT (maleic acid buffer with Tween20) at room temp for 30 mins, twice. Slides were blocked to reduce non-specific binding at room temp for 2-3 hours in blocking solution (with heat-inactivated sheep serum), then incubated overnight in a humidity chamber at 4 °C with blocking solution (active sheep serum) containing a 1:1000 dilution of anti-DIG alkaline phosphatase antibody (Roche, Sigma-Aldrich).

On day 3, slides were washed four times with 1X MABT for 30 mins each at room temp, then twice for 10 mins with AP (alkaline phosphatase) staining buffer, and left to stain with BM-Purple (Roche, Sigma-Aldrich) in a dark humidity chamber for at least 1 hour (up to a week in some cases). Once a noticeable signal was achieved, slides were washed with 1X PBS, three times for 5 mins each, then dehydrated, and mounted for imaging.

### **Immunohistochemistry**

IHC was performed on tissue sections as previously described (Eames et al., 2010), with modifications. Before starting the protocol, paraffin sections were deparaffinized and rehydrated in EtOH series to 70% EtOH, then kept in PBST (1X PBS/0.5% Triton X-100), whereas frozen sections were allowed to air dry for 10 min. Slides were post-fixed in 4% PFA at room temp for 20 mins (in slide mailers), then moved to a humidity chamber and rinsed twice in PBST for 5 mins

each, digested with 0.1% trypsin/1 mM EDTA/1X PBS for 15 mins (up to an hour) at 37 °C in a humidity chamber, rinsed twice in PBST for 5 mins each, digested with 0.5% hyaluronidase/PBST for 15 mins (up to an hour), rinsed twice in PBST for 5 mins each, blocked with blocking solution (4% goat serum/2% sheep serum/PBST) for 1 hour, and then incubated overnight in the cold room with a 1:100 dilution of mouse anti-COL II, monoclonal antibody II-II6B3 (DSHB) diluted with blocking solution. The next day, slides were rinsed three times with PBST for 2 mins each, incubated in the dark with a 1:1000 dilution of a fluorescent-labeled goat anti-mouse secondary antibody in blocking solution for at least 2 hours at room temp, rinsed three times with PBST for 2 mins each, stained with 300 nM DAPI/PBST for 15 mins, rinsed twice with PBST for 5 mins each, and then mounted for fluorescent microscopy imaging.

#### **Laser capture microdissection coupled with RNA sequencing**

For LCM-RNAseq, 10-16 µm cryosections were collected from freshly sacrificed, unfixed NF57 tadpoles on MMI membrane slides (#50102; MMI Molecular Machines & Industries), in RNase-free conditions, then stored at -80 °C until transport (on dry ice) to the MS Cameco Neuroscience lab on 5<sup>th</sup> floor at Saskatoon City Hospital for laser capture. Single slides containing sections of the medial angulosplenic were removed from -80 °C, then washed with 70% EtOH/0.1% DEPC for 1 min to fix the tissues, 1 min in cold 0.1% DEPC water to remove residual OCT, and dehydrated in EtOH/0.1% DEPC series (70%, 95%, 100%, 100%) for 1 min each to arrest the activity of RNases (Grover et al., 2012). Slides were shaken to dry then immediately mounted on an Olympus laser microdissection microscope (Molecular Machines & Industries CellCut system) for cell capture and care was taken to complete the task in 30 mins or less to minimize RNA degradation. Cells were captured into a MMI IsolationCap microtube (#50204; MMI Molecular Machines & Industries) before adding 50 µl of extraction buffer (Arcturus PicoPure RNA Isolation Kit) and transported on dry ice back to -80 °C storage at our lab. This was repeated for immature and mature cartilage from the humerus and all skeletal cell types were collected in triplicate. Captured areas were recorded for each sample (Table 4.1).

**Table 4.1| Captured areas from skeletal tissues of stage NF57 tadpoles.**

<i>Skeletal element</i>	<i>Cell type</i>	<i>Surface area captured (<math>\mu\text{m}^2</math>)</i>
<i>Medial angulosplenial</i>	OST 1	232183
<i>Medial angulosplenial</i>	OST 2	70451
<i>Medial angulosplenial</i>	OST 3	47422
<i>Humerus</i>	IMM 1	449442
<i>Humerus</i>	IMM 2	271954
<i>Humerus</i>	IMM 3	214610
<i>Humerus</i>	MAT 1	229000
<i>Humerus</i>	MAT 2	213630
<i>Humerus</i>	MAT 3	162322

Following laser capture, RNA was extracted with an Arcturus PicoPure RNA Isolation Kit (Cat #KIT0204; ThermoFisher) according to the protocol provided by the manufacturer. RNA was isolated from osteoblasts (n = 3), immature chondrocytes (n = 3), and mature chondrocytes (n = 3), and each sample was amplified twice using a MessageAmp II aRNA Kit (#AM1751; ThermoFisher). Amplified samples were brought to NRC (National Research Council) here on campus to evaluate RNA quality and concentration via a bioanalyzer, and samples meeting the minimum requirements according to an electropherogram summary were left with NRC to construct library preps and perform RNA sequencing. Raw RNA-seq data was downloaded from <https://lims.bioinfo.nrc.ca>.

#### **4.3.7 Preliminary RNA-seq analyses**

Dr. Katie Ovens normalized the raw RNA-seq data for frog, assigned gene IDs based on sequence alignments to online repositories (e.g., Ensembl), and determined threshold levels for gene counts to be considered biologically relevant for downstream analyses. Similar datasets in mouse, chick, and gar were also prepared in the same fashion thanks to previous work done collectively by Drs. Gómez Picos, Ashique, and Ovens. From these data, a list of candidate genes was generated (i.e., prominent chondrogenic, hypertrophic, and osteogenic markers according to classical definitions; Eames et al., 2003; Cole, 2011; Gómez-Picos & Eames, 2015) for a comparison across all four species. A manuscript in preparation by Drs. Gómez Picos, Ovens, Ashique, et al., analyzing mouse RNA-seq data, was also consulted to identify other early chondrogenic markers. Only one-to-one orthologs present in mouse, chick, gar, and frog were selected for comparative analysis.

### **Testing for significance of normalized gene counts using one-way ANOVA**

Normalized counts in frog were analyzed to see if RNA-seq would quantitatively support expression data from RNA *in situ* hybridization. Comparing candidate genes between IMM, MAT, and OST served as internal controls since each gene was expected to be higher in one cell type than the other two. A one-way ANOVA was also performed using IBM SPSS Statistics (Build 1.0.0.1447) to add statistical significance to any notable differences observed between the cell types, where specific differences (i.e., significant P-values) were identified via post-hoc analysis. Alpha levels were set at  $\alpha = 0.05$ .

### **Chondrogenic ratios from normalized counts**

A simple mathematical formula was employed to get a sense of chondrogenic expression levels among osteoblasts. This involved expressing average normalized counts of candidate cartilage genes as ratios and comparing these across species to see which animal had the most relative expression for each gene in their osteoblasts. For example, the average normalized counts for a chondrocyte gene (e.g., *acan*) in osteoblasts was divided by its average count in immature chondrocytes (OST:IMM), then mature chondrocytes (OST:MAT), and finally both (OST:IMM+MAT). From there, a heat map was created where chondrocyte genes were compared across all four species to see which osteoblast was 'most chondrogenic,' according to this metric. A deeper blue color was assigned to a species that had a higher ratio of a particular chondrocyte gene in its osteoblasts (e.g., less difference in normalized counts of *acan* between chondrocytes and osteoblasts), and darker reds denoted it had a lower ratio (e.g., greater difference due to lower *acan* counts in osteoblasts). The same color scheme was applied to each gene individually to gauge its relative level of expression in osteoblasts for each vertebrate model to see what kind of associations would emerge.

## **4.4 Results**

### **4.4.1 Perichondral bone from the humerus and dermal bone of the lower jaw were identified and characterized through dissected whole-mount and section histology**

The Nieuwkoop and Faber staging system describes the NF57 forelimb as being unerupted and having extensive perichondral ossification, whereas NF58 is characterized by an erupted forelimb that has undergone vascular invasion (Nieuwkoop & Faber, 1994). Gross observations of these

external events were possible thanks to some previous work done in the Eames lab by Yiwen Liu (Fig. 4.1), and were supplemented further with whole-mount histology (Fig. 4.2). Extraction of the forelimb from stages NF55-58 allowed for whole-mount visualization of the humerus undergoing endochondral ossification (Fig. 4.2C-F), where progressive ossification was evident according to increasing Alizarin red staining intensity. Histological sections of stages NF57 and NF58 stained with Safranin O and trichrome agreed with their Nieuwkoop and Faber descriptions. At stage NF57, the locations of immature cartilage in the epiphyses and mature cartilage in the diaphysis were confirmed (Fig. 4.3A), and extensive perichondral bone formation could be seen based on the position of osteoblasts (Fig. 4.3B). Vascular invasion was clearly visible at NF58 and demonstrated that this stage was not suitable for investigation since it introduced contaminating cells that would have affected the regions of interest (Fig. 4.3C,D). Downstream analyses and experiments were therefore focused on stage NF57, which presented uncontaminated perichondral bone for expression assays and uncontaminated mature and immature cartilage for laser capture.

According to independent comparisons of postembryonic *Xenopus laevis* skeletal development, the medial angulosplenic ossifies sometime around stages NF55-56 (Trümpy & Bernasconi, 1951; Sedra & Michael, 1957; Brown, 1980; Trueb & Hanken, 1992). This timeframe, in combination with some early larval stages (prior to ossification) previously assayed by Yiwen Liu, was used as a guide to narrow down when the medial angulosplenic might begin to develop in *Xenopus tropicalis*. A developmental series was generated surrounding the suspected stages of ossification with trichrome staining and revealed the lower jaw began to ossify between NF51-52 (Fig. 4.4). The minor amount of bone present at these stages and shortly after would likely not have been adequate for LCM-RNAseq based on surface areas captured from previous datasets. Since medial angulosplenic development would be more substantial by NF57, dermal osteoblasts from the lower jawbone were analyzed at the same stage as perichondral osteoblasts from the humerus.

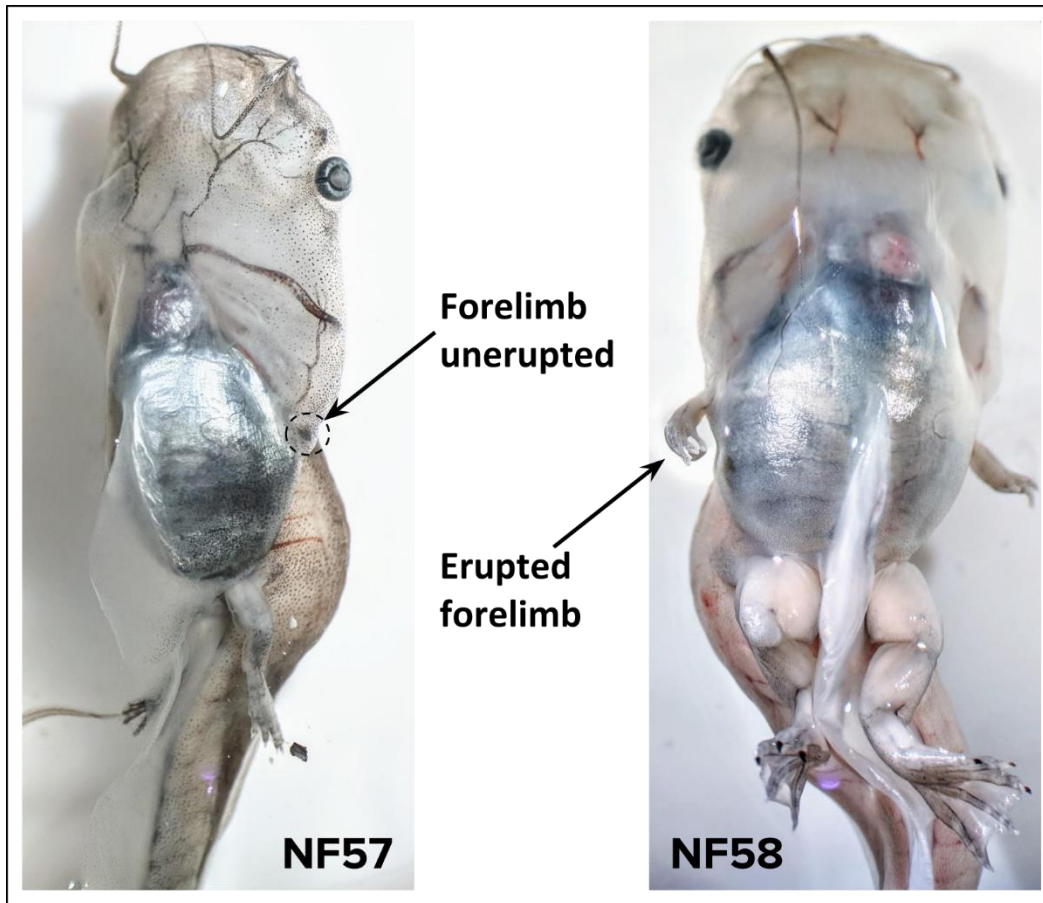


**Figure 4.1 | Forelimb eruption occurs at stage NF58.** According to the Nieuwkoop and Faber staging system, forelimb eruption corresponds with vascular invasion. (Credit: samples were raised by Yiwen Liu).

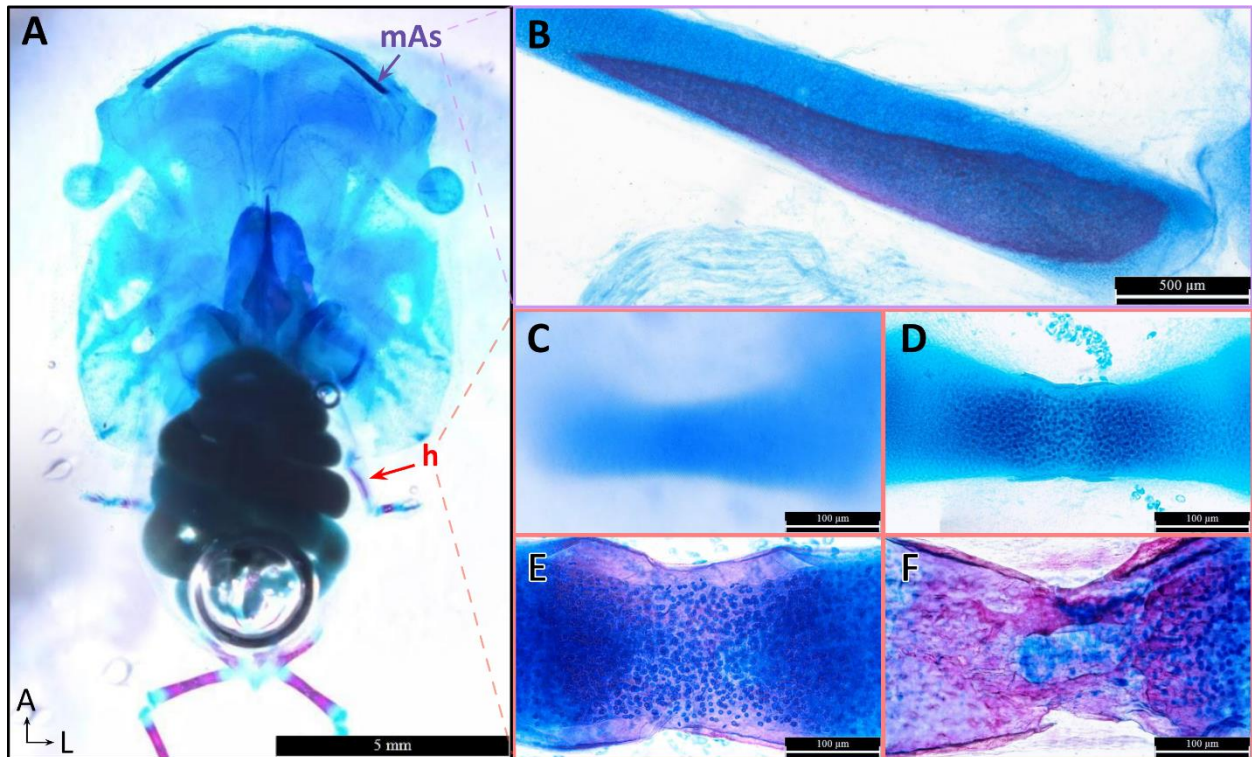


**Figure 4.2 | Whole-mount Alcian blue/Alizarin red staining shows ossification in the humerus and lower jaw.** [A] Skeletal prep of a stage NF58 tadpole revealing gross anatomical positions of the humerus and medial angulosplenic. [B] Meckel's cartilage dissected from stage NF58 showing that the medial angulosplenic has ossified extensively through Alizarin red staining. [C-F] Dissected forelimbs show the progression of endochondral ossification at the mid-diaphysis of the humerus from stages [C] NF55 (cartilaginous), [D] NF56 (early perichondral bone formation), [E] NF57 (extensive perichondral calcification), and [F] NF58 (erupted forelimb and vascular invasion). Abbreviations: h=humerus; mAs=medial angulosplenic. (Fig. 4.2C credit: Yiwen Liu).

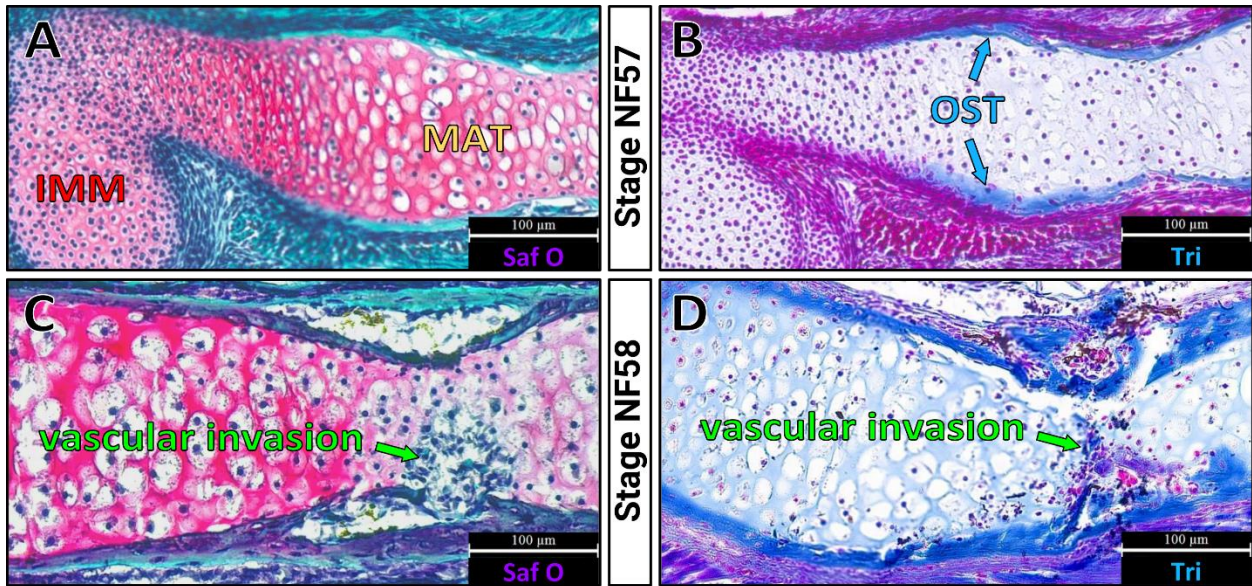


**Figure 4.3| Cartilage matures underneath perichondral bone before vascular invasion.** Longitudinal sections of the humerus stained with Safranin O and trichrome staining at stages (A,B) NF57 and (C,D) NF58. **[A]** Saf O shows immature chondrocytes in the epiphysis and hypertrophy of mature chondrocytes in the midsection of the diaphysis. **[B]** An adjacent NF57 section stained with trichrome indicating where the perichondral bone collar is located (Aniline blue color). **[C,D]** Vascular invasion occurs at stage NF58 and introduces red blood cells, chondroclasts, osteoblasts, and osteoclasts. Abbreviations: IMM=immature chondrocytes; MAT=mature chondrocytes; OST=osteoblasts; Saf O=Safranin O; Tri=trichrome.

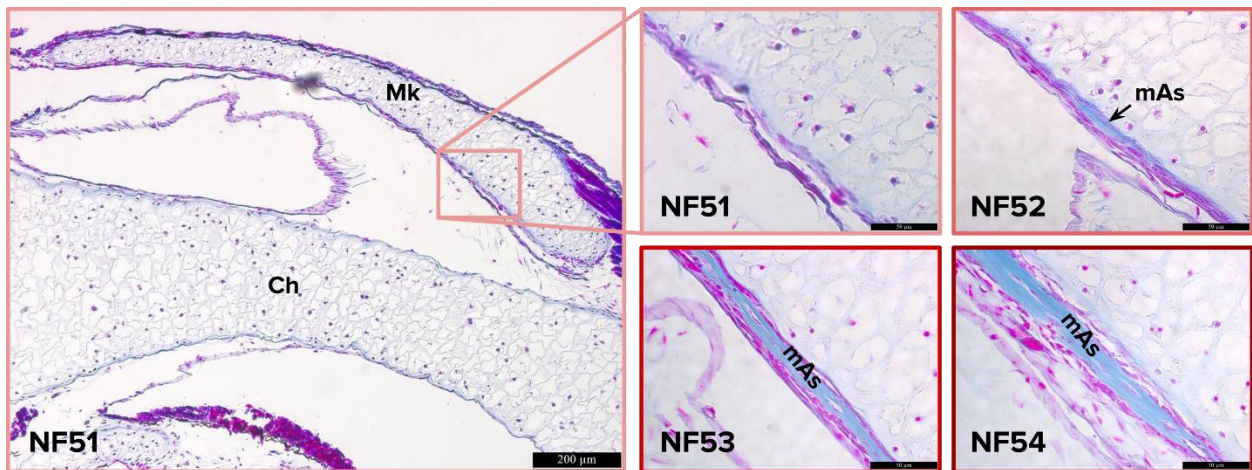


**Figure 4.4| A developmental series with trichrome pinpoints the exact moment of medial angulosplenic ossification.** The medial angulosplenic begins to develop around NF51-52 in *Xenopus tropicalis*, much earlier than *Xenopus laevis*. Abbreviations: Ch=ceratohyal; mAs=medial angulosplenic; Mk=Meckel's cartilage.

#### **4.4.2 The humerus has chondrogenic expression in layers inside and outside of perichondral bone**

A review of the current literature reveals that *sox9*, *col2a1*, and *col10a1* are expressed in osteoblasts of *X. tropicalis* (Aldea et al., 2013; Bertin et al., 2014; Enault et al., 2015). To search for these chondrogenic markers in perichondral bone of a stage NF57 humerus, expression assays were relied upon. RNA *in situ* hybridization was used for direct localization of mRNA transcripts and immunohistochemistry determined whether expression of any mRNA was functional, as well as provided an indirect means of transcript detection in case any had been translated into protein. Our data confirmed positive RNA ISH signals of *sox9* and *col2a1* in perichondral bone of frog, but not *col10a1*, and Col2 protein was not present anywhere in bone despite expression of *col2a1* (Fig. 4.5). This *col2a1*/Col2 discrepancy reinforced the notion that concordance rates between mRNA and protein expression can be notoriously undependable (Pascal et al., 2008).

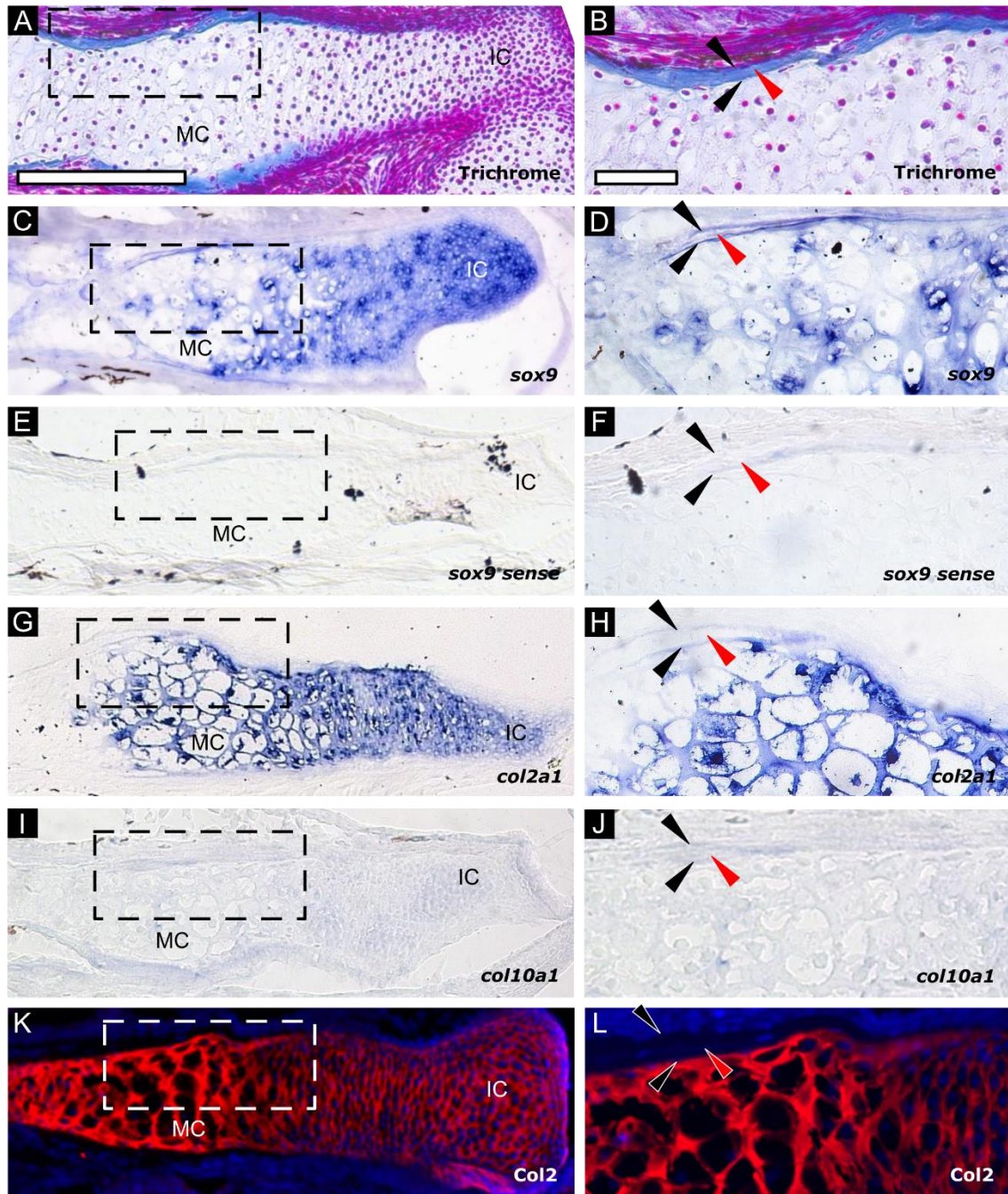


**Figure 4.5 | *sox9* and *col2a1* are expressed on the inner and outer layers of perichondral bone.** [A] Trichrome staining of a stage NF57 humerus distinguishes regions of immature cartilage (resting and proliferating chondrocytes), mature cartilage (hypertrophic chondrocytes), and perichondral bone (osteoblasts). [B] High magnification of the diaphysis focuses in on perichondral bone (blue), where *in situ* hybridization assays (C-H) reveal typical expression patterns of [C] *sox9* and [G] *col2a1* in cartilage. Higher magnification show [D] *sox9* and [H] *col2a1* are also found specifically in periosteum and perichondrium. [E, F] A *sox9* sense probe is absent from these distinct epithelial layers with some weak background staining in perichondral bone matrix. Likewise, [I, J] *col10a1* is negative throughout the entire humerus, save for non-specific binding in the perichondral region and weak background levels elsewhere. [K, L]

Fluorescent immunostaining of anti-Col2 merged with DAPI displays exclusive Col2 expression in cartilage, but none in bone. Black arrowheads point at internal and external layers of perichondral bone. Red arrowheads point at osteocytes or bone matrix. Scale bars: A, C, E, G, I, K=200µm; B, D, F, H, J, L=50µm. Abbreviations: IC=immature cartilage; MC=mature cartilage.

For reference, histological staining on longitudinal tissue sections of the humerus with trichrome denoted exactly where perichondral bone was located in Aniline blue (Fig. 4.5A,B). Other than in cartilage, the presence of *sox9* was confirmed in bone (Fig. 4.5C,D), but signals were isolated to the inner and outer regions of perichondral bone only (black arrowheads; Fig. 4.5D). The inner perichondrium and outer periosteum of perichondral bone originate from a common mesenchymal bilayer, the latter of which gives rise to osteoprogenitors (Egawa et al., 2014). This suggested the outer perichondral layer had a population of cells differentiating into osteoblasts that were expressing *sox9*, but osteocytes within bone matrix did not (red arrowheads point at bone matrix where osteocytes would be embedded; Fig. 4.5B,D,F,H,J,L). A negative *sox9* sense control confirmed the positive result for *sox9* was real (Fig. 4.5E,F). Similar expression was found for *col2a1*, although the signals in these layers were weaker (Fig. 4.5G,H). There was no indication of *col10a1* throughout the humerus aside from a false positive signal that was often observed in bone matrix (Fig. 4.5I,J). As an example, even the *sox9* sense probe showed false staining of bone matrix and nowhere else (Fig. 4.5E,F). This negative result for *col10a1* disagreed with the literature showing *col10a1* expression in perichondral osteoblasts of the femur (Aldea et al., 2013). To ensure that our *col10a1* anti-sense probe was not producing false negatives, its efficacy was tested on *X. tropicalis* teeth as a control. Teeth had recently been demonstrated as a positive site for *col10a1* (Debiais-Thibaud et al., 2019). A hydrolyzed *col10a1* anti-sense probe indeed produced a detectable signal in teeth at stage NF59 (Fig. 4.6), but neither a hydrolyzed nor a non-hydrolyzed *col10a1* probe showed up in the humerus, other than as a false positive or as non-specific background staining. Finally, immunohistochemical staining for Col2 protein found no evidence of its expression in bone matrix (Fig. 4.5K,L). In conclusion, there was chondrogenic expression of *sox9* and *col2a1* in perichondral bone of the frog humerus, but not *col10a1* or Col2 protein.

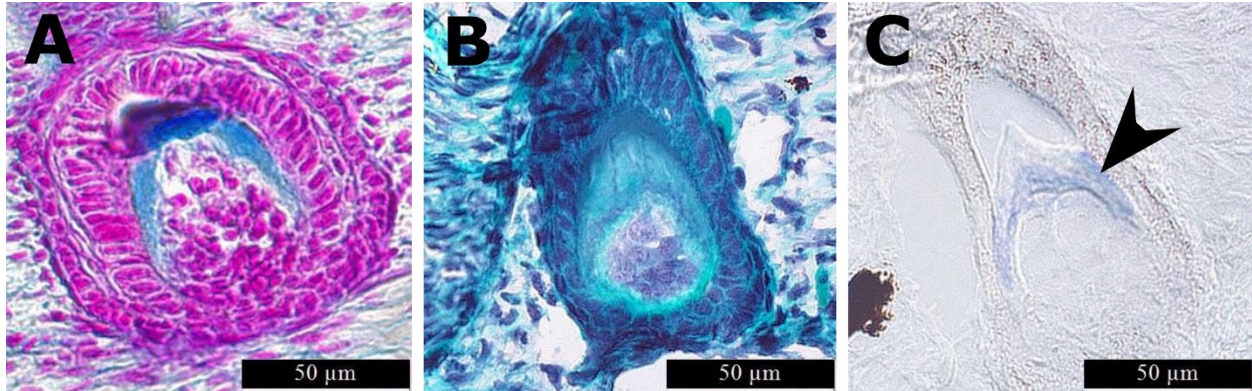


**Figure 4.6** | *col10a1* is expressed in maxillary teeth of a stage NF59 tadpole. **[A]** Trichrome and **[B]** Safranin O/Fast green reveal the morphology and staining patterns of a frog tooth in the upper jaw. **[C]** A black arrowhead indicates that *col10a1* expression appears to be specific to dentin, which has properties similar to osteoid found in bone (i.e., the organic component of bone matrix; Nanci, 2013).

#### 4.4.3 ISH and IHC show little to no chondrogenic expression in lower jaw osteoblasts

Again, trichrome revealed exactly the region of interest, this time from coronal sections of a dermal bone known as the medial angulosplenic (Fig. 4.7A,B). This skeletal element develops intramembranously along the posteromedial side of Meckel's cartilage. Unlike perichondral bone of the humerus, *in situs* of the medial angulosplenic showed no signs of *sox9* expression, which was restricted to staining of cartilage only (Fig. 4.7C,D). An identical negative result in bone was produced from a *sox9* sense probe (Fig. 4.7E,F). There appeared to be low to moderate expression of *col2a1* in dermal bone when compared to background levels and the darker staining of Meckel's cartilage (Fig. 4.7G,H). This signal was not as distinct as it was in perichondral bone and thus might not be real. Similar to the humerus though, the lower jaw exhibited no *col10a1* other than what appeared to be non-specific binding to bone matrix (Fig. 4.7I,J). Lastly, Col2 immunostaining revealed no protein was being expressed in dermal bone (Fig. 4.7K,L). Therefore, the lower jaw only showed low levels of *col2a1* (at best), but certainly no detectable expression of *sox9*, *col10a1*, or Col2.

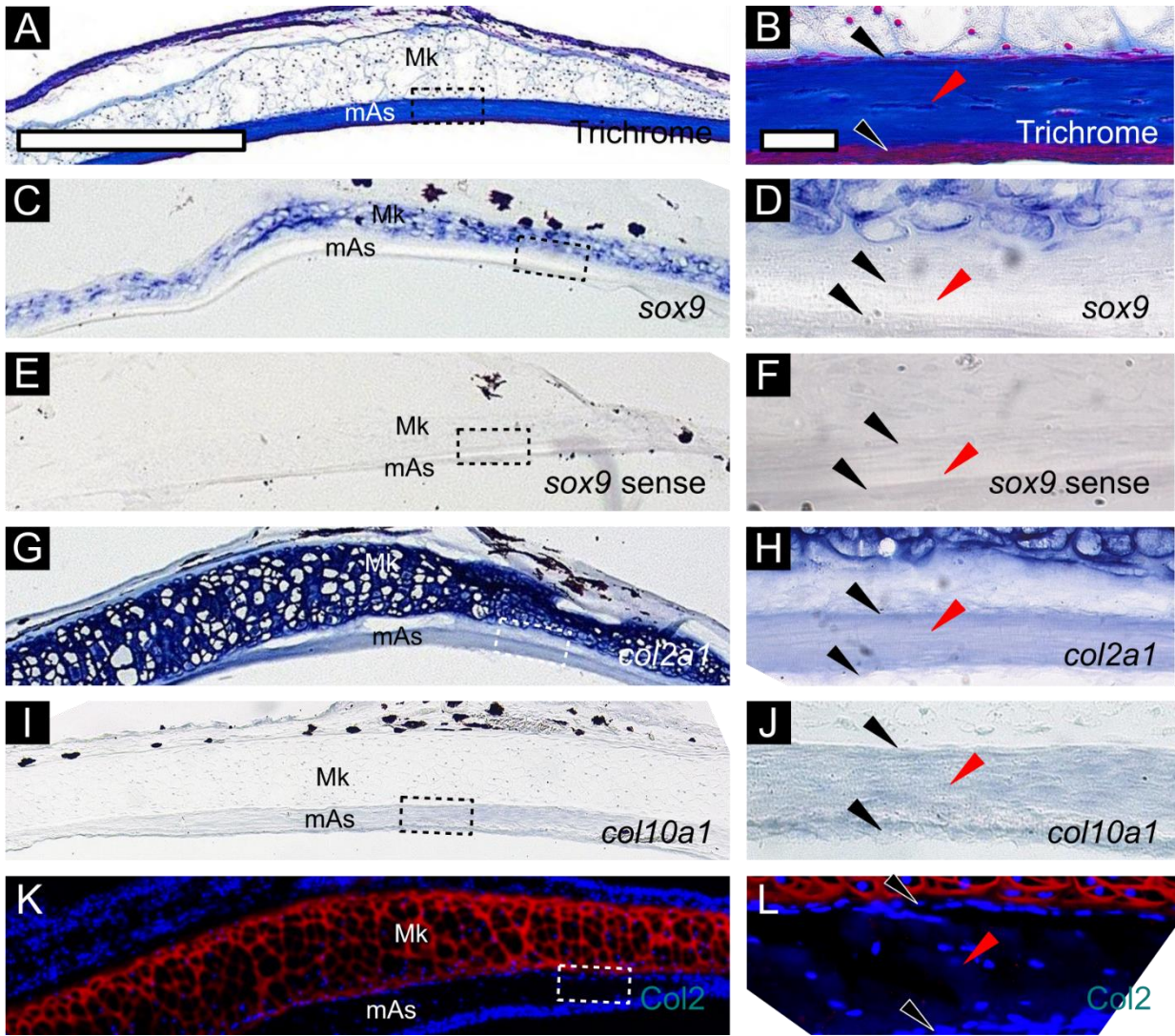


**Figure 4.7] Lower jaw osteoblasts of stage NF57 lack *sox9* expression, exhibit faint levels of *col2a1*, and have no Col2 protein expression. [A, B] Low and high magnifications of the developing lower jaw stained with trichrome show the medial angulosplenic dermal bone (blue) develops alongside Meckel's cartilage. (C-H) RNA *in situ* hybridization with [C, D] *sox9* and [E, F] *sox9* sense were completely negative in bone, but [G, H] *col2a1* exhibited weak expression in osteoblasts. [I, J] *col10a1* was negative throughout bone (signal is just background staining). [K, L] Merged images of anti-Col2 fluorescent immunostaining with DAPI showed Col2 was expressed in cartilage, but was absent in bone. Black arrowheads point at the epithelial layers on either side of the medial angulosplenic, where the bottom arrowhead is periosteum, and the top arrowhead may be periosteum and perichondrium. Red arrowheads point at osteocytes embedded within bone matrix or just bone matrix. Scale bars: A, C, E, G, I, K=500 $\mu$ m; B, D, F, H, J, L=50 $\mu$ m. Abbreviations: mAs=medial angulosplenic; Mk=Meckel's cartilage.**

#### 4.4.4 RNA-seq data confirmed chondrogenic expression in frog osteoblasts

LCM-RNAseq was performed on dermal osteoblasts of the medial angulosplenic as an independent measure of chondrogenic expression (Fig. 4.8). This method increased the level of sensitivity in detecting RNA transcripts that might not otherwise have appeared through standard expression assays. RNA-seq also allowed for a more quantitative assessment. Data normalization of raw counts and thresholds for each skeletal cell type (i.e., IMM, MAT, and OST) were determined by Dr. Katie Ovens (Table 4.2). Counts below threshold were put into parentheses to indicate expression levels that were considered to be background noise. Thresholds were: IMM = 12; MAT = 8; and OST = 8; where sample sizes for each were  $n = 3$ . While these thresholds appeared to be very low, it has been shown that low-count transcripts, particularly those of transcription factors, can still be biologically relevant (Raithel et al., 2016). As internal controls, average normalized counts of prominent skeletogenic genes were compared across IMM, MAT, and OST (Table 4.3). It was hypothesized that classic bone markers would be highest in OST of the medial angulosplenic, and likewise, traditional immature and mature cartilage genes would be upregulated in IMM and MAT captured from the humerus, respectively (Fig. 4.8). This was mostly true for MAT and OST, but not IMM.

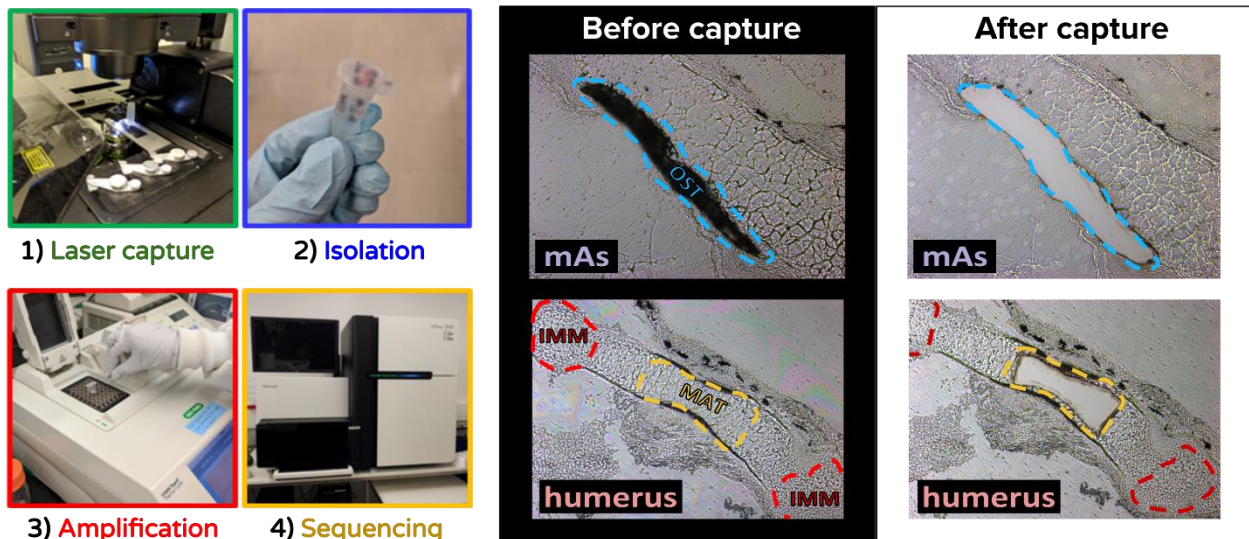


**Figure 4.8** | Skeletal cells were laser captured from the lower jaw and humerus for RNA-seq. Dashed lines indicate where OST were captured from the medial angulosplenic and IMM/MAT from the humerus (Note: the 'After capture' image for the humerus does not illustrate actual removal of IMM). RNA was

extracted from captured cells, put through two rounds of amplification, then submitted for Illumina sequencing.

**Table 4.2| Normalized counts of candidate skeletal genes in 3 different biological replicates for each skeletal cell type.** Typical immature cartilage genes are highlighted in red font, mature cartilage genes in yellow, and bone genes in blue. Counts below thresholds for IMM, MAT, and OST (12, 8, 8) are in parentheses and not considered biologically relevant. Abbreviations: IMM=immature chondrocytes; MAT=mature chondrocytes; OST=osteoblasts (Credit: data normalization and gene ID assignment by Dr. Katie Ovens).

Gene	<i>humerus</i>						<i>mAs</i>		
	IMM1	IMM2	IMM3	MAT1	MAT2	MAT3	OST1	OST2	OST3
<i>sox9</i>	1192	1331	953	1055	1330	1606	(0)	23	82
<i>col2a1</i>	38613	47240	34606	34077	148560	138671	1850	5363	8798
<i>acan</i>	8128	13835	6058	6020	24617	24908	1088	6973	1682
<i>sox5</i>	905	918	563	441	987	1357	(0)	155	82
<i>sox6</i>	386	409	121	123	325	221	14	299	72
<i>col9a1</i>	7972	10380	4592	7492	9376	2937	(4)	97	65
<i>col9a2</i>	120966	143017	171129	174276	278601	251745	5486	5180	3300
<i>col9a3</i>	(5)	(3)	(1)	(2)	(0)	(0)	10	15	32
<i>epyc</i>	24150	36120	29605	61703	13766	14169	1060	1266	419
<i>fmod</i>	(7)	(2)	(4)	(3)	(0)	(2)	316	520	162
<i>matn1</i>	(2)	(4)	(10)	10	(0)	10	133	30	(2)
<i>ihh</i>	(1)	23	(2)	(0)	3862	7501	(96)	568	(50)
<i>col10a1</i>	(8)	(1)	(0)	(0)	(0)	(0)	(3)	(1)	10
<i>runx2</i>	408	371	403	744	3251	3347	1056	3354	1530
<i>ibsp</i>	67	80	83	101	108	25	28	90	44
<i>sparc</i>	669	479	422	389	4736	6298	61687	73637	119277
<i>col1a1</i>	3026	1896	1350	1558	21627	27671	581043	1085835	846056
<i>col1a2</i>	231	434	499	407	2357	1906	25840	48308	125924
<i>bglap</i>	(0)	(0)	(0)	(0)	(0)	(0)	(0)	(0)	(0)

Unsurprisingly, average normalized counts of typical bone markers like *sparc* (secreted protein acidic and rich in cysteine, formerly *Osteonectin*), *col1a1*, and *col1a2* were highest in osteoblasts, displaying values of 84867, 837645, and 66691, respectively (Table 4.3); although only *sparc* and *col1a1* were statistically significant according to a preliminary one-way ANOVA, and *bglap* was not expressed at all. These reads served to somewhat alleviate any concerns regarding cross-contamination of the RNA-seq osteoblast data with other cell types since counts of these

osteogenic markers were much higher in bone than cartilage. Average counts of some well-known cartilage maturation markers, such as *ihh*, *runx2*, and *ibsp* (3788, 2447, and 78) appeared highest in MAT, but not significantly. *col10a1* was negligible across IMM, MAT, and OST (3, 0, and 5). Some unusual counts involved many important markers of immature cartilage, which were unexpectedly high in MAT (see Chapter 5 for a more thorough comparison and discussion of this result for cartilage), but given these genes were still more highly expressed in cartilage than bone, these could have simply been variations among IMM and MAT. Overall, a quick survey of the normalized counts showed low but non-negligible levels of major chondrogenic markers in OST, many of which were not significantly lower than their corresponding numbers in IMM. In fact, only *sox9*, *col9a1*, and *col9a2* were more significantly expressed in IMM (1159, 7648, 145037) than OST (35, 55, 4655). Instead, there were greater differences when comparing OST to MAT, where *sox9*, *col2a1*, *sox5*, *col9a1*, and *col9a2* were significantly higher in MAT (1330, 107103, 928, 6602, and 234874) than OST (35, 5337, 79, 55, and 4655). Conversely, there was one chondrogenic marker, *fmod*, that had significantly higher counts in OST (333) than IMM (4) and MAT (2). Another early immature cartilage marker, *col9a3*, was significantly higher in OST (19) than MAT (1). To gauge these levels of chondrogenic gene expression in osteoblasts, a preliminary analysis was conducted to see how these counts fared against other vertebrate models.

**Table 4.3| Average normalized counts of candidate skeletal genes in frog skeletal cells.** Counts bolded in blue observe for statistical significance of average normalized counts in OST only, compared to IMM and MAT, and was calculated by a one-way ANOVA. Asterisks indicate significance at \*p < 0.05, \*\*p < 0.01, and \*\*\*p < 0.001. Counts below threshold are in parentheses. Abbreviations: IMM=immature chondrocytes; MAT=mature chondrocytes; n = sample size; OST=osteoblasts. (Credit: data normalization and gene ID assignment by Dr. Katie Ovens).

<i>Gene</i>	<i>humerus</i>		<i>mAs</i>	
	<b>IMM</b> n = 3	<b>MAT</b> n = 3	<b>OST</b> n = 3	<b>OST</b> n = 3
<i>sox9</i>	1,159	*** 1330	***	<b>35</b>
<i>col2a1</i>	40,153	107103	*	<b>5337</b>
<i>acan</i>	9,340	18515		<b>3248</b>
<i>sox5</i>	795	928	*	<b>79</b>
<i>sox6</i>	305	223		<b>128</b>
<i>col9a1</i>	7648	* 6602	*	<b>55</b>
<i>col9a2</i>	145037	** 234874	***	<b>4655</b>
<i>col9a3</i>	(3)	(1)	*	<b>19</b>
<i>epyc</i>	29958	29879		<b>915</b>
<i>fmod</i>	(4)	* (2)	*	<b>333</b>
<i>matn1</i>	(5)	(7)		<b>55</b>
<i>ihh</i>	(9)	3788		<b>238</b>
<i>col10a1</i>	(3)	(0)		<b>(5)</b>
<i>runx2</i>	394	2447		<b>1980</b>
<i>ibsp</i>	77	78		<b>54</b>
<i>sparc</i>	523	** 3808	**	<b>84867</b>
<i>col1a1</i>	2,091	*** 16952	***	<b>837645</b>
<i>col1a2</i>	388	1557		<b>66691</b>
<i>bglap</i>	(0)	(0)		<b>(0)</b>

#### 4.4.5 Preliminary RNA-seq analysis suggests frog osteoblasts are highly chondrogenic

Frog RNA-seq data was compared against homologous datasets previously obtained by Drs. Amir Ashique and Patsy Gómez Picos in mouse, chick, and gar. Raw data from each species were

normalized and assigned gene IDs by Dr. Katie Ovens in order for a preliminary comparison of some candidate chondrocyte genes. As an alternative to the more comprehensive method of comparing of osteoblast molecular fingerprints via bioinformatics (presented in Chapter 3), a limited statistical approach was implemented. Normalized counts were used to calculate ratios that determined the relative levels of chondrogenic expression in osteoblasts (Table 4.4). This provided a rough idea of what the chondrogenic profile of frog osteoblasts might look like versus other vertebrates and suggested it was the most chondrogenic.

**Table 4.4| Heat map comparing chondrogenic ratios of osteoblasts in mouse, chick, gar, and frog.** Genes highlighted in light red are immature cartilage markers and genes highlighted in yellow are mature cartilage markers, but are also expressed in bone. Abbreviations: I=immature chondrocytes; M=mature chondrocytes; O=osteoblasts. (Credits: mouse, chick, and gar data collected by Drs. Patsy Gómez Picos and Amir Ashique; data normalization and gene ID assignment by Dr. Katie Ovens).

O/I	GAR	FROG	CHICK	MOUSE	O/M	GAR	FROG	CHICK	MOUSE	O/I+M	GAR	FROG	CHICK	MOUSE
<i>sox9</i>	0.356154	0.030207	0.040409	0.048937	<i>sox9</i>	0.617333	0.026309	0.072433	0.090617	<i>sox9</i>	0.465587	0.028124	0.053566	0.063552
<i>col2a1</i>	0.024011	0.132917	0.022838	0.053526	<i>col2a1</i>	0.043818	0.049831	0.042591	0.06572	<i>col2a1</i>	0.032063	0.072486	0.030765	0.059
<i>acan</i>	0.003114	0.347704	0.051402	0.001141	<i>acan</i>	0.005191	0.175407	0.066188	0.001215	<i>acan</i>	0.004004	0.233181	0.058685	0.001177
<i>sox5</i>	0.009501	0.099329	0.018019	0.020585	<i>sox5</i>	0.01557	0.085099	0.044422	0.090659	<i>sox5</i>	0.012127	0.091665	0.026902	0.033552
<i>sox6</i>	0.036989	0.420306	0.121732	0.281072	<i>sox6</i>	0.042747	0.575486	0.385106	0.712878	<i>sox6</i>	0.039981	0.485804	0.196324	0.40318
<i>col9a1</i>	0	0.007235	0.01283	0.002246	<i>col9a1</i>	0	0.008382	0.014128	0.001951	<i>col9a1</i>	0	0.007766	0.01352	0.002088
<i>col9a2</i>	0.000119	0.032097	0.003448	0.003205	<i>col9a2</i>	0.0005	0.019821	0.006719	0.005203	<i>col9a2</i>	0.000207	0.024507	0.004727	0.003966
<i>col9a3</i>	0.004325	6.333333	0.002979	0.001201	<i>col9a3</i>	0.012631	28.5	0.004143	0.001804	<i>col9a3</i>	0.006815	10.36364	0.00353	0.001442
<i>epyc</i>	0.004583	0.030542	0.005218	0.001201	<i>epyc</i>	0.007474	0.030623	0.010845	0.000512	<i>epyc</i>	0.005837	0.030583	0.007331	0.000718
<i>fmod</i>	0.001628	76.76923	0.738047	0.006465	<i>fmod</i>	0.026936	199.6	1.505495	0.29638	<i>fmod</i>	0.003406	110.8889	1.029645	0.012655
<i>matn1</i>	0.001286	10.3125	0.00329	0.00084	<i>matn1</i>	0.002124	8.25	0.001955	0.001065	<i>matn1</i>	0.001647	9.166667	0.002385	0.00094
<i>col10a1</i>	324.8771	1.555556	17.6	3.041667	<i>col10a1</i>	0.599836	---	0.004565	0.0008	<i>col10a1</i>	1.078113	3.111111	0.008215	0.001599
<i>runx2</i>	3.18902	5.025381	0.981675	15.46386	<i>runx2</i>	1.246475	0.809044	0.59989	1.961538	<i>runx2</i>	1.709201	1.393712	0.725249	3.481465
<i>ihh</i>	0.069314	27.46154	1.6	7.05	<i>ihh</i>	0.007009	0.062836	0.088496	0.020665	<i>ihh</i>	0.011673	0.125384	0.152542	0.04121



According to the heat map generated from chondrogenic ratios (Table 4.4), frog osteoblasts appeared to have the highest percentage of cartilage genes. This was very consistent regardless of whether the ratios were specifically comparing the level of cartilage gene expression in osteoblasts against their levels in immature chondrocytes, mature chondrocytes, or both. A deeper blue color meant higher counts of a candidate cartilage gene were present in osteoblasts relative to chondrocytes, and a deeper red meant less. For instance, *acan*, *col9a2*, *col9a3*, *epyc*, *fmod*, and *matn1* were more highly expressed in frog bone regardless of how the comparison was made. If ratios were restricted to chondrogenic expression in osteoblasts relative to immature chondrocytes—which would arguably be the most relevant comparison to be made since mature cartilage and bone have a strong overlap in gene expression (Vortkamp et al., 1996;

Inada et al., 1999; Neuhold et al., 2001; Zaragoza et al., 2006; Abzhanov et al., 2007; Mak et al., 2008; Eames et al., 2012; Huycke et al., 2012; Nishimura et al., 2012; Weng & Su, 2013)—then *col2a1*, *sox5*, and *sox6* could also be added to that list. This would mean 9 of 11 prominent markers of immature cartilage were highest in frog osteoblasts. When comparing individual ratios of candidate cartilage genes across clades, it seems from a relative standpoint that frogs consistently had a higher level of chondrogenic gene expression in their osteoblasts than mouse, chick, and gar (i.e., frog had the bluest ratios).

#### **4.5 Discussion**

Results in *X. tropicalis* were mixed when attempting to address whether the amphibian osteoblast had a chondrogenic level that was intermediate to earlier- and later-diverged vertebrates. Our findings both supported and disputed certain claims from the literature on chondrogenic expression in amphibian bone, but this depended on the cartilage gene being analyzed, the skeletal element, and/or whether the bone was of perichondral or dermal origin. While it generally appears as though frog osteoblasts express classic chondrogenic markers like *sox9* and *col2a1*, preliminary RNA-seq analysis suggested the expression levels of *col2a1* and other chondrocyte genes could be much higher than what is typically found in land tetrapods (Eames et al., 2004; Eames & Helms, 2004; Long & Ornitz, 2013). In fact, overall chondrogenic expression in frog osteoblasts might be even higher than gar osteoblasts (Eames et al., 2012). Gar were previously assumed to be the most chondrogenic of all the models being studied (Nguyen & Eames, 2020).

Frog RNA *in situ* hybridization data will be discussed first and compared to the literature (incorporating RNA-seq where relevant), then finish with a preliminary comparative analysis of RNA-seq data. More work needs to be done due to the challenge of comparing results obtained from different methods and skeletal elements at various stages of development (and to different species), but thus far some revelations have started to take shape. Amphibian osteoblasts do not appear to have a chondrogenic level that is intermediate to earlier- and later-diverged vertebrates. Furthermore, a possible consequence of this investigation might be the inadvertent discovery that perichondral bone has stronger chondrogenic expression than dermal bone.

#### **4.5.1 Chondrogenic expression was specific to layers outside perichondral bone matrix**

Starting with *sox9* and *col2a1*, the *in situ* signals obtained for these genes in the outer layer of perichondral bone of an NF57 humerus (Fig. 4.5D,H) were anatomically identical to a continuous layer of osteoblasts found in advanced stages of an NF58 or NF60 femur showing expression of *col10a1*, and other typical osteogenic markers, like *spp1*, *col1a1*, *col1a2*, and *sparc* (Espinoza et al., 2010; Aldea et al., 2013; Enault et al., 2015). This outer layer would have been homologous to any mouse or chick limb data as well, but unlike fish and frog (Eames et al., 2012; Bertin et al., 2014; Enault et al., 2015), mouse/chick osteoblasts typically do not express *Sox9/SOX9* and *Col2a1/COL2A1* (Nakashima et al., 2002; Eames & Helms, 2004; Yoshida et al., 2004). Likewise, signals found in the inner perichondral layer (Fig. 4.5D,H) may have been osteoblasts, but since chondroprogenitors were also a possibility there (Aghajanian & Mohan, 2018), chondrogenic expression would have been less surprising if that were the case. Positive RNA ISH results for *sox9* in perichondral bone of the humerus (Fig. 4.5D) seemed to agree with published results from perichondral bone of the femur (Bertin et al., 2014). However, femoral *sox9* detection was produced by RT-PCR, which was a more sensitive technique, and those tissues were not free of chondrocyte contamination (Bertin et al., 2014).

#### **4.5.2 *sox9* in situ expression is more prominent in perichondral than dermal bone**

Observations from perichondral bone of the humerus were not obviously translatable to dermal bone of the lower jaw. Expression assays showed no expression of *sox9* (Fig. 4.7C,D), but RNA-seq was able to detect very low levels (Table 4.3). Published RT-PCR results from dermal bone of the calvaria, which was devoid of cartilage, showed a drastic drop in *sox9* compared to perichondral bone of the femur (Bertin et al., 2014). This low detection in the skull disagreed with our *sox9* *in situ* data from the medial angulosplenial (Fig. 4.7D), but somewhat re-aligned with the added sensitivity of RNA-seq (Table 4.3). The same paper also managed to produce a stronger *sox9* signal in cultured osteoblasts harvested from the frontoparietal (an intramembranous bone of the skull; Trueb & Hanken, 1992; Bertin et al., 2014), but this was not a fair comparison given the significant difference in experimental conditions.

The *sox9* femoral, calvarial, and primary osteoblast culture data referenced in this section (and the last) belong to the Marcellini lab at the University of Concepción in Chile (Bertin et al., 2014). They had also kindly provided us with unpublished data showing weak-to-moderate *sox9* RNA ISH signals in perichondral osteoblasts of a stage NF60 femur and NF58 of the ventral neural arch (Cervantes et al., in preparation). Their *in situ* results for the femur have been the most analogous data in agreement with ours in the humerus. Once peer-reviewed, our results will be published in collaboration with theirs (Figs. 4.5 and 4.7). For now, the evidence seems to suggest that perichondral osteoblasts in the frog have higher expression of *sox9* than dermal osteoblasts.

#### **4.5.3 *col2a1* might have reduced expression in dermal bone, too**

When comparing our *col2a1* data to similarly published results in the femur, calvaria, and primary osteoblasts from cell culture (Bertin et al., 2014), a moderate difference between perichondral and dermal expression of *col2a1* existed as well. There were some distinctions worth mentioning, however. In our data, *col2a1* was positive in the humerus (Fig. 4.5H), and possibly the lower jaw (Fig 13H), though appeared weak in either case. Signals in the medial angulosplenic were especially ambiguous and it could not be ascertained if chondrogenic expression was localized to the periosteal layer outside of dermal bone matrix (Fig. 4.7H). If background levels could be accounted for, a slightly darker expression layer of osteoblasts might have been resolved (like in the humerus). From the literature, older cultured dermal osteoblasts experienced a dramatic fall off in *col2a1* expression (Bertin et al., 2014). This further fueled the idea that dermal expression of chondrogenic genes might be weaker. Moreover, the *col2a1* signal in dermal bone of the lower jaw was difficult to distinguish due to moderate staining of the bone matrix (Fig. 4.7G,H). Regardless, the corresponding *col2a1* counts from RNA-seq of the medial angulosplenic seemed relatively high considering how nondescript the *in situ* signal was (Table 4.2). This could have been a technical issue with the RNA ISH protocol, but at least the differences in relation to RNA-seq were consistent for *col2a1* as they had been for *sox9* in dermal bone. Both genes seemed weaker in RNA ISH only to have more noticeable expression in RNA-seq. One way to reconcile these discrepancies would be to perform LCM-RNAseq on perichondral osteoblasts to see if the pattern persisted (i.e., counts of *sox9* and *col2a1* would be expected to be higher than in dermal osteoblasts). There was also some conflicting *col2a1* published data that had shown negative *in*

*situ* results from NF60 perichondral osteoblasts of the femur (Enault et al., 2015). Yet the same paper also managed to present positive *col2a1 in situ* data from stage NF57 perichondral osteoblasts of the vertebrae (Enault et al., 2015), a chondral bone in *X. tropicalis* (Slater et al., 2009). Despite both being limbs, perichondral data from the femur (*col2a1*-negative; Enault et al., 2015) contradicted ours from the humerus (*col2a1*-positive; Fig. 4.5H). The femur and humerus are long bones that undergo endochondral ossification, so presumably they should have exhibited similar traits. Considering how weak *col2a1* expression was already in the humerus, it could be the femur was simply weaker. Developmental timing might also have been a factor in this instance since the femur develops much earlier than the humerus (Nieuwkoop & Faber, 1994). As demonstrated by the loss of *col2a1* signal strength in older cultured osteoblasts (Bertin et al., 2014), timing can affect its level of expression. At the very least, it was quite clear there was no Col2 protein in frog bone, regardless of location or levels of *col2a1* expression (Figs. 4.5K,L and 4.7K,L). This result was similar to previous findings in chick, where *COL2A1* mRNA was expressed but COL2 protein was not (Abzhanov et al., 2007).

The discrepancies in *sox9* and *col2a1* expression between perichondral and dermal osteoblasts might be due to subtle differences in the ossification process itself, anatomical location, timing of development, or other technical issues like sensitivity of the experiment. For instance, osteoblast differentiation during perichondral ossification relies on signals from prehypertrophic chondrocytes (St-Jacques et al., 1999; Eames et al., 2003), whereas dermal osteoblasts that form intramembranously are cartilage-independent (Eames & Helms, 2004). Since *sox9* and *col2a1* are heavily associated with cartilage development, perhaps this dependence (i.e., on the immediate presence and transduction signals from nearby chondrocytes) was a differentiating factor somehow. The timing of development could have influenced results as well since ossification of the lower jaw occurred earlier at NF51-52 (Fig. 4.4), whereas the humerus ossified much later at NF55-56 (Fig. 4.2C,D). Given that each skeletal element developed at a different rate and were at different phases of development by NF57, this might have affected levels of *sox9* and possibly *col2a1* as well (Bertin et al., 2014; Enault et al., 2015). As a counterargument, however, osteoblasts are usually at different phases of development at any given time. Generally speaking,

sensitive techniques like RT-PCR and RNA-seq can detect very low levels of RNA transcripts that RNA ISH might not, which could impact the interpretation of positive versus negative results.

#### **4.5.4 Expression assay results were insufficient to draw any definitive conclusions**

RNA ISH assays of *sox9* and *col2a1* alone could not determine clearly whether chondrogenic expression in frog osteoblasts was intermediate to earlier-diverged fish and later-diverged mouse and chick. Perichondral bone expression of *sox9* and *col2a1* would appear to be more similar to earlier-diverged vertebrates (Eames et al., 2012), which does not support an alternative hypothesis that frog osteoblasts are more similar to other tetrapods. On the other hand, a lack of *sox9* and weak *col2a1* dermal bone expression would seem to be more similar to land tetrapods (Eames et al., 2004; Eames & Helms, 2004; Abzhanov et al., 2007; Long & Ornitz, 2013). Together, these conflicting perichondral and dermal data could potentially support that chondrogenic expression in frog osteoblasts is intermediate to earlier- and later-diverged vertebrates. Though ultimately, a comprehensive look at the RNA-seq data through comparative transcriptomics should provide a more definitive answer.

#### **4.5.5 The humerus and medial angulosplenial have little to no *col10a1* expression**

Comparison of *col10a1* expression in frog osteoblasts with published results was discordant, but technical issues and differences in the protocols used were likely significant contributors. From our RNA ISH data, *col10a1* was essentially absent from osteoblasts of the humerus and lower jaw (Figs. 4.5I,J and 4.7I,J), but present in published results from similar testing of the femur (Aldea et al., 2013). RT-PCR of cultured dermal osteoblasts, calvaria, and hindlimb also presented positive results, although signals seemed very low in the hindlimb and extremely low in calvarial osteoblasts compared to primary cultures (Bertin et al., 2014). This reaffirmed an earlier comment that culture conditions perhaps amplified chondrogenic signals and were not comparable to *in situ* data. Firstly, some support could still be derived from these published RT-PCR data. It was more sensitive—although still only semi-quantitative, at best—yet *col10a1* barely registered in calvaria and was still quite weak even in the hindlimb (Bertin et al., 2014). Secondly, this was another example of weaker dermal expression of a cartilage gene (i.e., *col10a1* was weaker in calvaria than hindlimb osteoblasts; Bertin et al., 2014). Thirdly, our negative

*col10a1 in situ* results from the humerus (Fig. 4.5I,J) were independently validated by the same result in the medial angulosplenic (Fig. 4.7I,J), then again from RNA-seq data (Table 4.2). And finally, it had been consistently demonstrated that cultured osteoblasts seemed to inflate the expression strength of chondrogenic genes (e.g., *sox9*, *col2a1*, and *col10a1*) when compared to their levels *in situ* (Bertin et al., 2014), so those findings may not be as relevant. Once again, it is up for debate whether anatomical location, developmental timing, or sensitivity of the protocols used might account for these differences, but it is telling that the two most sensitive protocols (i.e., RT-PCR and RNA-seq) agreed with our data more.

Opposing conclusions were drawn based on the presence or lack of *col10a1* expression in amphibian bone. It was pointed out that since *col10a1* expression was found in bone of actinopterygians but not mammals (Eames et al., 2012), amphibian osteoblasts must be more similar to that of earlier-diverged fishes (Aldea et al., 2013). According to our findings, bone in frog is more like that of other tetrapods in this respect since mouse/chick bone typically only have trace levels of *Col10a1/COL10A1* (Nakashima et al., 2002; Eames & Helms, 2004; Yoshida et al., 2004). However, if expression in osteoblasts of mouse and chick are above the negligible *col10a1* amounts found in frog, this would suggest the amphibian osteoblast does not have a chondrogenic profile intermediate to earlier- and later-diverged vertebrates. Then again, it must also be taken into consideration that *col10a1* is a marker of mature cartilage, which has more similarities to bone than to immature cartilage (Vortkamp et al., 1996; Inada et al., 1999; Neuhold et al., 2001; Zaragoza et al., 2006; Abzhanov et al., 2007; Mak et al., 2008; Eames et al., 2012; Huycke et al., 2012; Nishimura et al., 2012; Weng & Su, 2013). A preliminary look at the RNA-seq data between mouse, chick, frog, and gar will attempt to address chondrogenic expression levels.

#### **4.5.6 Amphibian osteoblasts might be more chondrogenic than mouse, chick, and gar**

An early examination of the RNA-seq data appeared to refute the hypothesis and suggested the frog osteoblast may be more chondrogenic than earlier- and later-diverged clades. Stronger conclusions can certainly be drawn once more thorough bioinformatic analyses are performed, but further collaborative work is needed in that area. According to a heat map generated of 14 cartilage candidate genes shared among all four species (Table 4.4), the ratios of their expression in osteoblasts relative to chondrocytes showed that frog was the most chondrogenic. This was

overwhelmingly true when restricting analysis to just immature cartilage markers (11 of the 14 genes), which further strengthened the case since many markers of mature cartilage (e.g., *col10a1*, *runx2*, and *ihh*) are often found in bone (Vortkamp et al., 1996; Inada et al., 1999; Neuhold et al., 2001; Zaragoza et al., 2006; Abzhanov et al., 2007; Mak et al., 2008; Eames et al., 2012; Huycke et al., 2012; Nishimura et al., 2012; Weng & Su, 2013). In that situation, at least 6 of 11 to as many as 9 of the 11 genes, were in favor of the frog being the most chondrogenic. This depended on whether chondrogenic expression levels in osteoblasts were being compared to expression levels in immature chondrocytes (arguably the most relevant), mature chondrocytes, or both.

The limited approach employed here seems inherently biased at first, but the list of candidate genes purposely highlighted some of the most important markers of cartilage (Eames et al., 2003; Cole, 2011; Gómez-Picos & Eames, 2015; Gómez-Picos et al., in preparation), so this was not an insignificant result. These genes generally define what a chondrocyte is, in terms of gene regulation and cellular makeup, at least in a classical sense. This list also contained the single most important driver of cartilage differentiation, *sox9*. Interestingly enough, *sox9* had the highest ratio in gar osteoblasts, relative to mouse, chick, and frog (Table 4.4).

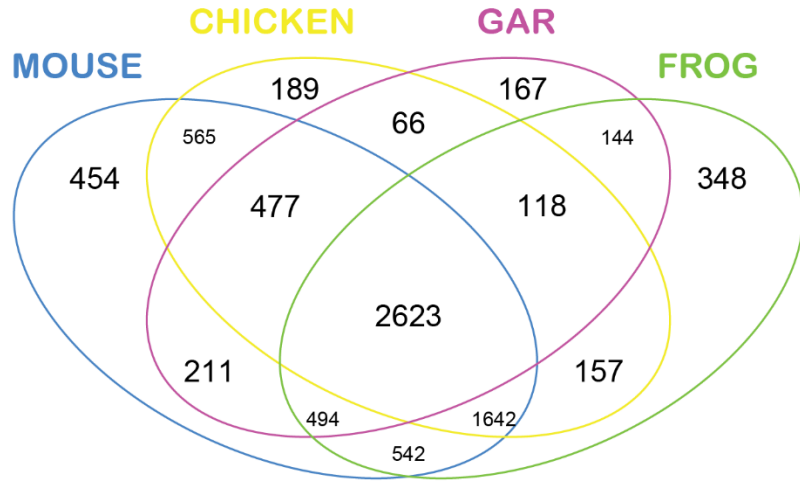
In reality, most of these ratios were very low amongst all groups with very few exceptions, but relatively speaking, frog was consistently highest. For instance, a previous assessment of *col2a1* expression in amphibian osteoblasts had been described as being “moderate” (Enault et al., 2015) and comparable to levels in mouse (Hilton et al., 2007) and chick (Abzhanov et al., 2007). If this was true, then levels of *col2a1* must be considered moderate across all vertebrates, including fish. This preliminary analysis offered support to the frog as being the most chondrogenic because it appeared to have the most high levels of chondrocyte genes being expressed in its osteoblasts. As a consequence, the current interpretation of this data does not support the hypothesis that frog osteoblasts have a level of chondrogenic expression intermediate to other clades. Any limitation due to gene selection bias, though, does emphasize the importance of the work being done by Drs. Patsy Gómez Picos and Katie Ovens in the Eames lab on skeletal GRNs (gene regulatory networks). The most comprehensive definition of what makes a chondrocyte, an osteoblast, or how similar an osteoblast is to a chondrocyte involves

not only all the genes being expressed, but how they regulate and interact with one another. It seems reasonable that GRNs should be the most convincing method to evaluate and support whichever vertebrate is most chondrogenic when it comes to comparing the osteoblast molecular fingerprints from each clade.

On a related note, Drs. Patsy Gómez Picos and Katie Ovens kindly supplied some differential gene expression data from osteoblasts incorporating frog with mouse, chick, and gar (Fig. 4.9). A gene was considered to be differentially expressed if the  $\log_2$  fold change was  $\pm 2$ . While this comparison was comprehensive and unbiased, as it contained all genes that were one-to-one orthologs in osteoblasts of all four species, it did not tell us which osteoblast was the most chondrogenic, or even how chondrogenic. To do this, the focus would still have to be on genes expressed in osteoblasts that were shared with chondrocytes, particularly those which defined the cartilage cell type, classical or otherwise. The resulting Venn diagram depicted the gene expression distribution of all genes expressed in osteoblasts above threshold that were shared across all four species (2623, or  $\sim 32\%$  of 8197 total genes; Fig. 4.9A). It was found that frog osteoblasts shared more genes with osteoblasts of land tetrapods (52% with mouse and chick), than with osteoblasts of an aquatic animal (41% with gar). This suggested that frog osteoblasts were more like other tetrapods in terms of all genes being expressed, not necessarily genes that characterized them as being osteoblasts or made them chondrogenic. While gene ontology analysis showed enriched biological processes that included osteoblast differentiation and bone mineralization, many housekeeping genes that occur in every cell were also enriched (Fig. 4.9B).

A

OST



B

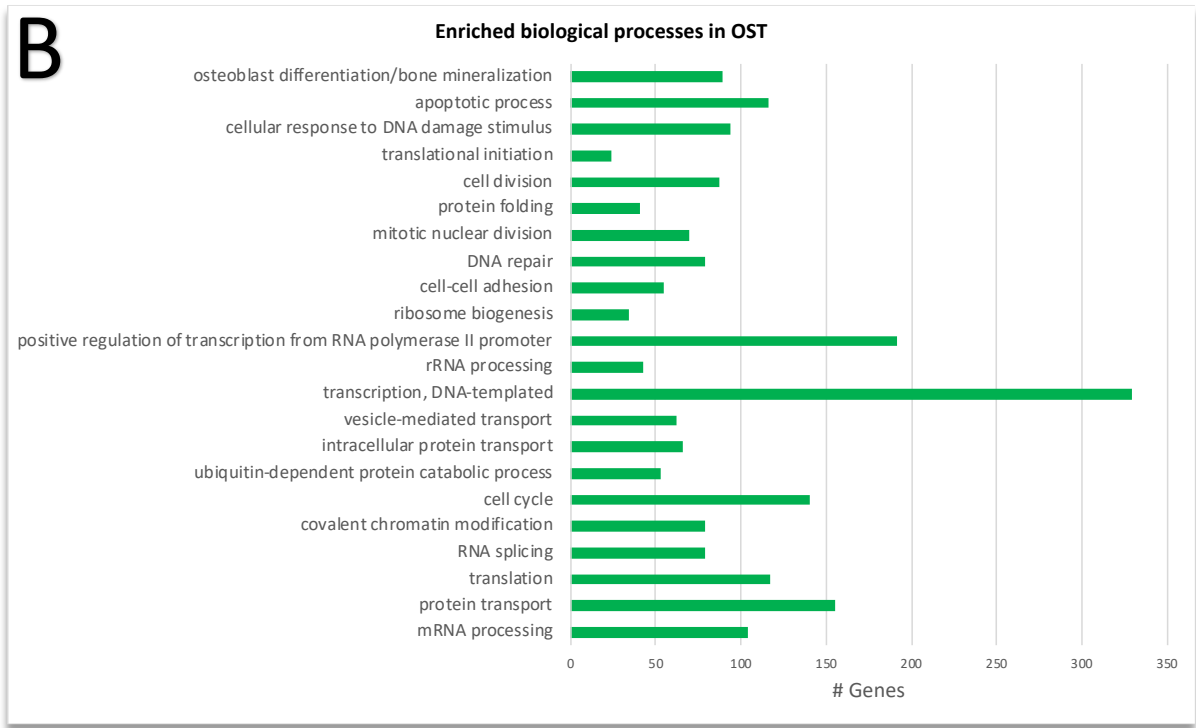


**Figure 4.9| Evolution of the osteoblast gene regulatory network. [A]** Venn diagram showing gene expression distribution among mouse, chick, gar, and frog. Total genes in OST among the four species expressed above threshold: 8197 genes. Genes shared between OST of the four species: 2623, or ~32% of total genes. Tetrapods (mouse, chick, and frog) share 4265 genes (2623 + 1642), or 52% of total genes. Land tetrapods (mouse and chick) share 5307 genes (2623 + 1642 + 565 + 477), or 65% of total genes.

Aquatic animals (frog and gar) share 3379 genes (2623 + 144 + 118 + 494), or 41% of total genes. **[B]** Gene ontology analyses of enriched biological processes. (Credit: Patsy Gómez Picos and Katie Ovens).

#### 4.5.7 Summary

In summary, the data presented here regarding chondrogenic expression in amphibian osteoblasts have mostly agreed with published results, though a notable disagreement had been whether or not *col10a1* was expressed. Previous data demonstrated that *col10a1* was present in bone of *X. tropicalis* (Aldea et al., 2013), whereas we did not. Our respective results came from different skeletal elements and stages of development so perhaps these were confounding factors. We did find support that amphibian osteoblasts appeared to be more chondrogenic than later-diverged vertebrates. Furthermore, preliminary analysis of candidate genes through RNA-seq suggested amphibians may be more chondrogenic than earlier-diverged vertebrates as well. This would be a novel finding if confirmed further through validation studies. Additionally, it may have been discovered that expression of *sox9* and *col2a1* are stronger in perichondral bone than dermal bone, which had not been stated explicitly before despite more examples supporting this than not from the literature. Based on the data available, the hypothesis that amphibian osteoblasts have a chondrogenic level intermediate to earlier- and later-diverged vertebrates was not supported. If this is the case, it would also suggest that chondrogenic expression during the evolution of the vertebrate osteoblast might have actually increased before being lost, and therefore, was not a gradually repressive event as previously hypothesized (Nguyen & Eames, 2020). There is still much work left to be done, specifically regarding bioinformatic analyses before stronger conclusions can be drawn. It is possible a gradual repressive trend might still be established once more thorough data are incorporated into this study.

## CHAPTER 5

### Characterizing hypertrophy of amphibian chondrocytes

*Nguyen, J. K. B., Gómez-Picos, P., Liu, Y., Ovens, K., and Eames, B. F.*

#### 5.1 Abstract

Hypertrophic chondrocytes are enlarged cartilage cells that are one of the more obvious morphological features of endochondral ossification (a process by which bone forms indirectly via a cartilage template). All common vertebrate lab models, including mouse, chick, and zebrafish, basically undergo the same histological and molecular progressions during hypertrophy. Examples of chondral bones are the humerus and ceratohyal. In frog, previous research had shown ossification of these skeletal elements was delayed or incomplete, though chondrocytes matured and became hypertrophic as usual. Therefore, we hypothesized that maturation of amphibian cartilages still followed the standard hypertrophic cascade. To test this, we analyzed histological and molecular markers of developing limb and head cartilages of the western clawed frog, *Xenopus tropicalis*. Indeed, the standard histological pattern occurred during development of the humerus, where chondrocytes gradually became hypertrophic prior to ossification. Consistent with the standard molecular cascade, the chondrogenic markers *col2a1* and *sox9* were downregulated in hypertrophic chondrocytes of the humerus. Interestingly, however, expression of the classical hypertrophic marker *col10a1* was not upregulated in these chondrocytes. Unexpectedly, some head cartilages, such as the ceratohyal, a skeletal element homologous to the hyoid bone of the larynx, underwent histological hypertrophy extremely rapidly (within mere hours of becoming chondrocytes). In addition, the ceratohyal halted at the hypertrophic stage and persisted as such throughout metamorphosis into adulthood, never ossifying. Meckel's cartilage and the palatoquadrate also displayed similar behavior. Unlike the humerus, hypertrophic chondrocytes in the head cartilages continued to express relatively high levels of *col2a1* and *sox9*, but similarly lacked *col10a1* expression. As such, these unusual discoveries present a unique opportunity to investigate the molecular mechanisms that might explain why frog cartilages deviate from the standard histological and molecular

hypertrophic cascade of other vertebrates. Such findings might shed light upon osteoarthritic cartilage, which often has ectopic hypertrophic differentiation.

## 5.2 Introduction: Cartilage development and the hypertrophic cascade

Cartilage cells can be categorized as either resting and proliferating (immature) chondrocytes, or prehypertrophic and hypertrophic (mature) chondrocytes. Both immature and mature chondrocytes can remain indefinitely as hyaline cartilage at the articular surfaces of joints (Gray & Williams, 1989; Leboy et al., 1988; Eames et al., 2003, 2004; Eames & Helms, 2004; Yang et al., 2014; Zhou et al., 2014; Hinton et al., 2017; Aghajanian & Mohan, 2018). However, many immature chondrocytes also become part of cartilage templates that mature to form chondral bone (Kronenberg, 2003; Mackie et al., 2008; Long & Ornitz, 2013). The hypertrophic enlargement of chondrocytes during maturation tends to be a progressive and gradual morphological event. Usually hypertrophy begins centrally within a cartilage model before spreading outwards over the course of several days and/or weeks as endochondral ossification transforms cartilage into bone (Pechak et al., 1986; Nieuwkoop & Faber, 1994; Marks et al., 2000; Miura et al., 2008; Eames et al., 2012; Kozhemyakina et al., 2015). Predictable changes also occur at the molecular level in terms of gene expression (Eames et al., 2003, 2004; Miura et al., 2008). Maturing chondrocytes that progress to hypertrophic differentiation typically show decreased levels of *Sox9* and *Col2a1* (Eames et al., 2003; Tchetina et al., 2014). Mature markers like *Ihh*, *Runx2*, and *Col10a1* instead start to increase (Eames et al., 2003; Tchetina et al., 2014). *Ihh* is recognized as a marker of prehypertrophic chondrocytes (St-Jacques et al., 1999; Karsenty & Wagner, 2002; Kronenberg, 2003; Long & Ornitz, 2013). *Runx2* is generally expressed throughout the entire maturation process and regulates the expression of many downstream targets (Eames et al., 2003; Zheng et al., 2003; Mackie et al., 2008; Li et al., 2011; Nishimura et al., 2012). This includes *Ihh* (Yoshida et al., 2004), *Col10a1* (Linsenmayer et al., 1991; Poole, 1991), and a late marker of mature cartilage, *Ibsp* (Komori, 2010). Incidentally, if *Sox9* levels remain high, *Runx2* is unable to guide chondrocytes through maturation and highlights the importance of this coordinated regulation (Eames et al., 2004; G. Zhou et al., 2006; Gómez-Picos & Eames, 2015). Together, these histological and molecular changes characterize the hypertrophic cascade (Eames et al., 2003, 2004; Mackie et al., 2008). Given that cartilage maturation is highly conserved among vertebrates (Eames et al., 2004, 2011, 2012; Eames & Helms, 2004), we were interested to see if the hypertrophic cascade was conserved in amphibian cartilages as well.

In *Xenopus tropicalis*, hypertrophy was analyzed within the limb (humerus) and head (ceratohyal). We hypothesize that maturing chondrocytes of the amphibian undergo the same histological and molecular progressions of the hypertrophic cascade common to all vertebrates. To test this, we characterized the development of cartilages from the limb and head of frog by using histology, RNA *in situ* hybridization, immunohistochemistry, and RNA sequencing, then compared these results within the frog and to other vertebrate models.

Our results suggested hypertrophy was mostly conserved in amphibian limb cartilage, but not molecularly or temporally conserved in the head. Compared to other vertebrates, mature cartilage in the amphibian maintained or upregulated many chondrogenic genes that would normally be more highly expressed in immature cartilage. The hypothesis was therefore only partially supported and makes the frog a very unique model for studying hypertrophy.

### **5.2.1 Amphibian cartilage maturation has some differences versus other vertebrates**

A general overview of cartilage development in the amphibian was important in order to pinpoint the pertinent stages for analysis of hypertrophy. The humerus and ceratohyal specifically probed cartilage maturation from the appendicular as well as the cranial skeleton. This gauged the consistency of development within an amphibian from anatomically and mechanically different sources of cartilage. These skeletal elements also allowed for a comparative study since homologous datasets were already available in other vertebrate models, from the literature and from previous work in our lab. Unpublished studies of limb cartilage had been done in mouse and chick, whereas head cartilage data came from chick and gar (previous work by Drs. Gómez Picos, Ashique, and Ovens). Expression assays and LCM-RNAseq had been performed on stages where skeletal elements were undergoing overt maturation (i.e., hypertrophy) during endochondral ossification, just prior to vascular invasion (Kronenberg, 2003; Mackie et al., 2008; Long & Ornitz, 2013). This was to ensure no cellular contaminants were introduced, while abundant amounts of immature and mature chondrocytes would be available for downstream analyses. To further remain consistent with previous data collection, comparable stages of development needed to be ascertained in the frog. This minimized the differences between models with fewer variables to account for when drawing conclusions.

A review of humerus development had determined that stage NF57 would be the ideal stage for analysis of hypertrophy. The Nieuwkoop and Faber staging system describes the forelimb as being cartilaginous at stage NF55 and having extensive perichondral ossification by NF57 (Nieuwkoop & Faber, 1994). Stage NF58 was noted for forelimb eruption and vascular invasion (Nieuwkoop & Faber, 1994). This meant NF58 was to be avoided and many chondrocytes of the diaphysis should have been maturing and hypertrophic at NF57. Specific details regarding the hypertrophic cascade in the humerus of *X. tropicalis* were limited from published results. Hindlimb data (e.g., femur, tibia, and fibula) indicated endochondral ossification was delayed, resulting in less trabecular bone and poor growth plates compared to other vertebrates, and sometimes even lacked secondary ossification sites (Moriishi et al., 2005; Miura et al., 2008). Typical early chondrogenic markers like *sox9* and *col2a1* were upregulated in immature cartilage and downregulated in mature cartilage (Miura et al., 2008; Enault et al., 2015). Hypertrophic chondrocytes of the femur had been shown not to express *col10a1* at all, which would differentiate the frog from other models (Aldea et al., 2013). While *ihh* was upregulated in prehypertrophic chondrocytes, these cells were noted as being slightly offset (i.e., more towards the epiphyses) from where they would usually be found in the growth plates of mice (Moriishi et al., 2005). An interesting observation related to this was that Hedgehog signaling did not result in expression of typical downstream targets like *ptch1* (protein patched homolog 1) and *gli1* (glioma-associated oncogene 1) in proliferating chondrocytes (St-Jacques et al., 1999; Moriishi et al., 2005; Hadden, 2014). Given that this pathway and the involvement of proliferating chondrocytes are critical for the differentiation of mesenchymal cells into osteoblasts (St-Jacques et al., 1999; Long et al., 2004), and the regulation of cartilage maturation (Vortkamp et al., 1996; Chen et al., 2008); Macica et al., 2011), this was speculated as a possible reason for the slight abnormalities observed in frogs pertaining to endochondral ossification (Moriishi et al., 2005). Lastly, expression of *runx2* was said to be weak in hypertrophic chondrocytes of the hindlimb compared to other animals (Miura et al., 2008).

The literature on amphibian head cartilage development was not overly extensive. Most papers focused on chondrogenesis and very little was published about hypertrophy or exactly when it occurred (Lukas & Olsson, 2017). A review of the ceratohyal—a structure homologous to the

hyoid, which is a chondral bone situated in the upper larynx of humans—revealed that it remained cartilaginous, hypertrophic, and did not ossify in *Xenopus laevis* (Thomson, 1986). Upon further review, it appears this phenotype is a common trait among anuran frogs that separates them from more ancient amphibians (Porter & Vial, 1974). In contrast, elements homologous to the ceratohyal in other animals would normally progress through the usual stages of cartilage maturation beyond hypertrophy to become chondral bone (Eames et al., 2004, 2011, 2012; Eames & Helms, 2004). Persistent hypertrophy of the ceratohyal and Meckel’s cartilage were demonstrated from light and electron microscopy of *Xenopus laevis*, which had focused on head cartilage development at stages just before, during, and after metamorphosis (i.e., from NF57 to NF66; Thomson, 1986). Similar observations had not yet been made in *Xenopus tropicalis*. Lineage tracing experiments confirmed that larval chondrocytes contributed to the post-metamorphic forms of both the ceratohyal (known as the hyale after metamorphosis; Rose, 2009) and Meckel’s cartilage (Kerney et al., 2012). RNA *in situ* hybridization assays revealed *sox9* and *col2a1* were upregulated in many NF57 head cartilages despite chondrocytes being hypertrophic (Kerney, Hall, et al., 2010); even by NF64, *col2a1* was still being expressed (Kerney, Hall, et al., 2010). The only notable change in morphology was a slight decrease in size experienced by hypertrophic chondrocytes at later stages (e.g., NF60 and beyond; Thomson, 1986). This was eventually attributed to increased cartilage ECM pushing against the lacunar spaces in which the cells resided (Thomson, 1986, 1987).

Considering how sparse the literature was on characterizing amphibian cartilage maturation, some atypical results had already begun to stand out. This was especially true of head cartilage, which displayed persistent hypertrophic features that were atypical of homologous elements found in other vertebrate models (Porter & Vial, 1974; Thomson, 1986). Instead of ossifying, the ceratohyal remained cartilaginous (Rose, 2009). These observations and insufficient published resources describing the precise timing of amphibian cartilage hypertrophy warranted further investigation. We discovered hypertrophy in the head occurred very rapidly, shortly after cartilage differentiation, and did so globally, rather than progressively like in the limb. Both maturing head and limb cartilages were revealed to lack a prominent hypertrophic marker in *col10a1*. And finally, early chondrogenic markers of cartilage (e.g., *sox9* and *col2a1*) were found

to either persist (in head cartilage) or have prolonged expression (in limb cartilage) during hypertrophy.

### 5.2.2 Higher precision ZO staging was used to track head cartilage development

A finer ZO staging system was utilized to interrogate cartilage development of the ceratohyal in *Xenopus tropicalis* (Ziermann & Olsson, 2007). This alternative system was especially relevant given its focus on the condensation to cartilage differentiation stages (Lukas & Olsson, 2017). ZO staging also claimed higher accuracy at time points that were specifically targeted for study (i.e., the early larval stages, or around when chondrogenesis began in the head). These stages corresponded traditionally to NF32-46, but were further subdivided into 20 ZO stages (Fig. 5.1; Ziermann & Olsson, 2007). ZO staging detailed more internal and external landmarks, allowing for an increase in the precision and timing of development.

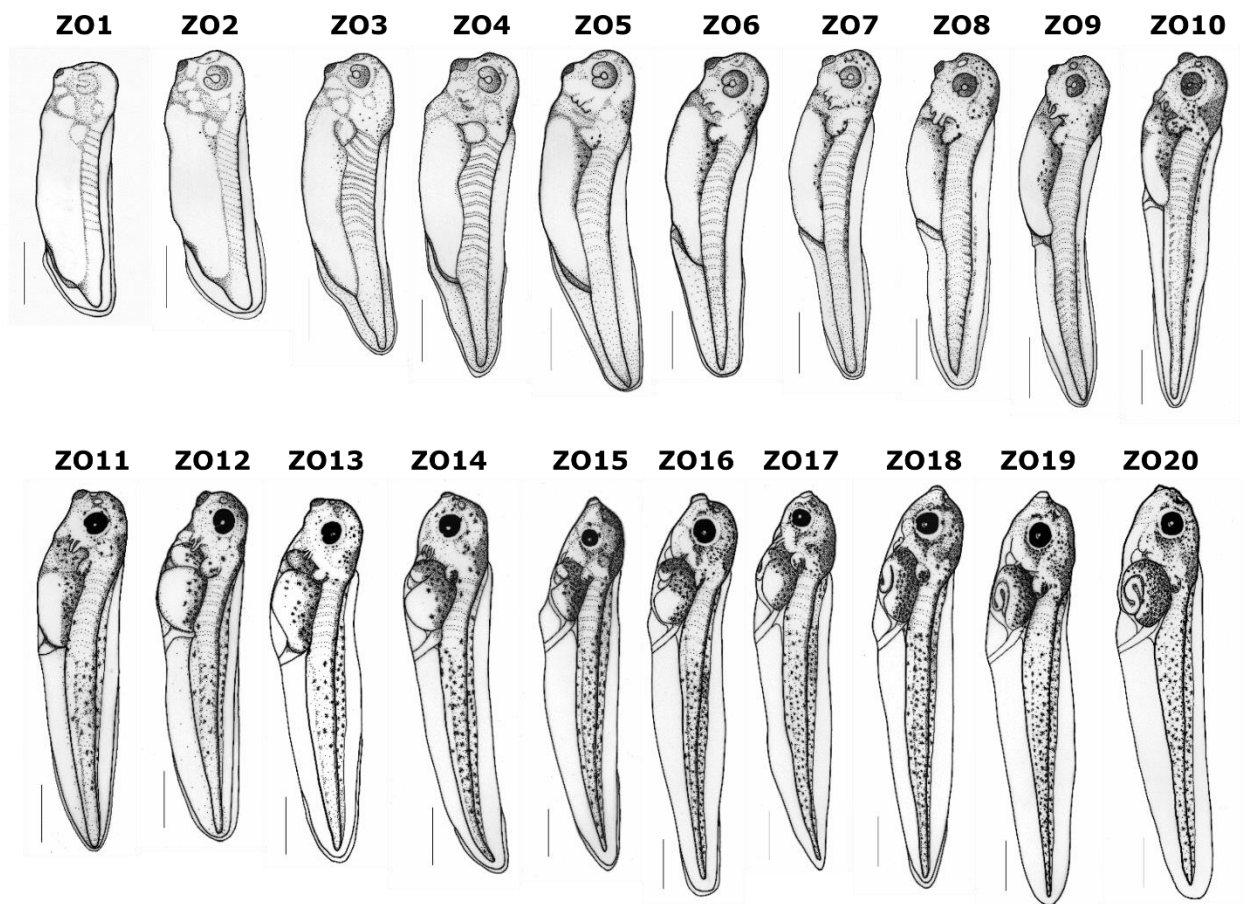


**Figure 5.1| ZO staging subdivides NF stages of early larval development in *Xenopus tropicalis*.** The 20 stages of Ziermann and Olson correspond to stages NF32-46 of early larval development. These figures

are meant to show physical features only. Scale bars are not accurate. Only side profiles are depicted here, but ventral views were also available for staging purposes. Images were extracted from their original supplementary files and reoriented for comparative purposes. (Credit: Ziermann & Olsson, 2007).

## **5.3 Materials and methods**

### **5.3.1 Use of lab animals**

*Please refer to previous materials and methods in Chapter 4 (see page 29).*

### **5.3.2 Frog mating**

*Please refer to previous materials and methods in Chapter 4 (see page 29).*

### **5.3.3 Raising tadpoles to stages of interest**

*Please refer to previous materials and methods in Chapter 4 (see page 30).*

### **5.3.4 Fixation, processing, and sectioning for histology**

*Please refer to previous materials and methods in Chapter 4 for tissue fixation, processing, and sectioning protocols (see page 31).* Longitudinal sections were obtained from the humerus (stages NF55 and NF57) and coronal sections were obtained from the ceratohyal (stages NF39 up to NF63).

### **5.3.5 Histology**

#### **Whole mount Alcian blue/Alizarin red acid-free staining**

*Please refer to previous materials and methods in Chapter 4 (see page 32).*

#### **Safranin O and trichrome section histology**

*Please refer to previous materials and methods in Chapter 4 (see page 32).*

### **5.3.6 Expression assays**

#### **RNA *in situ* hybridization**

*Please refer to previous materials and methods in Chapter 4 for preparatory steps prior to RNA ISH (see page 33).* RNA ISH was carried out on tissue sections as previously described (Strähle et al., 1994; Jowett & Yan, 1996; Eames et al., 2011), with modifications, on stages NF55 and NF57 of the humerus and NF40 to NF44 of the ceratohyal. Results from RNA ISH assays were compared to similar data in other species from the literature.

## **Immunohistochemistry**

*Please refer to previous materials and methods in Chapter 4 (see page 34).*

## **Laser capture microdissection coupled with RNA sequencing**

*Please refer to previous materials and methods in Chapter 4 for details of immature and mature chondrocyte capture from an NF57 humerus (see page 35).*

### **5.3.7 Preliminary RNA-seq analyses**

*Please refer to previous materials and methods in Chapter 4 (see page 36).* Dr. Katie Ovens normalized the raw RNA-seq data from the frog humerus, assigned gene IDs based on sequence alignments to online repositories (e.g., Ensembl), and determined thresholds for counts in immature and mature chondrocytes to be considered relevant (IMM = 12; MAT = 8). Similar datasets in mouse and chick humeri were also available for comparison thanks to previous work done collectively by Drs. Gómez Picos, Ashique, and Ovens. Immature and mature cartilage RNA-seq data from the ceratobranchial in chick and ceratohyal in gar were provided by Drs. Gómez Picos and Ovens.

### **Testing for significance of normalized gene counts using an independent samples t-test**

Normalized counts in frog were analyzed to see if RNA-seq would quantitatively support expression data from RNA *in situ* hybridization. An independent samples t-test was also performed using IBM SPSS Statistics (Build 1.0.0.1447) to determine if the differences in expression (normalized counts) of candidate cartilage genes were statistically significant between immature and mature cartilage for each species. Alpha levels were set at  $\alpha = 0.05$ . Frog results were aligned against mouse, chick, and gar to compare gene expression of prominent chondrogenic and hypertrophic markers during hypertrophy.

## **5.4 Results**

### **5.4.1 Stage NF57 of the humerus was determined to be consistent with previous datasets in the mouse and chick for analysis of immature and mature cartilage**

Some preliminary results on the humerus had previously been analyzed by Yiwen Liu and Dr. Patsy Gómez Picos. In continuing their work, it was confirmed through histology that stages NF57 and NF58 indeed followed their Nieuwkoop and Faber descriptions. This was done through

external staging, skeletal preps, and section histology, which were previously shared in Figures 4.1-4.3 from Chapter 4. From there, the project was advanced further by illustrating the developmental timing and patterning of hypertrophy. This involved comparing section histology and expression assays from stages before overt hypertrophy (NF55) and during hypertrophy (NF57) (Fig. 5.2).

Safranin O staining of stage NF55 showed most chondrocytes throughout the humerus were similar in size to epiphyseal chondrocytes of NF57 (Fig. 5.2A,B). Maturing diaphyseal chondrocytes of NF57 were comparatively larger as they had become hypertrophic (Fig. 5.2A,B). These histological results confirmed the expected progression of chondrocyte hypertrophy spatially within the developing humerus. Hypertrophy began in the middle of the diaphysis first before progressing slowly towards the epiphyses. The elapsed time between NF55 and NF57 was estimated to be 9 days at 23 °C for *X. laevis* (Nieuwkoop & Faber, 1994). Based on two separate clutches of *X. tropicalis* at 27-28 °C (data not shown), NF55 and NF57 humeri demonstrated that limb cartilage became hypertrophic in as little as 4 days, up to a week or longer, depending on husbandry conditions. Thus, the gradual, temporal aspect of the hypertrophic cascade was also satisfied.

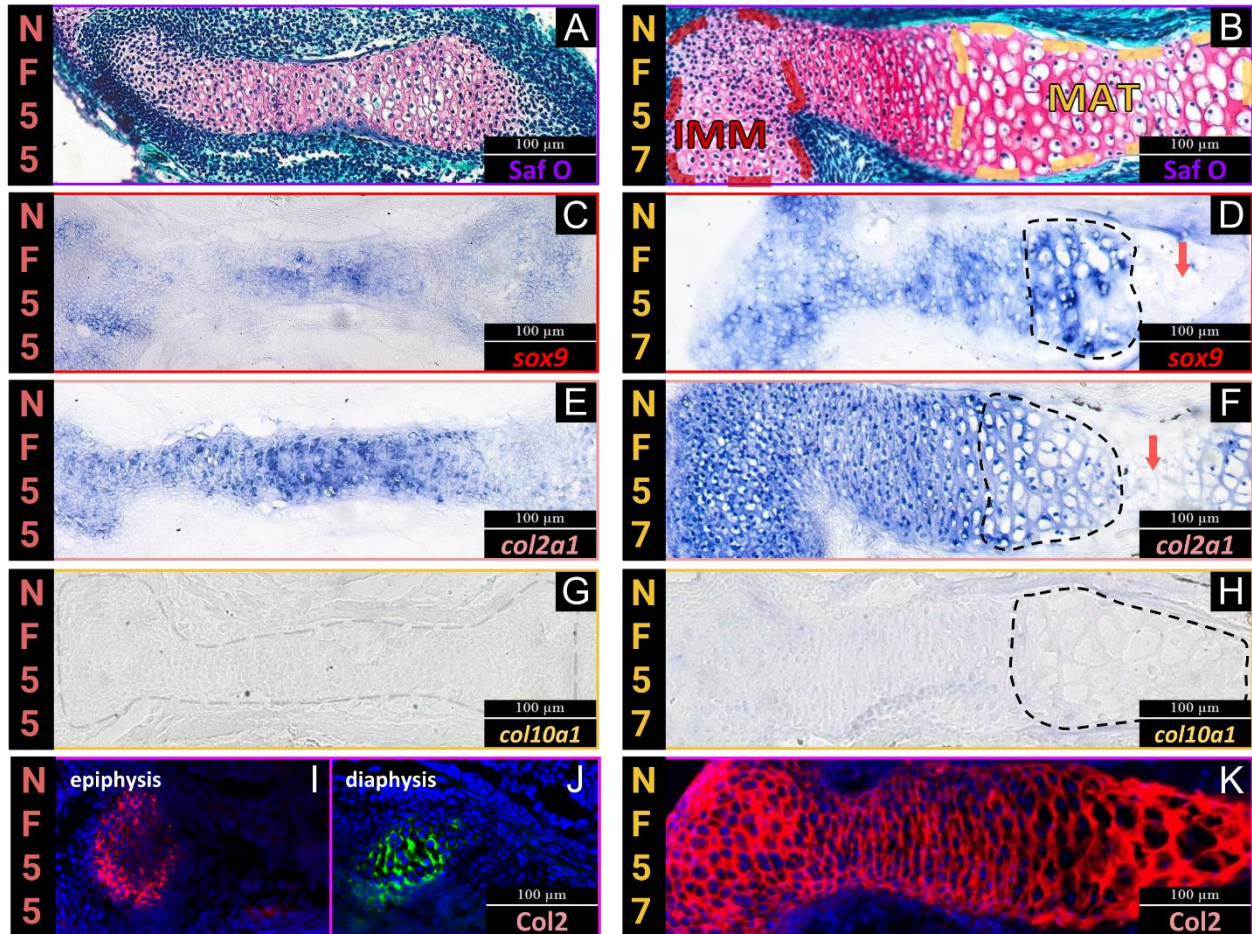


**Figure 5.2| Expression assays of the humerus mostly showed the expected patterns of the hypertrophic cascade.** (A, C, E, G, I, J) Images are longitudinal sections of the humerus at stage NF55 and (B, D, F, H, K) stage NF57. Only half the humerus is shown at stage NF57 in order to emphasize chondrocyte morphology and gene expression from the epiphysis to the diaphysis. **[A]** Saf O staining of cartilage show chondrocytes throughout NF55 are mostly small with some signs of prehypertrophy in the diaphysis. **[B]** Chondrocytes become overtly hypertrophic in the diaphysis of NF57. Immature cartilage markers, such as **[C]** *sox9* and **[E]** *col2a1* are upregulated throughout the entire humerus at NF55. In addition to the epiphyses, **[D]** *sox9* and **[F]** *col2a1* are also highly expressed in prehypertrophic and hypertrophic regions of NF57 as indicated by dashed black lines, before the signals become downregulated in the mid-diaphysis (downward facing red arrows). **[G, H]** The hypertrophic marker *col10a1* is completely negative in the humerus at NF55 (translucent dashes outline the humerus), and even in hypertrophic chondrocytes of NF57 (dashed black lines). **[I, J]** Separate immunostaining of the epiphysis and diaphysis show expression of Col2 protein (the full humerus would have signal; data not shown). **[K]** Col2 is also expressed in cartilage of NF57.

#### 5.4.2 Molecular data showed hypertrophy was mostly conserved in the humerus

At first glance, RNA *in situ* hybridization assays revealed the transition from immature to mature cartilage in the humerus to be fairly typical and in-line with published results from the femur (Miura et al., 2008; Aldea et al., 2013; Enault et al., 2015). Early chondrogenic markers like *sox9*

(Fig. 5.2C,D) and *col2a1* (Fig. 5.2E,F) were downregulated, and expression of the hypertrophic marker *col10a1* was absent (Fig. 5.2G,H). Upon further inspection, it was noted specifically that there were regions of hypertrophic chondrocytes that still exhibited expression of *sox9* (Fig. 5.2D) and *col2a1* (Fig. 5.2F). Immunostaining showed that Col2 protein was present in cartilage throughout the entire humerus at stages NF55 (Fig. 5.2I,J) and NF57 (Fig. 5.2K).

#### **5.4.3 Average normalized counts from RNA-seq revealed mature cartilage in the frog humerus had high expression of many immature cartilage markers**

In frog, 11 immature cartilage genes were assessed (Table 5.1), of which only 5 exhibited higher counts in IMM (immature chondrocytes) than MAT (mature chondrocytes): *sox6* (305 vs 223), *col9a1* (7648 vs 6602), *col9a3* (3 vs 1), *epyc* (29958 vs 29879), and *fmod* (4 vs 2); although none were statistically significant, according to a preliminary independent samples t-test, and two (*col9a3* and *fmod*) were well below the threshold levels for IMM and MAT (thresholds were 12 and 8, respectively) to even be considered biologically relevant. Frog had higher average normalized counts for the 6 other immature cartilage genes analyzed in MAT than IMM: *sox9* (1330 vs 1159), *col2a1* (107103 vs 40153), *acan* (18515 vs 9340), *sox5* (928 vs 795), *col9a2* (234874 vs 145037), and *matn1* (7 vs 5). Only *col9a2* counts were significantly higher in MAT than IMM and counts for *matn1* were below threshold, and therefore, not relevant in either cell type. The remaining candidate genes were prominent markers of mature cartilage and displayed higher average counts in MAT than IMM: *ihh* (3788 vs 9), *runx2* (2447 vs 394), and *ibsp* (78 vs 77), except for *col10a1* (0 vs 3), which was negligible throughout cartilage.

When comparing cartilage RNA-seq data from the frog humerus to datasets previously obtained in mouse, chick, and gar, frog had consistently higher expression levels of several early (immature) chondrogenic markers in MAT (Table 5.1). In gar, all immature cartilage genes tested had higher counts in IMM. Chick had higher counts of only one immature cartilage marker: *matn1* in MAT than IMM (74474 vs 44262), although this was not statistically significant. Mouse had two genes with higher counts in MAT than IMM: *col9a1* (28533 vs 24782) and *epyc* (1952 vs 833), but neither were significantly different from their counts in IMM. Generally speaking, the difference in counts for most candidate genes was not statistically significant across all datasets, even though almost all counts were higher in their expected cell types (except frog). The remaining

four candidate genes were markers of mature cartilage (*ihh*, *col10a1*, *runx2*, and *ibsp*) and all had expression that were highest in MAT across all species, except two: *ibsp* in *gar* and *col10a1* in frog. Counts for these genes were essentially negligible in both immature and mature chondrocytes of both species. The lack of *col10a1* transcripts in MAT of frog matched its RNA ISH result. RNA-seq also validated that *sox9* and *col2a1* were still being expressed at high levels in MAT. Taking the RNA-seq and *in situ* data together, it appeared early hypertrophic chondrocytes in the frog humerus might have increased expression of early chondrogenic markers like *sox9* and *col2a1* before dropping as they continued to mature. Also, it was determined that *col10a1* was not a marker of hypertrophy, according to RNA ISH, RNA-seq, and published results (Aldea et al., 2013).

**Table 5.1| Comparison of candidate cartilage gene counts in immature and mature chondrocytes of mouse, chick, gar, and frog.** Average normalized counts of 11 early chondrogenic markers and 4 hypertrophic markers. Higher counts are bolded and counts below threshold in frog are in parentheses. An independent samples t-test was employed to determine any differences between counts of IMM and MAT. Asterisks indicate significance at \*p < 0.05 and \*\*p < 0.01. Abbreviations: IMM=immature chondrocytes; MAT=mature chondrocytes; n = sample size. (Credits: mouse, chick, and gar data collected by Drs. Patsy Gómez Picos and Amir Ashique; data normalization and gene ID assignment by Dr. Katie Ovens).

Gene								
	IMM n=4	MAT n=5	IMM n=3	MAT n=3	IMM n=4	MAT n=5	IMM n=3	MAT n=3
<i>sox9</i>	<b>260</b>	150	1,159	<b>1330</b>	<b>1198</b>	668	<b>11723</b>	* 6331
<i>col2a1</i>	<b>194955</b>	106827	40,153	<b>107103</b>	<b>23224</b>	12453	<b>129705</b>	105639
<i>acan</i>	<b>25628</b>	15372	9,340	<b>18515</b>	<b>12186</b>	9464	<b>16072</b>	15086
<i>sox5</i>	<b>3852</b>	2351	795	<b>928</b>	<b>3408</b>	** 1382	<b>4275</b>	** 971
<i>sox6</i>	<b>3298</b>	2854	<b>305</b>	223	<b>595</b>	* 188	<b>3519</b>	* 1387
<i>col9a1</i>	<b>1106</b>	* 108	<b>7648</b>	6602	<b>141205</b>	128227	24782	<b>28533</b>
<i>col9a2</i>	<b>1677</b>	* 400	145037	* <b>234874</b>	<b>78122</b>	* 40093	<b>11442</b>	7047
<i>col9a3</i>	<b>29364</b>	* 10055	<b>(3)</b>	(1)	<b>62368</b>	44842	<b>32478</b>	* 21619
<i>epyc</i>	<b>2270</b>	1391	<b>29958</b>	29879	<b>8126</b>	3910	833	<b>1952</b>
<i>fmod</i>	<b>983</b>	* 59	<b>(4)</b>	(2)	<b>74</b>	36	<b>6754</b>	147
<i>matn1</i>	<b>2333</b>	1412	(5)	<b>(7)</b>	44262	<b>74474</b>	<b>25385</b>	20027
<i>ihh</i>	69	<b>685</b>	(9)	<b>3788</b>	1	<b>23</b>	7	* <b>2274</b>
<i>col10a1</i>	21	<b>11238</b>	<b>(3)</b>	(0)	1	<b>1928</b>	8	<b>30432</b>
<i>runx2</i>	128	<b>326</b>	394	* <b>2447</b>	890	<b>1456</b>	332	** <b>2617</b>
<i>ibsp</i>	<b>2</b>	0	77	<b>78</b>	10	* <b>143</b>	169	<b>38662</b>

#### 5.4.4 The frog ceratohyal undergoes rapid hypertrophy early and remains cartilaginous

These results built upon preliminary work done by Yiwen Liu, who had investigated many of the later larval stages when hypertrophy was already evident. These narrowed down the stages of interest for this histological study (i.e., NF39 to NF44).

A developmental series with Safranin O revealed precisely when hypertrophic differentiation took place within the ceratohyal (Fig. 5.3). Mesenchymal condensations were completing the process of shaping the cartilage model from stages NF39-40.5 (ZO7 to ZO10-11). Within a few hours, the rising intensity of Saf O became apparent as chondroblasts increased secretions of sulfated proteoglycans into the ECM, indicating that chondroblasts had differentiated into chondrocytes by NF41.5-NF42 (ZO13-14). Flattened cells surrounding the element were also

beginning to form the perichondrium. Less than 8 hours after chondrocyte differentiation, signs of hypertrophy were obvious by NF43 (ZO15). From NF44 (ZO17) onwards, chondrocytes continued to increase in size, but always remained hypertrophic (Fig. 5.4). These findings for stages NF57 and up agreed with published results (Thomson, 1986).

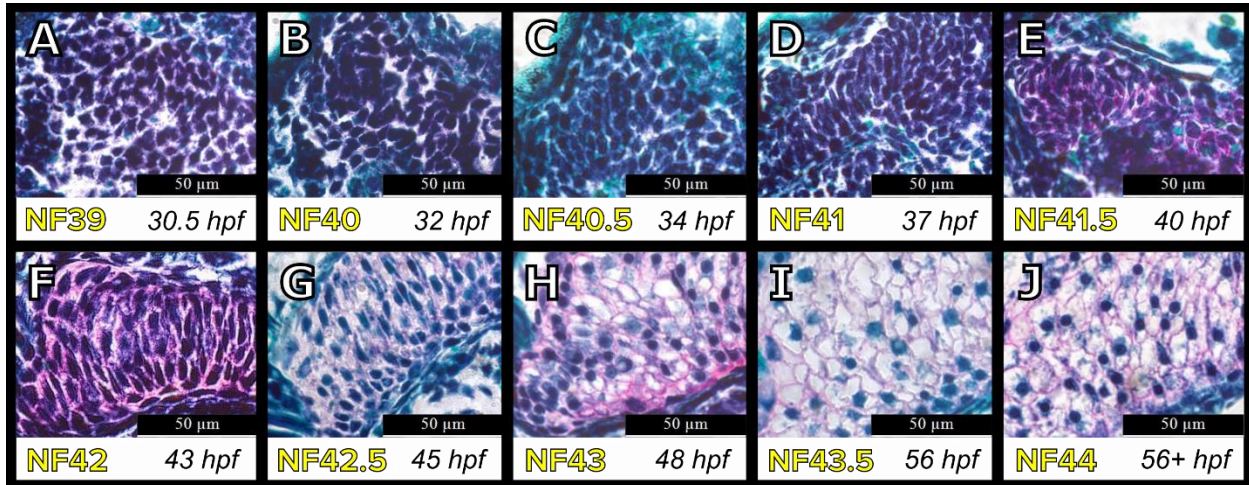


**Figure 5.3| Sub-staging early ceratohyal development revealed chondrocyte differentiation and hypertrophy.** (A-J) Saf O staining of early larval stages show the progression of ceratohyal development from stages NF39 to NF44. Mesenchyme condenses from [A-D] NF39 to N41. Overt chondrocyte differentiation occurs from [E] NF41.5 to [F] NF42. Hypertrophy begins around [G] NF42.5 to [H] NF43 and takes less than 5 hours to become noticeable. From [I] NF43.5 and beyond [J] NF44, chondrocytes remain hypertrophic. The ceratohyal differentiates and becomes hypertrophic in less than 24 hours. Approximate developmental times underneath images are based on 6 matings at 27-28 °C.

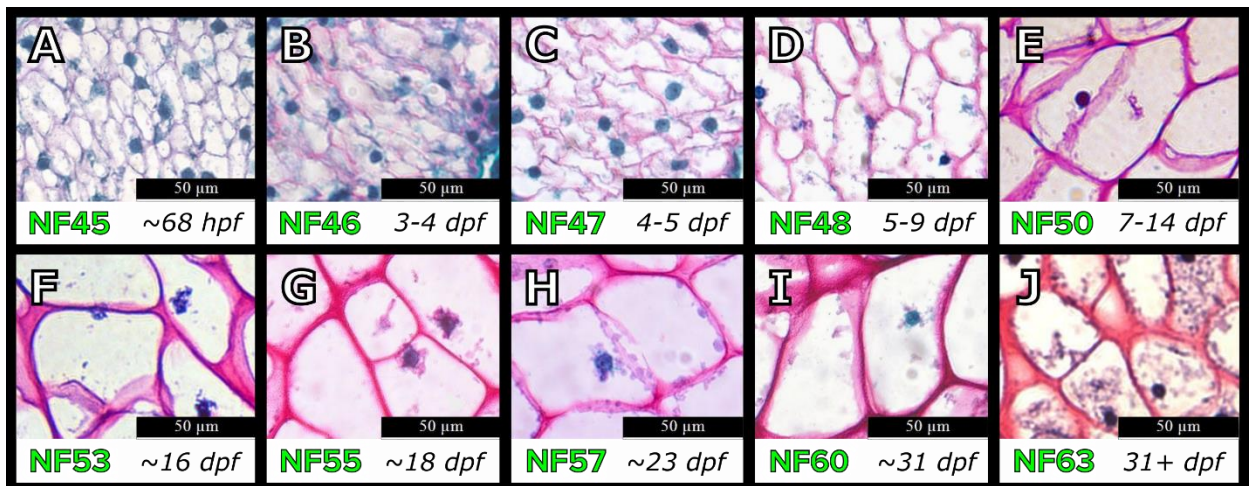


**Figure 5.4| From stages NF45 onwards, ceratohyal chondrocytes remained hypertrophic and never ossified.** (A-J) Chondrocytes of the ceratohyal further increase in size, but are always hypertrophic. Approximate developmental times for [A-D] NF45 to NF48 were based on 6 matings at 27-28 °C.

Developmental times for [E-J] NF50 and up were only based on the average of 2 matings. (Credit: Images for Figs. 5.4I,J were taken by Yiwen Liu).

Col2 immunostaining further validated cartilage differentiation and hypertrophy of the ceratohyal (Fig. 5.5). No Col2 protein was detected at stage NF40 (ZO8-9; Fig. 5.5A). By NF41.5, extracellular Col2 was abundant and yet another sign that chondrocytes had differentiated (Fig. 5.5B). From NF42 to NF44 (Fig. 5.5C-E), it could be seen that hypertrophy was occurring and that it happened throughout the entire element all at once.

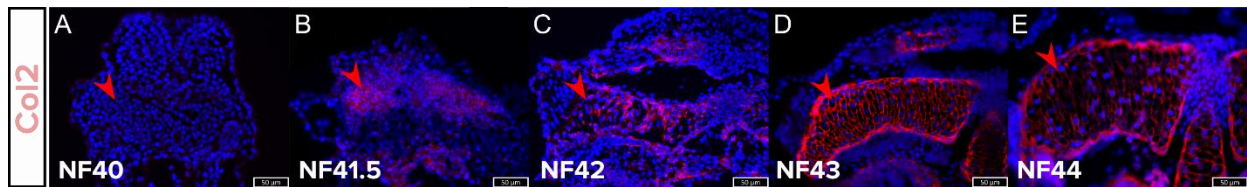


**Figure 5.5| Col2 immunostaining independently confirmed differentiation and hypertrophy of ceratohyal cartilage.** Red arrowheads point at one half of the ceratohyal. [A] No Col2 protein was expressed at NF40. [B] The presence of Col2 protein indicated chondrocytes had formed by NF41.5. [C] NF42, [D] NF43, and [E] NF44 showed chondrocytes became hypertrophic all at once.

From a histological standpoint, ceratohyal chondrocytes increased in size and satisfied one major morphological feature of hypertrophy. The temporal and spatial aspects of the hypertrophic cascade, however, were not followed at all by amphibian head cartilages. Ceratohyal chondrocytes became hypertrophic very rapidly and hypertrophy did not progress gradually from the middle of the element outwards, as had been the case in the humerus. Instead, it appeared as though all chondrocytes increased in size at the same time.

#### 5.4.5 Regulation of chondrogenic genes is not conserved in amphibian head cartilage

RNA ISH and IHC assays of the ceratohyal were focused on the differences between stages NF42 and NF43, when chondrocytes had first become overtly hypertrophic (Fig. 5.6). During this transition, there was no downregulation of *sox9* or *col2a1*, and no upregulation of *col10a1* in hypertrophic chondrocytes of the ceratohyal. Immunostaining showed Col2 protein was expressed throughout the entire element before and during hypertrophy. Even analysis of a much later stage NF57 revealed expression of *sox9*, *col2a1*, and Col2 had never ceased completely (Fig. 5.7A,B,D). In contrast, *col10a1* was still not present in hypertrophic chondrocytes

(Fig. 5.7C). It appeared that molecularly, the frog ceratohyal did not follow the hallmark patterns of *sox9* and *col2a1* downregulation and *col10a1* upregulation during the hypertrophic cascade (Eames et al., 2003; Tchetina et al., 2014). This makes amphibian head cartilage very unique among vertebrates.

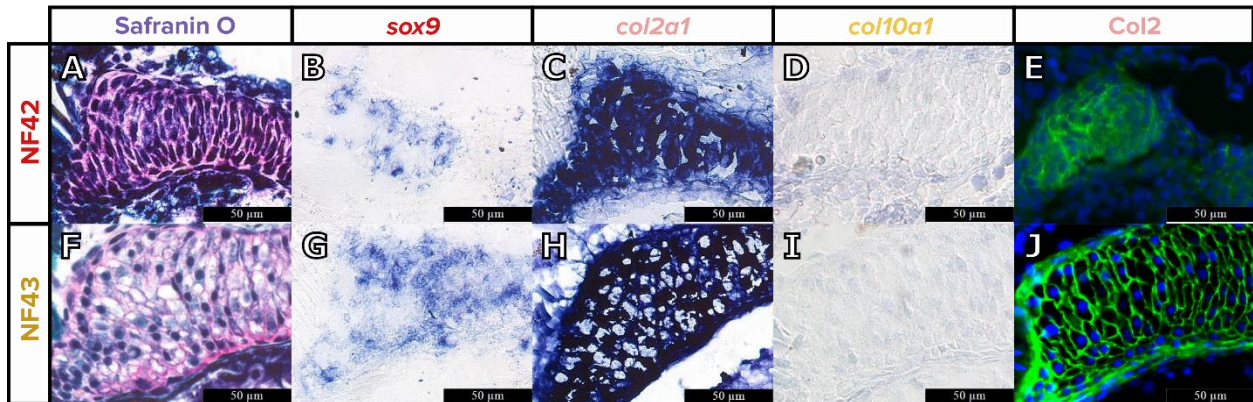


**Figure 5.6 | Analysis of the ceratohyal during hypertrophy showed gene regulation was not conserved.** (A-E) Stage NF42 of the ceratohyal just before or as hypertrophy was about to begin. (F-J) Stage NF43 shows that hypertrophy has clearly begun as chondrocytes have visibly increased in size. Saf O staining demonstrates the difference in chondrocyte size before [A] and after [F] the onset of hypertrophy. Neither *sox9* [B, G] nor *col2a1* [C, H] were downregulated as chondrocytes entered hypertrophy. [D, I] The hypertrophic marker *col10a1* was not expressed at all. [E, J] Col2 protein continued to present before and during hypertrophy and reaffirmed that hypertrophy occurred throughout the entire element at once.

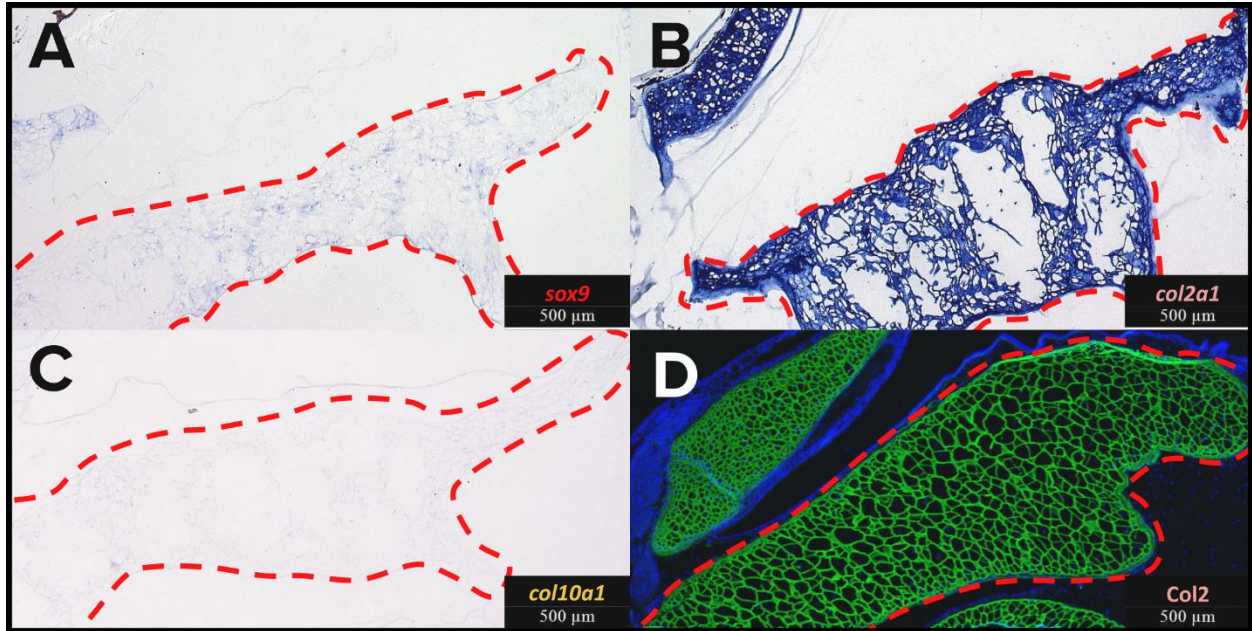


**Figure 5.7 | Expression assays of *sox9*, *col2a1*, and Col2 continued to be expressed at stage NF57 and *col10a1* was still negative.** Dashed red lines indicate one half of a stage NF57 ceratohyal. (A-C) were frozen sections of RNA ISH and (D) was a paraffin section of IHC. Approximately 3 weeks after ceratohyal chondrocytes first became hypertrophic, [A] *sox9* and [B] *col2a1* still had signals, but [C] *col10a1* remained negative. [D] Col2 protein expression was present throughout the ceratohyal and other head cartilages.

## 5.5 Discussion

The hypothesis that maturing chondrocytes of the amphibian undergo the standard histological and molecular progressions of hypertrophy common to all vertebrates was mostly supported in humerus cartilage, but not in ceratohyal cartilage. We discovered hypertrophy in the humerus was comparable to that of other models with the exceptions that *sox9* and *col2a1* did not immediately downregulate (Fig. 5.2D,F), and no expression of *col10a1* was found in mature cartilage (Fig. 5.2G,H). Eventually, *sox9* and *col2a1* did downregulate in more advanced hypertrophic chondrocytes located centrally in the mid-diaphysis when cartilage maturation progressed towards the epiphyses. Similar to the humerus, maturing chondrocytes of the ceratohyal had high levels of *sox9* and *col2a1*, with no indication that the hypertrophic marker *col10a1* was present (Figs. 5.6 and 5.7). Likewise, both the humerus (Fig. 5.2I-K) and ceratohyal (Fig. 5.6) expressed Col2 protein before and during hypertrophy. These patterns of Col2 protein expression were similar to what had been seen in other tetrapods (Von Der Mark et al., 1976; Blitz et al., 2013). Unlike the humerus, *sox9* and *col2a1* expression continued in the ceratohyal

and chondrocytes underwent hypertrophy very rapidly, almost all at once, then remained this way without ever ossifying. In most other vertebrate models, the ceratohyal—or a skeletal element homologous to it (e.g., the ceratobranchial in chick)—undergoes endochondral ossification (Eames et al., 2004, 2011, 2012; Eames & Helms, 2004). The continued expression of *sox9* and *col2a1* during hypertrophy were consistent with the literature, which had previously been reported in other head cartilages at stage NF57, and at NF64 for *col2a1* (Kerney, Hall, et al., 2010). The lack of *col10a1* was also in agreement with negative results that were published in mature cartilage of a stage NF58 femur (Aldea et al., 2013). In fact, there were no observations throughout this cartilage study that were discordant with published data on the *Xenopus* frog. The unusual findings pertaining to *sox9*, *col2a1*, and *col10a1* in amphibian cartilage had simply not been recognized as abnormal before, and thus, were never subjected to further scrutiny. Therefore, our novel findings revealed that hypertrophy in the frog can occur without the immediate downregulation of immature cartilage markers like *sox9* and *col2a1*, without the need for expression of a mature cartilage marker like *col10a1*, and that sustained levels of *sox9* and *col2a1* corresponded to (and possibly have something to do with) the rapid maturation and persistent hypertrophy of the head cartilages.

### **5.5.1 Early chondrogenic markers are highly expressed in mature cartilage of frogs**

A molecular aspect of the hypertrophic cascade not being followed by maturing chondrocytes of the humerus was the sustained expression of early chondrogenic markers like *sox9* and *col2a1*. Although unusual, these genes did eventually downregulate dramatically in older, more advanced hypertrophic chondrocytes of the humerus, but not the ceratohyal. Their contradictory expression levels at the start of hypertrophy, however, could be parsed out and corroborated quantitatively by RNA-seq. Average normalized counts in the frog humerus revealed that *sox9*, *col2a1*, and other prominent markers of immature cartilage (e.g., *acan*, *sox5*, *sox6*, *col9a1*, *col9a2*, etc.) had higher counts in MAT rather than IMM (Table 4.4). This was generally not the case for normalized counts in mouse, chick, or gar, with the caveat being that gar cartilage data was collected from the ceratohyal since gar are limbless. These non-amphibian species expectantly had higher counts of early cartilage genes in IMM, with very few exceptions (e.g., *col9a1* and *epyc* in mouse, and *matn1* in chick were higher in MAT). If RNA ISH and RNA-seq from

the frog data are analyzed together, it seems newly hypertrophic chondrocytes were responsible for the higher counts of *sox9* and *col2a1* in MAT. This suggests these genes might have been upregulated during the initial phases of hypertrophy, which would be a trait unique to amphibians, if verified. Had LCM-RNAseq been performed specifically on more centralized and advanced hypertrophic chondrocytes of the mid-diaphysis, the relative counts for these early chondrogenic markers likely would have been reversed (i.e., higher in IMM than MAT). Such a result would be more typical of the expression patterns seen in other vertebrate models.

*In situ* data from the frog ceratohyal during the initial phases of hypertrophy were consistent with results from the humerus. Signals for *sox9* and *col2a1* remained intense during hypertrophy, which could lend support the notion that levels of *sox9* and *col2a1* might actually be higher in chondrocytes when they first became hypertrophic. What distinguished the ceratohyal from the humerus was that *sox9* and *col2a1* levels never dropped completely as hypertrophic chondrocytes advanced. Furthermore, this persisted into adulthood as the ceratohyal remained cartilaginous and hypertrophic. This also differentiates the amphibian from other vertebrates.

### **5.5.2 *col10a1* did not appear to be a marker of hypertrophy in amphibians**

The absence of *col10a1* during cartilage maturation was also an atypical finding in frog. Neither limb nor head cartilages exhibited this hypertrophic marker in RNA ISH assays. Normalized counts of *col10a1* from RNA-seq were negligible in both immature and mature cartilage of the humerus (3 and 0 counts, respectively; Table 4.4), further validating these negative results. Of the other candidate genes considered to be hypertrophic markers (*ihh*, *runx2*, and *ibsp*), all averaged more counts in MAT than IMM. Only *runx2* was statistically significant (2447 vs 394), even though the difference in average counts for *ihh* was actually larger (3788 vs 9). The lack of *col10a1* expression in hypertrophic chondrocytes was not entirely unprecedented. Studies of *Col10a1*-null mice had determined its expression was not necessary for hypertrophy itself (Kwan et al., 1997; Rosati et al., 1994). Data from the frog appears to support this idea, but one major difference would be that this happened naturally without gene manipulation.

### 5.5.3 Amphibian head cartilage is especially unique compared to other cartilages

One of the most fascinating observations from this study was how rapidly hypertrophic the ceratohyal became in the frog, mere hours after differentiating into cartilage (Fig. 5.3). This was apparent even externally as the rounded head shape of an NF41.5-NF42 tadpole could be witnessed transforming into a wedge shape through to NF42.5-NF43 in roughly eight hours or less (presumably due mostly to hypertrophy; Zahn et al., 2017). The initial transition of cells from tightly packed immature chondrocytes to visibly prehypertrophic chondrocytes occurred in only 2-3 hours and could be reliably timed. Hypertrophy happened very soon after fertilization (~48 hpf) and occurred throughout the entire ceratohyal, unlike in zebrafish, gar, and chick, which happen more slowly and progressively (Eames & Helms, 2004; Eames et al., 2012). The humerus took days to become mature in comparison, where hypertrophy started off in the mid-diaphysis before progressively spreading outwards. Since this was not the case for the ceratohyal, a transition zone did not exist. Unlike the humerus, there were no flattened columns of proliferating cells that could be distinguished from prehypertrophic and progressively more hypertrophic chondrocytes. Only proliferating chondrocytes at the perichondrium of the ceratohyal were non-hypertrophic. This suggested that the rapid pace of hypertrophy was continually taking place as new cells were added from stage NF44 onwards. Hence, the ceratohyal always appeared hypertrophic, even at much later stages (Fig. 5.4).

The closest comparison to the frog ceratohyal in terms of timing might be the zebrafish ceratohyal. These results are unpublished, but according to histological studies done by Elham Koosha, a PhD candidate in the Eames lab, the ceratohyal in zebrafish underwent cartilage differentiation sometime between 48 and 72 hpf. Furthermore, her molecular data presented *col10a1* expression at ~96 hpf, suggesting signs of hypertrophy, which aligned with previous reports (Eames et al., 2011, 2012). Thus, in terms of developmental timing, it appears frog head cartilages are more similar to teleosts than other tetrapods. In regards to the developmental arrest of bony cranial structures, the non-ossification of head cartilages had been deemed a novel trait in anurans (Porter & Vial, 1974). These data do not support the hypothesis that maturation is conserved within amphibian head cartilages and highlights that hypertrophy seems to be very unique in this particular region.

### 5.5.4 Summary

The following statements can be made regarding amphibian cartilage (summarized in Table 5.2):

- 1) *sox9* and *col2a1* are highly expressed early in hypertrophy.
- 2) *col10a1* is not a marker of hypertrophy.
- 3) Amphibian limb cartilage follows the hypertrophic cascade as most vertebrates (with the exceptions noted above).
- 4) Amphibian head cartilages do not follow the standard molecular, temporal, or spatial progressions of hypertrophy.

Table 5.2| The similarities and differences between limb and head cartilage maturation in *Xenopus*.

Skeletal element	Similarities	Differences
Humerus	<ul style="list-style-type: none"> <li><i>sox9</i> and <i>col2a1</i> highly expressed during early hypertrophy</li> </ul>	<ul style="list-style-type: none"> <li>Hypertrophy initiates in the mid-diaphysis and spreads gradually</li> <li><i>sox9</i> and <i>col2a1</i> decrease dramatically as cartilage maturation progresses</li> <li>Ossifies as chondrocytes terminally differentiate and die</li> </ul>
Ceratohyal	<ul style="list-style-type: none"> <li>No <i>col10a1</i> expression</li> </ul>	<ul style="list-style-type: none"> <li>Hypertrophy occurs rapidly shortly after chondrogenesis and is global</li> <li><i>sox9</i> and <i>col2a1</i> expression persist indefinitely</li> <li>Remains cartilaginous and chondrocytes stay hypertrophic</li> </ul>

The hypertrophic cascade appears mostly conserved in the frog humerus, with some minor exceptions, namely delayed *sox9* and *col2a1* downregulation and the absence of *col10a1* upregulation. On the other hand, it seemed quite clear that ceratohyal development was very unique on multiple fronts, and thus, not conserved. The ceratohyal did not follow the molecular, temporal, or spatial aspects of the hypertrophic cascade: gene regulation was not conserved since *sox9* and *col2a1* never downregulated completely; hypertrophy occurred much more rapidly compared to other models; and almost all chondrocytes became hypertrophic at once, regardless of location.

Given that sustained hypertrophic cartilage can be a natural phenomenon in frog, yet an aberrant condition in humans that often accompanies osteoarthritis (Bayles, 1950; Dreier, 2010), amphibian cartilage could be a useful model for studying this widespread disease. Regardless, the driving forces behind hypertrophy are poorly understood (Cooper et al., 2013), and since

interesting things are happening in the frog that do not occur in other vertebrate models, this might teach us something new about cartilage disease, development, and evolution.

## CHAPTER 6

### Discussion, limitations, and future directions

#### 6.1 Discussion

The goal of this thesis was to unravel a small part of skeletal cell evolution by investigating specific aspects of bone and cartilage development in an amphibian. This was accomplished primarily through histological and gene expression assays. Amphibian results were compared against other vertebrate models to uncover any similarities, differences, and patterns among representatives of earlier- and later-diverged clades. In theory, this could potentially provide an estimation of what might have occurred in the past, although enticing insights into the unique development of a present-day frog were revealed as well. Traditional functional studies were not the main focus here as the purpose was to infer how the transcriptome (i.e., the molecular fingerprint) of skeletal cells may have evolved through these comparisons. We argue that the ultimate assay for elucidating the functional roles of transcription factors, such as ones known to drive skeletogenesis like Sox9 and Runx2 (Eames et al., 2003, 2004; Eames & Helms, 2004), involves analyzing the very outputs generated by them. There has been substantial evidence over the years to support that certain portions of these transcriptional outputs are critical for skeletal cell differentiation (Gómez-Picos & Eames, 2015; Gómez-Picos et al., in preparation). For instance, Sox9 and Runx2 control downstream expression of genes that characterize cartilage like *col2a1* and *col10a1*, respectively, and can regulate many other factors that are either necessary or often important for cartilage and bone development in most vertebrates, such as Sox5, Sox6, and Sp7 (Linsenmayer et al., 1991; Poole, 1991; Lefebvre et al., 1996; Bell et al., 1997; Ducy & Zhang, 1997; Komori et al., 1997; Otto et al., 1997; Akiyama et al., 2002; Eames et al., 2003, 2004; Zheng et al., 2003; Eames & Helms, 2004; Nishio et al., 2006; Komori, 2011; Li et al., 2011; Gómez-Picos & Eames, 2015; Kague et al., 2016; Yu et al., 2017). However, quantitating these outputs comprehensively through comparative transcriptomics in an attempt to reconstruct skeletal cell evolution is a novel approach that is still in its infancy. Any changes in expression of skeletal genes across species have yet to be investigated thoroughly, particularly in amphibians. This gap in the

literature has led to biased notions as to what genes characterize skeletal cells and what the standard progression of skeletal development is currently understood to be.

Our investigation has revealed a novel transcriptional output which is likely driving some atypical developmental patterns observed in frog skeletal cells. Osteoblasts of the frog appeared to be more chondrogenic compared to other animals but lost this feature once they became osteocytes, which is somewhat similar to what happened during osteoblast evolution. Some speculation will be offered as to why this may have taken place. Furthermore, some differences in chondrogenic expression were discovered that depended on where and how bone formed. Regarding amphibian cartilage, it appeared as though chondrocyte hypertrophy in the head and limb displayed some conserved features, but development of the head cartilages was especially peculiar compared to other models. Overall, it seems amphibian skeletal cells expressed high levels of early (immature) chondrogenic genes, relatively speaking. How much this contributes or relates to some of the unusual traits found in the frog remains to be seen.

### **6.1.1 Osteoblast evolution**

In bone, it was discovered that osteoblasts of fishes expressed cartilage genes that, by classical definition, were typically not found in osteoblasts of land tetrapods (Eames et al., 2012). Follow-up studies were presented in Chapter 4 which seemed to suggest that amphibian bone might be more chondrogenic than fish, though these findings were preliminary and require more in-depth bioinformatical support. The basis for this observation came from a limited comparison that showed many prominent cartilage genes had relatively higher expression in amphibian osteoblasts than other species (Table 4.4). If supported, this could mean chondrogenic genes were not gradually repressed during the evolution of the osteoblast as previously hypothesized in Chapter 3 (Nguyen & Eames, 2020). However, this interpretation hinged upon the assumption that osteoblasts of earlier-diverged fishes were more chondrogenic to begin with, which these results have also called into question (i.e., gar exhibited the reddest ratios in Table 4.4). The same preliminary analysis used to measure chondrogenic expression in the frog appeared to place the gar on a similar level to the mouse and chick, meaning that frog was the outlier. Recent dissertations by Drs. Patsy Gómez Picos and Katie Ovens have only partially supported gar osteoblasts as being more chondrogenic than osteoblasts of mouse and chick. Therefore, the

possibility that the frog osteoblast is most chondrogenic could actually be valid. Comparative transcriptomic analyses incorporating frog data with mouse, chick, and gar should provide further resolution and elucidate if this is truly the case. Evolutionarily speaking, the current analysis suggests chondrogenic gene expression in osteoblasts may have actually increased in the amphibian lineage first, before being repressed in later-diverged tetrapods (Eames et al., 2012; Aldea et al., 2013). Since frogs are a transitional animal that can exist in both aquatic and terrestrial environments, perhaps the expression of this trait may be related somehow. This remains highly speculative, however. The path moving forward to address these issues and other discrepancies are presented in future directions.

### **6.1.2 Amphibian osteoblasts appeared to downregulate chondrogenic expression before maturing into osteocytes**

Chondrogenic signals from RNA *in situ* hybridization assays have thus far been restricted to layers outside of the bone matrix. To recap these findings, *sox9* (Cervantes et al., in preparation) and *col10a1* (Aldea et al., 2013) expression were found in osteoblasts of the femur, and our data showed *col2a1* in humerus osteoblasts (Fig. 4.5H). Two important observations follow as a result: 1) The cells inside the bone matrix (osteocytes) appeared not to express chondrocyte genes, and 2) osteoblasts must have downregulated chondrocyte genes as they matured into osteocytes. Rephrased another way, amphibian osteoblasts expressed similar molecular characteristics to chondrocytes early in their development, only to lose them later on. This could offer some support to the hypothetical evolutionary loss of chondrogenic markers in osteoblasts as a recapitulation event (Nguyen & Eames, 2020). Given that osteoblasts and chondrocytes develop from common osteochondroprogenitors (Nakahara et al., 1990), their subsequent differentiation into more specialized cells could have also involved losing the expression of genes that initially made them similar. A recent chondrocyte-to-osteogenic precursor model supports this idea, where a population of chondrocytes (or chondrogenic cells) lose the expression of genes that classified them as chondrogenic, before transdifferentiating into osteoblasts (Ono et al., 2014; Aghajanian & Mohan, 2018). Whether or not this has any relation to how the osteoblast evolved has yet to be determined, but this could possibly be an explanation for why expression of chondrogenic markers is present in osteoblasts of earlier-diverged vertebrates (Benjamin, 1988,

1989; Benjamin & Ralphs, 1991; Eames et al., 2012; Aldea et al., 2013; Bertin et al., 2014; Enault et al., 2015).

### **6.1.3 Why did bone of later-diverged vertebrates lose chondrogenic expression?**

Cartilage has increased flexibility since chondrocytes have an ECM containing mostly loose Col2 fibers, whereas mineralized bone matrix is more rigid partly due to tightly wound collagen fibers like Col1 secreted by osteoblasts (Gómez-Picos & Eames, 2015). A skeleton predominantly fortified by bone rather than cartilage likely aided in the diversification of life on land (Volkman & Baluška, 2006; Wood & Nakamura, 2018). Therefore, losing any skeletal traits associated with cartilage could theoretically make bone stronger to resist the additional mechanical load of living in this new environment (Volkman & Baluška, 2006). This might be a potential reason for why bone of later-diverged vertebrates no longer needed the (arguably weaker) characteristics associated with cartilage. Further support for this idea can be tested for by analyzing aquatic mammalian osteoblasts. If the hypothesis is correct, these cells should have a molecular profile that reverted back to a more 'chondrogenic' form. This would offer some insight into how an osteoblast was capable of evolving and provide yet another step in clarifying whether or not bone might have evolved from cartilage (Gómez-Picos & Eames, 2015). If chondrogenic expression is a trait that osteoblasts can lose or regain during its evolution, that means the programming was there all along. It could be a relic that was shared between osteoblasts and chondrocytes before these cell types diverged that still persists today.

### **6.1.4 Perichondral and intramembranous ossification are similar, but different**

In Chapter 4, it had been suggested that chondrogenic expression might be higher in osteoblasts of perichondral bone than of dermal bone. Perichondral and intramembranous ossification are often referred to as being the same, but these osteogenic programs evolved at different times (intramembranous is thought to have evolved first; Vaškaninová, 2020). Many texts and papers will refer to the formation of perichondral bone as being an intramembranous process. This is due to the fact that descriptively, they sound identical since mesenchymal cells of the perichondrium differentiate directly into osteoblasts (Egawa et al., 2014). However, one key difference is that perichondral ossification requires *Ihh* signals from prehypertrophic and

hypertrophic chondrocytes (St-Jacques et al., 1999), whereas intramembranous bone forms without the need for cartilage at all (Eames & Helms, 2004; Abzhanov et al., 2007; Huycke et al., 2012). Moreover, increased Hedgehog signaling has been shown to induce transdifferentiation of hypertrophic chondrocytes into osteoblasts during endochondral ossification, further adding to the complexity of skeletal development (Vortkamp et al., 1996; Hammond & Schulte-Merker, 2009). Since *hh* is also important for regulating cartilage maturation (Vortkamp et al., 1996), we can begin to appreciate these minor differences between perichondral and intramembranous ossification could actually be important details of skeletal cell evolution (Vaškaninová, 2020). Our RNA *in situ* hybridization results showing increased chondrogenic expression in perichondral over dermal osteoblasts might yet be another example that separates these ossification types.

#### **6.1.5 Where and how skeletal cells form could be clues into evolution**

From an evolutionary perspective, these findings in the head and limb might be telling us something about previous iterations of the chondrogenic and ossification programs. This relates to the fact that limbs developed as a novel trait in tetrapods during vertebrate evolution (Shubin, 2002; Wood & Nakamura, 2018). Since the appendicular skeleton evolved after the axial and cranial skeleton (Berendsen & Olsen, 2015), the pathways associated with forming bone in the head might be showcasing more primitive features than those from the limb, assuming these pathways have been constrained. Likewise, this could explain the differences observed between the head and limb when comparing how their cartilages mature. Many bones of the skull are dermal, but some are chondral as well. Since perichondral bone typically accompanies endochondral ossification, this adds yet another layer to be considered when comparing evolution and development. It has been hypothesized that intramembranous bone predates endochondral bone (Hirasawa & Kuratani, 2015; Cervantes-Diaz et al., 2017; Wood & Nakamura, 2018), and that perichondral bone likely evolved somewhere in between (Vaškaninová, 2020). This might also be why chondrogenic expression levels in perichondral and dermal osteoblasts have been shown to vary.

### 6.1.6 Chondrocyte hypertrophy

Our research into cartilage evolution and development has also yielded some very interesting results, particularly regarding chondrocyte hypertrophy—an integral part of endochondral ossification. Hypertrophy is highly conserved within vertebrates, following a very particular histological and molecular progression that had not been thoroughly characterized in frog yet. The hypertrophic cascade has associated changes in terms of gene regulation, morphology, and developmental timing that have been very consistent across non-amphibian clades (Eames et al., 2004, 2011, 2012; Eames & Helms, 2004). Given that previous studies imaging head cartilage of *Xenopus laevis* showed them to be permanently hypertrophic (Thomson, 1986), this raised the question of whether or not the standard hypertrophic cascade was still valid for this unusual phenotype. It was found that arrested endochondral development in head cartilage was a common feature of anuran frogs (Porter & Vial, 1974). Our results confirmed this and elaborated further on the molecular and histological details that made this trait unique. On the other hand, a review of humerus development revealed some notable deviations from the norm, such as decreased trabecular bone and incomplete Hedgehog signaling in proliferating chondrocytes (Moriishi et al., 2005; Miura et al., 2008). These were described as possible causes for what appeared to be delayed endochondral ossification in frog limbs. We are not certain these were valid arguments for such a conclusion, however. Our own analyses of the humerus and ceratohyal confirmed that *col10a1* was not a hypertrophic marker in frogs (Figs. 5.2 and 5.6; Table 4.1). This had been previously shown in the femur as well (Aldea et al., 2013). Together, these negative results supported past studies that had revealed hypertrophy could occur unimpeded in *Col10a1*-null mice (Rosati et al., 1994; Kwan et al., 1997). Instead, we showed early hypertrophy in frog cartilage was associated with high levels of *sox9* and *col2a1* expression. These genes would eventually become downregulated completely in the humerus as cartilage maturation progressed (Fig. 5.2), but not in the head cartilages (Figs. 5.6 and 5.7). High chondrogenic expression of *sox9* and *col2a1* during the initial phases of hypertrophy in the humerus could be considered a subtle variation, but the continued levels of *sox9* and *col2a1* long after hypertrophy had occurred in the ceratohyal certainly were not. Either result might be considered novel discoveries given these markers are normally associated with immature and not mature cartilage.

Overall, hypertrophy in amphibian limb cartilage was fairly conserved, especially with later-diverged tetrapods since more aspects of the hypertrophic cascade were followed than not. Amphibian head cartilages, however, appeared more conserved with earlier-diverged teleosts in terms of its early development and timing (Eames et al., 2012). Although, as a separate clade, anurans featured some very specific properties like rapid and global hypertrophy that have expanded our views on how chondrocytes can develop.

### **6.1.7 Amphibians have many unusual features during development compared to other vertebrates that generate more questions than answers about skeletal cell evolution**

Finally, to address the general hypothesis posited back in Chapter 1, our findings suggested amphibian bone and head cartilages did NOT have molecular and histological profiles intermediate to that of earlier- and later-diverged vertebrates. Osteoblasts of frog were more chondrogenic than other vertebrate models and chondrocytes from frog head cartilages underwent rapid hypertrophy, coupled with associated patterns of gene regulation that were non-standard. Hypertrophy of amphibian limb cartilage, on the other hand, matured in a manner similar to other models. This could be considered relatively intermediate (and thus, conserved) since the hypertrophic cascade within amphibian limb cartilage did not deviate much compared to earlier- and later-diverged clades (Leboy et al., 1988; Karsenty & Wagner, 2002; Eames et al., 2003; Kronenberg, 2003; Eames & Helms, 2004; Mackie et al., 2008; Eames et al., 2012; Long & Ornitz, 2013).

## **6.2 Limitations**

While precautions were taken to produce the best possible data and analyses for this thesis, there were certain issues that could not be overcome and will be expanded upon further. As much as we would like to reconstruct the past, it is impossible to know with absolute certainty what happened during evolution. All that can be done is to gather as much information as possible in the hopes of building and improving a model that best represents what might have occurred. Further complicating this particular endeavor was the fact that amphibians underwent drastic changes during their skeletal development (i.e., metamorphosis), whereas other vertebrate models generally did not need to take that into account. Finally, there were other variables, such as technical limitations or erroneous practices that could have unintentionally

impacted results adversely, though efforts were always taken to minimize these as much as possible. Each of these limiting factors will be expanded upon in the next several sections.

### **6.2.1 Phyletic constraint is an unproven hypothesis**

Although phyletic constraint might allow us to learn about the past (S. J. Gould & Lewontin, 1979), convergent evolution could also be leading us astray (Doyle, 1996; Wake et al., 2011; Currie, 2013). All modern-day animals have evolved for the same amount of time, meaning there have been ample opportunities for certain traits to evolve independently. What might seem like an evolutionary pattern of connected events could turn out to be chance, and therefore, completely unrelated. Many similar biological traits can also evolve out of necessity or because of some adaptive advantage being offered, not because they were inherited from a common ancestor (Blackburn, 1992; Doolittle, 1994; Kozmik et al., 2008; McGhee, 2011). Furthermore, evolution could have potentially wiped out or warped the history of an event beyond recognition, erasing the very information needed to trace back the lineage of a particular trait. Clade-specific adaptations could have altered or hidden ancestral features to an extent that animals today no longer contain a decipherable record of a distant relationship. Though on an evolutionary scale, with the enormous number of connections that currently exist, continue to form, and are available as evidence for phylogenetic reconstruction, remnants of the past are not so easily lost (S. J. Gould & Lewontin, 1979; Woese & Fox, 1977). All life on earth (discovered thus far) has been constrained to same building blocks after all, which has allowed science to confidently establish connections from hundreds of millions to billions of years ago (Woese & Fox, 1977; Chiappe, 2009). Perhaps in the far future, if the world encounters some greater catastrophic event that we have yet to anticipate, or through some technological advance that may alter the course of evolution, then life as we currently know it might no longer be recognizable or quantifiable (Bostrom, 2002; Rowe & Beard, 2018).

### **6.2.2 More species are needed for a robust evolutionary study**

With all the model systems available for evolutionary and developmental study, relying on a single species to represent an entire clade is not reasonable and limits the strength of the conclusions that can be drawn (Weinstein & Ciszek, 2002). This is especially true when attempting

to discern among the variety of traits that have arisen due to evolution. The same can be said for any biological study, where incorporating multi-species data will almost always undoubtedly improve the resolution of what is being observed (Block et al., 1999; Hollowed et al., 2000). The feasibility of performing experiments on as many different organisms as we would like must also be considered, and is yet another limitation. At some point a balance must be struck between working with the resources available in order to maximize useful data, and deciding whether the time, cost, and effort of expansion is worth the trouble, or will only result in diminishing returns (Fleming & Alexander, 2002). That said, if more frog species and other representative vertebrates can be incorporated into this study, such as data from even earlier-diverged cartilaginous fishes like little skate and ratfish—work that is currently being researched by PhD candidate, Oghenevwogaga (Joseph) Atake—those datasets should add much greater insight into the evolution of skeletal cells. Other underutilized non-avian reptilian and non-anuran amphibian models, such as *Anolis* lizards and urodelian salamanders should also be considered (Kulyk & Zalik, 1982; Benton, 1990; Rasys et al., 2019), especially for this type of study which placed emphasis on intermediate clades for discerning patterns within vertebrate evolution.

### **6.2.3 Vertebrate metamorphosis is unique to amphibians**

Comparing skeletal development in the amphibian to other vertebrate models is complicated by metamorphosis (Laudet, 2011). An equivalent process is generally not found in other vertebrates, at least to the extent experienced by amphibians. For instance, even though zebrafish undergo metamorphosis (McMenamin & Parichy, 2013), the changes are nowhere near as dramatic, and it could technically be argued that all vertebrates undergo a minor version of metamorphosis during their development. The extreme transformation of a tadpole to a frog is a limitation that must be considered when drawing conclusions. While the ceratohyal was mostly studied before the premetamorphic stages (early NF40s; Segerdell et al., 2013), analysis of the humerus and medial angulosplenic occurred just as metamorphosis was beginning (NF57; Nieuwkoop & Faber, 1994). This might account for the deviations that were observed during skeletal development. Publications have illustrated in great detail how drastic the reshaping and reorganization of amphibian skeletal elements can be through apoptosis and resorption—especially in the head, which makes up most of the tadpole (Rose, 2009; Rose et al., 2015). It is

possible fluctuations in the levels of chondrogenic (and osteogenic) genes being studied could be a direct consequence of these metamorphic changes alone and nothing to do with an evolutionary pattern or connection.

#### **6.2.4 Technical limitations**

In terms of technical limitations, it had been mentioned before that some protocols (e.g., RNA *in situ* hybridization) might not have been sensitive enough to detect low levels of gene expression, or not quantitative enough to gauge the difference between higher and lower levels. This could have potentially led to incorrect conclusions. For example, perhaps *col10a1* expression was present in mature cartilage or the expression of chondrogenic markers was much stronger in frog osteoblasts than what had been observed. This could explain why others had shown *col10a1* expression in bone, whereas our experiments did not (Aldea et al., 2013). The added sensitivity of RNA-seq should have alleviated most of those concerns, although a third independent validation study (e.g., qPCR) would certainly have been useful to resolve this issue. Other limitations regarding developmental timing and the different sources from where skeletal cells had been analyzed were already addressed in Chapter 4.

Another issue pertaining to RNA *in situ* assays involved the use of plasmids that were sent from other labs, some of which belonged to *Xenopus laevis*. While *X. laevis* and *X. tropicalis* genomes are highly conserved (Yanai et al., 2011), there was a chance that expression patterns were not as representative or as strong as they could have been. For every RNA probe that was used, the same concentrations, temperatures, hybridization times, etc., were followed, but ideally these steps should have been optimized for each since nucleic acids react differently according to their GC content (Yang et al., 1999); although the concentrations and hybridization times followed here were likely in excess. The potential for cross-reactivity of anti-sense RNA probes with mRNA isoforms was also a concern that could have affected results. For example, *col2a1* has alternative splice forms, a shorter and longer version, where only the short-form characterizes cartilage (Nah et al., 2001). Therefore, an improperly designed probe might be detecting non-cartilage tissues as well. This issue should have been resolved by comparing expression signals with regions of interest through histology. Adjacent sections were stained with Safranin O or trichrome to determine where cartilage or bone was located, respectively. Signals from RNA ISH were overlaid

with these regions to confirm that expression was specific to a particular tissue type and not the surrounding tissues.

LCM-RNAseq required cells to be captured within 30 mins or less since RNA has a tendency to degrade, but what if some RNA transcripts were more prone to degradation than others (Bernstein et al., 2002; Wang et al., 2002; Schwanhäusser et al., 2011)? During laser capture, this possibility could lead to inaccurate results, making it seem as though there were higher or lower counts of a particular gene. Another concern with LCM-RNAseq was the possible misrepresentation of captured cells from mature cartilage of the humerus. As highlighted in Chapter 5, hypertrophy has a very unusual expression pattern in the frog. Newly hypertrophic chondrocytes expressed higher levels of *sox9* and *col2a1* than older, more advanced hypertrophic chondrocytes (Fig. 5.2). This information was not known before LCM-RNAseq was performed. Therefore, the possibility exists that captured regions may have been more biased towards cells that were more lateral to the mid-diaphysis (and newly hypertrophic) than to centralized (and older hypertrophic) cells of the mid-diaphysis. This could have affected results and been a potential reason for why average normalized counts of early chondrogenic markers in MAT were so high compared to IMM (Table 4.4). When sectioning a humerus, the majority of sections would have been collected from these more lateral regions of higher expression since they exist on either side of the mid-diaphysis.

Preliminary analysis of the RNA-seq data was limited and biased since candidate cartilage genes were chosen. However, these genes were selected based on their importance in cartilage and bone development (Eames et al., 2003; Cole, 2011; Gómez-Picos & Eames, 2015). A problem inherent to the RNA-seq data itself was the variation in counts between samples that could have affected the calculations of candidate gene ratios in osteoblasts. This was evidenced by the large fluctuation in values from sample to sample (Table 4.1), which resulted in only a small percentage of genes having statistical significance. This was true for all species (not shown). Even with comprehensive data, there was still the potential issue of a small sample size ( $n = 3$ ) affecting results due to this misrepresentation.

Finally, the sheer amount of data generated by RNA-seq meant there was the potential for mishandling or mislabeling of information due to outdated (or even incorrectly updated) online repositories (e.g., NCBI, Ensembl). For instance, relying on the automated process of assigning gene IDs could accidentally result in the wrong gene(s) being assigned, or a gene of interest being missed altogether. These databases are maintained by highly qualified personnel (<https://www.ncbi.nlm.nih.gov/books/NBK3840/>), but there was always the possibility of human error. Albeit, the benefits far outweigh any risks of inaccuracy given it would be impossible to handle these large volumes of data otherwise.

## **6.3 Future directions**

### **6.3.1 Two frogs are better than one**

Despite anecdotal evidence that *Xenopus* frogs can move on land if drier conditions required them to migrate to new water sources (Loveridge, 1976; De Villiers & Measey, 2017), they are classified as fully aquatic. Therefore, to complement and bolster the skeletal observations that have been made thus far in an aquatic frog species, similar research should be performed on a truly land-based frog, like *Rana pipiens*. This would narrow the types of developmental constraints that might have been at play in shaping amphibian skeletal cell development. Other than phyletic constraint, physical constraints can also place a limit on what biological processes can occur (Gilbert & Barresi, 2016). Life in water versus on land are subject to a different set of conditions that have affected how organisms have evolved and can develop (Stearns, 1992; Volkmann & Baluška, 2006; Dawson & Hamner, 2008; Webb, 2012; Gearty et al., 2018). The idea is to eliminate the effects of external forces and attribute the strength of phyletic constraint to the observations being made. If land-based and aquatic frogs show similar traits, then likely it was a constraint imposed upon them by a common ancestor. If a trait of interest, like chondrogenic expression in osteoblasts, was completely lost in land frogs, then this would support the environment as being the more probable cause for its disappearance in land tetrapods.

### 6.3.2 Expression data of many important skeletogenic markers still need to be assayed

Many mature cartilage and bone genes (e.g., *runx2*, *col1a1*, *col1a2*, *bglap*, *spp1*, *sparc*, *dmp1*, and more) were provided to us by collaborators that, unfortunately, have not been thoroughly tested yet due to the Covid-19 pandemic. Future experimental assays should prioritize two prominent markers of mature cartilage, *runx2* (Eames et al., 2003, 2004; Eames & Helms, 2004; Yoshida et al., 2004) and *spp1* (also known as bone sialoprotein, or formerly, osteopontin; Gerstenfeld & Shapiro, 1996), to see if they are expressed where *col10a1* expression was lacking in hypertrophic chondrocytes. Even then according to one report, *runx2* was poorly expressed in hypertrophic chondrocytes of *X. tropicalis* (Miura et al., 2008). Considering the role of Runx2 during cartilage maturation and its direct control in regulating *Col10a1* expression (Zheng et al., 2003; Li et al., 2011), this might account for some of the discrepancies (e.g., negative *col10a1* results) we see in frog skeletal development versus other species. Published results have also shown *runx2* expression in mesenchymal precursors of the skull (Kerney et al., 2007). This was confirmed with a trial run of *runx2* that was found to be positive in the condensation phases of some early-to-mid NF30s samples before the pandemic hit (Fig. 6.1). *runx2* should be highly expressed in bone as well and can serve as a positive control in that regard (Ducy & Zhang, 1997; Komori et al., 1997; Otto et al., 1997; Eames et al., 2003, 2004; Eames & Helms, 2004). *spp1* is a late mature cartilage marker (Gerstenfeld & Shapiro, 1996) that might show up where *col10a1* was expected to be during hypertrophy. PhD candidate, Rafa Grecco Machado, had previously demonstrated a similar scenario in the chick humerus (data not shown). Though unlikely, transient *col10a1* expression could be the reason why it was not detected in mature cartilage of the frog. It is possible that *spp1* might immediately follow this hypothetical rapid downregulation of *col10a1*. Previous RNA ISH and RT-PCR studies in *Xenopus tropicalis* have characterized *spp1* expression patterns in earlier and later stages of calvarial and limb bone development (Espinoza et al., 2010). Another interesting skeletal gene to investigate would be *bglap*, a marker of cartilage and bone maturation (McKee et al., 1992; Nakase et al., 1994; Roach, 1994; Lui et al., 2019), since our RNA-seq data showed no *bglap* expression whatsoever in cartilage or bone of the frog (Table 4.3).

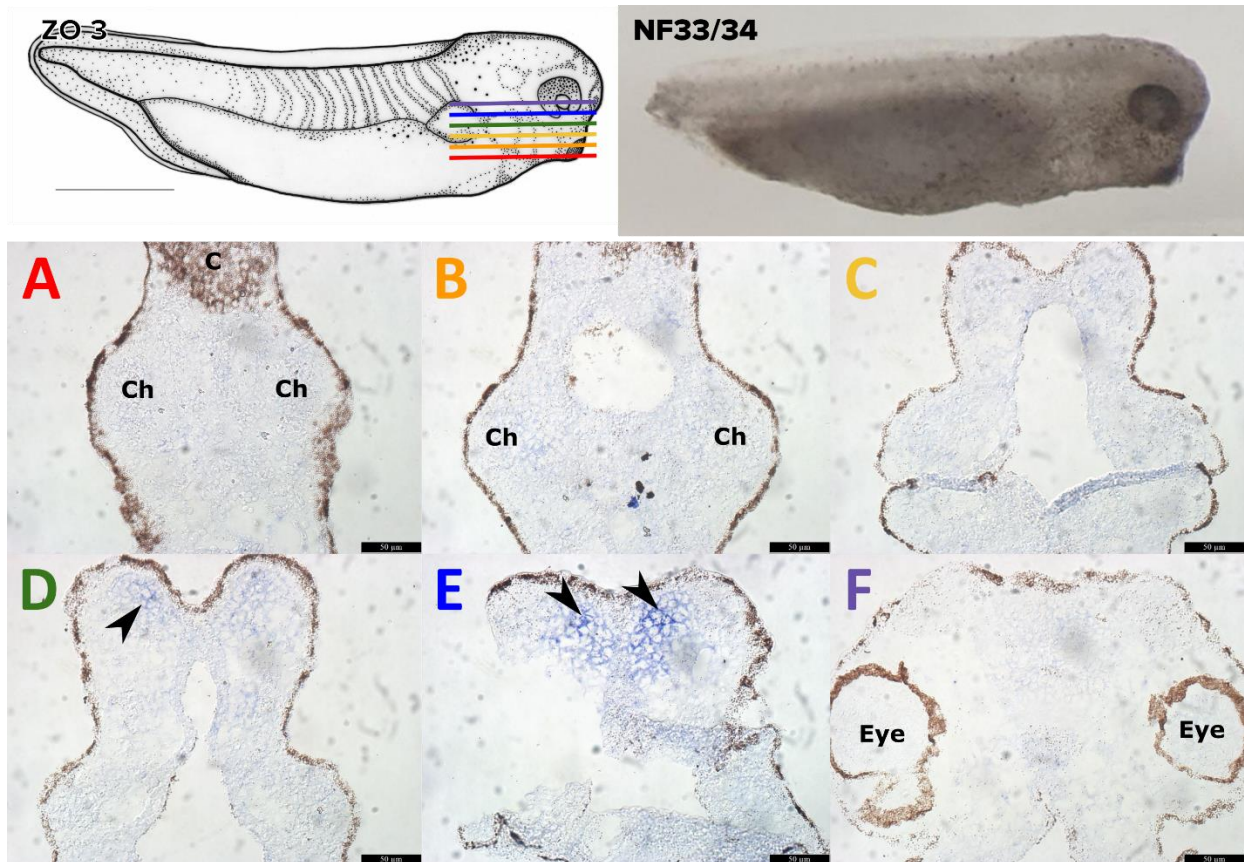


**Figure 6.1 | Preliminary RNA *in situ* hybridization assays of *runx2* show expression at stages NF33/34. [A-F] Coronal sections from ventral to dorsal are color coded and approximately correspond to the colored lines in a ZO 3 (NF33/34) schematic taken from Ziermann & Olsson, 2007. Arrowheads point at expression of *runx2* in anterior head structures. Abbreviations: C=cement gland; Ch=ceratohyal. (Credit: ZO 3 image adapted from Ziermann & Olsson, 2007).**

To further validate RNA-seq and ISH data, immunohistochemical and other functional studies with Sox9 and Col10 (collagen type X protein encoded by the *Col10a1* gene; Apte et al., 1991) should be performed to complement those already completed with Col2. In fact, unpublished data from our collaborators have already demonstrated Sox9 protein expression in frog osteoblasts (Cervantes et al., in preparation), which supports the notion that low counts of transcription factors (e.g., seemingly negligible *sox9* levels from our RNA-seq data) can still be biologically relevant (Raithel et al., 2016). It is expected that Col10 protein would be negative throughout the skeletal regions being investigated, given previous *col10a1* RNA *in situ* results. For a positive control, Col10 could be tested on teeth of a stage NF59 (or later) since *col10a1* appeared to be expressed in dentin of the teeth (Fig. 4.6). Also, qPCR (quantitative PCR)

experiments would be highly recommended to serve as yet another independent method to verify all the results presented in this thesis.

### **6.3.3 Hedgehog signaling may have a different role in amphibian skeletogenesis**

Comparison of limb and head structures within the frog and to published results may have led to some novel discoveries. There appeared to be molecular features that distinguished frog skeletal cells based on anatomical location and mode of ossification that had not previously been characterized before. Firstly, our results demonstrated that the maturation of chondrocytes can vary in the humerus and ceratohyal. Secondly, and more speculatively, perichondral osteoblasts of the limb versus dermal osteoblasts of the lower jaw might have different levels of chondrogenic expression. A common thread amongst all these observations is the expression of *Ihh* (Indian hedgehog), which regulates cartilage maturation and is needed for bone formation (Vortkamp et al., 1996; St-Jacques et al., 1999; Abzhanov et al., 2007; Huycke et al., 2012; Shi et al., 2015).

Hedgehog signaling is a ligand-dependent transcription pathway mediated by two transmembrane protein receptors, Patched (PTC, encoded by the *Ptch1* gene) and Smoothen (SMO) (Wilson & Chuang, 2010; Hadden, 2014). PTC exerts inhibitory control over SMO, and as such, releases this blockage when bound by IHH or one of its homologs (Vortkamp et al., 1996). This leads to a cascade of phosphorylation events that culminates in the activation and nuclear translocation of a GLI transcription factor (encoded by *Gli1*), which subsequently drives expression of Hedgehog target genes (Wilson and Chuang 2010). One of these downstream targets, either directly or indirectly, is *PTHrP* (parathyroid hormone-related protein; Vortkamp et al., 1996). Together, *Ihh* and *PTHrP* form a negative feedback loop that regulates chondrocyte proliferation and the rate of hypertrophy (Vortkamp et al., 1996; Chen et al., 2008). During endochondral ossification, *Ihh* signals are required from prehypertrophic chondrocytes to activate *PTHrP* in periarticular and proliferating chondrocytes, and this *PTHrP* expression, in turn, limits hypertrophy by suppressing *Ihh* (Minina et al., 2001; Chen et al., 2008; Long & Ornitz, 2013; Yang et al., 2015). The complexities of this interaction might account for why both over- and under-expression of *Ihh* in transgenic and mutant mice have demonstrated the ability to delay hypertrophic differentiation of chondrocytes (St-Jacques et al., 1999; Minina et al., 2001). On the

other hand, mice that have *Ihh* knocked out completely fail to produce *PTHrP*, whose under-expression results in the premature hypertrophic differentiation of chondrocytes (Karaplis et al., 1994), since *PTHrP* is normally needed to keep chondrocytes in a proliferative state (Kronenberg, 2003); further validation of this is seen when *PTHrP* overexpression instead causes a delay in hypertrophy (Weir et al., 1996). Control of chondrocyte hypertrophy by *Ihh* can also be more direct with opposing effects that are independent of *PTHrP* (Vortkamp et al., 1996; Kobayashi et al., 2002, 2005; Mak et al., 2008). *PTHrP*-null mice that have *Ihh* knocked out experience delays in chondrocyte hypertrophy, whereas overexpressing *Ihh* in these same mutants promotes hypertrophy (Mak et al., 2008). With *PTHrP* deactivated, acceleration of hypertrophy can similarly be achieved through inactivation of *Ptch1*, a negative regulator of Hedgehog signaling, (Mak et al., 2008).

It would be interesting to do functional studies involving Hedgehog signaling given its importance in limb development and craniofacial morphogenesis (Riddle et al., 1993; Cordero et al., 2007), to see if similar effects are observed in the frog. Published results on the *Xenopus* homolog of *ihh* during endochondral ossification have already shown that the usual downstream targets of Hedgehog signaling, like *gli1* and *ptch1*, are absent in proliferating chondrocytes (Moriishi et al., 2005). Proliferating chondrocytes from articular cartilage and the growth plates express *PTHrP* and therefore have a very important role in regulating the rate of cartilage maturation (Lee, 1995; Vortkamp et al., 1996; Kronenberg, 2003; Chen et al., 2008; Macica et al., 2011). Perhaps this has something to do with why early chondrogenic markers are so highly expressed during amphibian skeletal cell development, since *gli1* and *ptch1* are part of the Hedgehog pathway that (directly or indirectly) regulates chondrocyte proliferation and maturation (Vortkamp et al., 1996; Karp et al., 2000). If this pathway is disrupted, proliferating chondrocytes might not be able to control the rate of hypertrophic differentiation by repressing prehypertrophy through *ihh*-induced *PTHrP* expression (Vortkamp et al., 1996; Chung et al., 1998). This could be a factor for why hypertrophy occurs so quickly in the head cartilages. The rapid rate of expansion could also be related to why immature cartilage markers remain so high even once chondrocytes begin to mature (i.e., not enough time for downregulation). Therefore, in limb cartilage and bone, knocking out *ihh* (or *PTHrP*) warrants further investigation. A working hypothesis is that this may have less deleterious

effects in the frog compared to other vertebrates since the Hedgehog pathway appears to be incomplete even under normal conditions. Based on the preliminary information available, it seems Hedgehog signaling could have something to do with the unusual development of amphibian skeletal cells.

#### **6.3.4 Why are chondrogenic genes so highly expressed in amphibian skeletal cells?**

Immature cartilage markers like *sox9* and *col2a1* (and possibly more) were being expressed in mature cartilage and bone of amphibians at levels not usually found in other vertebrate models (Table 4.3). Do the persistent expression of these genes have anything to do with the rapid and sustained hypertrophy of the head cartilages? Could this be preventing parts of the anuran cranial skeleton from undergoing endochondral ossification (Porter & Vial, 1974)? Sustained *Sox9* expression is known to suppress *Runx2*—and hence, prevent cartilage maturation and bone formation (Eames et al., 2003, 2004; Eames & Helms, 2004; Zhou et al., 2006)—though more specific to this situation, persistent levels of *Sox9* in hypertrophic chondrocytes have been shown to impair their transdifferentiation into osteoblasts in mice (Lui et al., 2019). It would be interesting to knock down or silence these chondrogenic genes with siRNA and/or miRNA to see what effect this might have on skeletal development in the frog. Some studies have shown that the ceratohyal can calcify in tadpoles with underdeveloped or missing thyroid glands, though in a very specific region (Kerney, Wassersug, et al., 2010). This demonstrates a slight possibility that the frog ceratohyal might still have the ability to undergo endochondral ossification. Moreover, if *col10a1* is not associated with hypertrophy in the larval head cartilages of the frog, perhaps persistent or increasing levels of *sox9* and *col2a1* can be considered frog-specific hypertrophic signatures. Overexpressing these genes should be able to test this hypothesis since the timing of hypertrophy in both the head and limbs have been well established. It would be possible to make precise measurements to see if ectopically inducing *sox9* and *col2a1* were able to reduce the amount of time it takes to become hypertrophic. In adult skate, it has been shown that the persistence of *sox9* and *col2a1* (also *sox5* and *sox6*) correlate with their ability to spontaneously repair cartilage injuries (Marconi et al., 2020). Could this be related to the ability of *Xenopus* frogs to regenerate limbs and quickly repair skull injuries as well (Suzuki et al., 2006; Mitogawa et al., 2018; Muñoz et al., 2018)?

### **6.3.5 Mature chondrocytes may share more genes with immature chondrocytes than osteoblasts in the amphibian**

Originally, it had been proposed that osteoblasts may have evolved by co-opting the gene regulatory network of mature chondrocytes (Gómez-Picos & Eames, 2015). This arose from the observation that mature chondrocytes have more genetic overlap with osteoblasts than immature chondrocytes (Vortkamp et al., 1996; Inada et al., 1999; Neuhold et al., 2001; Zaragoza et al., 2006; Abzhanov et al., 2007; Mak et al., 2008; Eames et al., 2012; Huycke et al., 2012; Nishimura et al., 2012; Weng & Su, 2013). It would be interesting to see if this were still true in the frog as well, or if the expression of *sox9* and *col2a1* in persistently hypertrophic chondrocytes was a sign of a stronger overlap between mature and immature cartilage instead. Normalized counts from the frog humerus showed many early chondrogenic genes were at higher levels in mature cartilage than immature cartilage (Table 5.1), which seemed to blur the line between these two cell types. LCM-RNAseq on immature and mature cartilage from the ceratohyal would be the next logical step to verify if this trend continued. It would be challenging to capture immature cartilage from the ceratohyal for two reasons: 1) there is a very small window of opportunity to capture cells before they become hypertrophic, so immature and mature cartilage would have to be captured at different stages; 2) the immature ceratohyal is miniscule, therefore multiple samples would need to be pooled together in order to have enough RNA concentration for sequencing.

### **6.3.6 Thyroid hormone inhibition**

Due to the rapid maturation of amphibian head cartilages and known role of thyroid hormone in facilitating hypertrophy in mammals (Bassett & Williams, 2016), we were interested in what effect inhibiting thyroid hormone would have on cartilage development. This experiment had actually already been carried out (see Appendix A), but results were preliminary. To summarize, the goal was to slow down ceratohyal development specifically, but inhibiting thyroid hormone seemed to introduce a global delay instead. These initial findings were promising nonetheless and worth reproducing with a different inhibitor to verify if those observations were indeed accurate.

### 6.3.7 Amphibian head cartilage could be a useful model for osteoarthritis

The persistent hypertrophy of amphibian head cartilage could potentially serve as a model for osteoarthritis research. Ectopic hypertrophic differentiation of chondrocytes frequently accompanies osteoarthritic cartilage, but it is unclear why (Bayles, 1950; Dreier, 2010). While mature cartilage can persist in healthy adults, this is generally restricted to certain regions, like articular cartilage (Yang et al., 2014; Zhou et al., 2014; Hinton et al., 2017; Aghajanian & Mohan, 2018). Articular joints also contain resting chondrocytes, and it is the abnormal hypertrophy of these chondrocytes that are associated with osteoarthritis (Dreier, 2010). In the amphibian, hypertrophic cartilage makes up major structures of the cranial skeleton, such as the ceratohyal, palatoquadrate, and Meckel's cartilage (Porter & Vial, 1974; Rose, 2009; Rose et al., 2015). What is the difference between hypertrophic cartilage that can exist indefinitely as healthy tissue versus hypertrophic cartilage that becomes pathological? Furthermore, hypertrophic cartilage can also mineralize and die during a normal process like endochondral ossification (Kronenberg, 2003; Mackie et al., 2008; Long & Ornitz, 2013). Even though *Col10a1* is a classical hypertrophic marker, here we have an amphibian model that naturally lacks its expression and lives with arthritic-like cartilage in its head. Are frogs able to maintain 'healthy' hypertrophy because of the absence of a gene that would normally be upregulated? Or perhaps are higher levels of *sox9* and *col2a1* important for maintaining this phenotype without having any deleterious effects? What would happen if these genes were ectopically expressed or knocked down? The driving mechanism behind chondrocyte hypertrophy is still poorly understood despite recent advances in this area of research (Cooper et al., 2013). Perhaps this is a yet-to-be defined subclass of cartilage that can be considered as "hypertrophic" immature cartilage. Investigating how amphibian head cartilages develop and are able to maintain this hypertrophic state may provide new insights into osteoarthritis that had previously not been explored.

In closing, these are just some of the potential topics for future research that can give us insight into evolution, development, and health. For the time being, there are plans for myself, Dr. Patsy Gómez Picos, and Dr. Katie Ovens to collaborate on an osteoblast evolution paper that will incorporate my frog data with theirs to address some of these issues. Dr. Eames and I also have

plans to publish of our cartilage results and are working on a skeletal development manuscript for *Xenopus tropicalis*.

## APPENDIX A

### Thyroid hormone inhibition

#### **A1.1 Thyroid hormone affects many aspects of skeletal development**

The thyroid is an endocrine gland best known for maintaining metabolic homeostasis (Mullur et al., 2014). It also has important roles in skeletal development, bone maintenance, and repair (Mackie et al., 2008; Kim & Mohan, 2013; Bassett & Williams, 2016). Whether the thyroid had a part to play in skeletal cell evolution (or other systems and cell types, in general) is currently not known (Sachs & Campinho, 2019). In recent years, some prominent skeletal biologists have even begun to advocate that bone itself should be considered as part of the endocrine system, due to its own ability to regulate certain metabolic processes (Guntur & Rosen, 2012; Karsenty & Oury, 2012; Kim & Mohan, 2013). The hormones secreted by the thyroid gland have two forms (Fig. A1):  $T_4$  (inactive thyroxine) and  $T_3$  (biologically active triiodothyronine), the latter of which directly influences many skeletogenic pathways, including, but not limited to the proliferation and differentiation of chondrocytes and osteoblasts (Kim & Mohan, 2013). Of particular interest to us was the direct influence  $T_3$  had over hypertrophy (Bassett & Williams, 2018). This was due to the observation that head cartilages of *Xenopus tropicalis* became hypertrophic very rapidly, early in development (Fig. 5.3), and then remained this way into adulthood (Porter & Vial, 1974; Thomson, 1986). Since thyroid hormone (TH) has been known to influence hypertrophy (Bassett & Williams, 2016), we hypothesize inhibiting thyroid hormone slows the rate of hypertrophy.

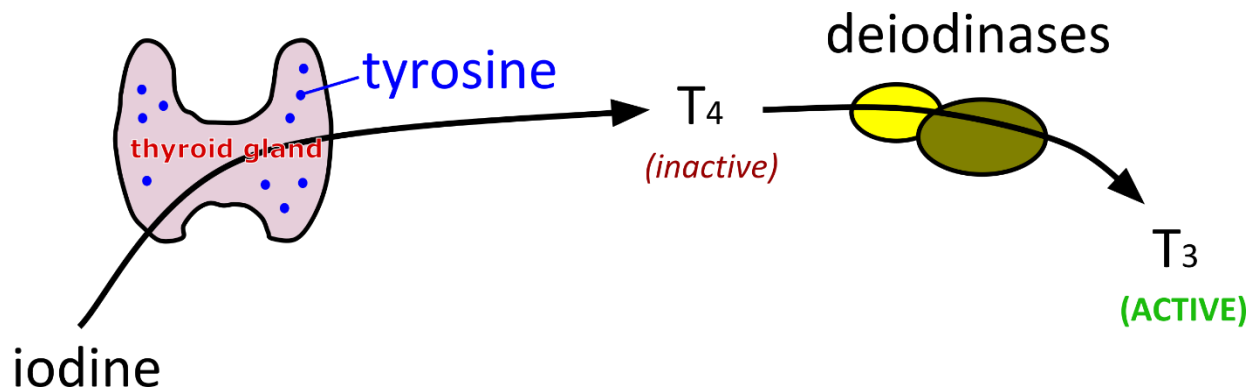


**Figure A1| A simple schematic illustrates how thyroid hormone is biologically activated.** Iodine uptake by the thyroid gland combines with tyrosine to form T<sub>4</sub>, which is converted to T<sub>3</sub> by deiodinases.

### **T<sub>3</sub> is active even before the thyroid begins to function**

The thyroid forms at stage NF43 but does not begin to secrete TH until NF48 (Fini et al., 2012). Some TH could potentially be introduced exogenously at NF45/46, around the time when tadpoles lose their yolk and begin to feed on their own (Brown et al., 2005; Rose, 2014). It had been discovered recently that levels of TH were already present at the embryonic and very early larval stages (before a functional or fully formed thyroid gland) thanks to maternally-provided stocks of both T<sub>4</sub> and T<sub>3</sub> (Morvan-Dubois et al., 2008; Fini et al., 2012). These levels were also demonstrated to be biologically relevant since blocking endogenous T<sub>3</sub> impacted neuronal development (Fini et al., 2012). This was highly informative as TH is famously known for facilitating metamorphosis, but does not begin to ramp up production until stage NF56 (Brown & Cai, 2007; Wen & Shi, 2016). Synthesis of TH receptors begins around stage NF35 (Yaoita & Brown, 1990; Eliceiri & Brown, 1994; Brown & Cai, 2007). Unbound TH receptors repress nuclear transcription to slow growth and development (Hu & Lazar, 2000; Morvan-Dubois et al., 2008). Further evidence to support this came from knocking down TH receptors, which increased the rate at which tadpoles grew (Wen & Shi, 2015; Wen & Shi, 2016). Once bound to a T<sub>3</sub> ligand, this releases the inhibition and allows for the regulatory processes that drive metamorphosis (Buchholz et al., 2006; Brown & Cai, 2007; Wen & Shi, 2016).

### **T<sub>3</sub> competitors were required to inhibit binding of thyroid hormone to receptors**

Since it was revealed that thyroid hormone could indeed play a role at the stages our skeletal studies were focused on, an inhibitor was needed that would specifically bind to or compete

against T<sub>3</sub>. Most thyroid research in frogs used drugs designed to block TH production during the metamorphic stages (Callery & Elinson, 2000; Degitz et al., 2005; Buchholz et al., 2006; Coady et al., 2010; Tietge et al., 2010; Smirnov & Vassilieva, 2014; Rose & Cahill, 2019). This would not have been suitable for our purposes since our investigations were much earlier in development (pre-NF44), when T<sub>3</sub> had not begun production but was already present (Morvan-Dubois et al., 2008; Fini et al., 2012). Two candidates known to block thyroid activity in *Xenopus* frogs at stages before thyroid gland formation were found: 1) TBBPA (tetrabromobisphenol A), a naturally-occurring flame retardant with structural similarities to TH (Johnson-Restrepo et al., 2008; Fini et al., 2012; Zhang et al., 2014; Yamauchi, 2016; Mengeling et al., 2017; Wang et al., 2017) and 2) NH-3, a synthetic T<sub>3</sub> antagonist (Lim et al., 2002; Nguyen et al., 2002; Fini et al., 2012; Mengeling et al., 2017). NH-3 was kindly sent to us by Drs. Jean-Baptiste Fini and Barbara Demeneix from the National Museum of Natural History in France.

### **Rationale for the thyroid hormone inhibition experiment**

The purpose of this experiment was to learn what effect TH had on the maturation of chondrocytes in the skeletal head structures of the developing tadpole. From Chapter 5, it was shown that the ceratohyal became hypertrophic in mere hours after differentiating into cartilage. By exposing early larvae to a TH inhibitor just prior to the formation of the ceratohyal, the hope was to induce a delay in maturation. Instead, our preliminary results from a single trial of TBBPA exposure demonstrated a global delay in development, not just cartilage maturation. This was consistent with previous research which had sped up tadpole development by knocking down TH receptors (Wen & Shi, 2015, 2016).

## **A1.2 Materials and Methods**

### **Use of lab animals**

*Please refer to previous materials and methods in Chapter 4 (see page 29).*

### **Frog mating**

*Please refer to previous materials and methods in Chapter 4 (see page 29).*

## Exposure of tadpoles to thyroid hormone inhibitor

We adapted a thyroid inhibition protocol based on work described previously (Fini et al., 2012; Zhang et al., 2014; Wang et al., 2017), with modifications to suit our stages of interest (Fig. A2). Stage NF35 tadpoles were targeted since this was when TH receptor synthesis began (Yaoita & Brown, 1990; Eliceiri & Brown, 1994; Brown & Cai, 2007) and chondrogenesis had not yet begun (NF40-41; Lukas & Olsson, 2017). Ten individual beakers containing NF35 tadpoles were placed into a 27-28 °C water bath. Each beaker was an experimental group filled with 100 ml of TBBPA or TBBPA with 1 nM T<sub>3</sub> at concentrations of 10 nM, 100 nM, 500 nM, and 1000 nM, respectively. The remaining control groups were 0.01% DMSO and 1 nM T<sub>3</sub>. Experimental groups were exposed for 5 hrs, 7 hrs, 10 hrs, 26 hrs, and 30 hrs, then compared to untreated tadpoles through Safranin O staining. Untreated tadpoles were raised in standard 0.1X MBS alongside experiment groups.

## Fixation, processing, and sectioning for histology

*Please refer to previous materials and methods in Chapter 4 for tissue fixation, processing, and sectioning protocols (see page 31).* Coronal sections were obtained from the ceratohyal at stages NF35 to NF45.

## Histology

### Safranin O and trichrome section histology

*Please refer to previous materials and methods in Chapter 4 (see page 32).*

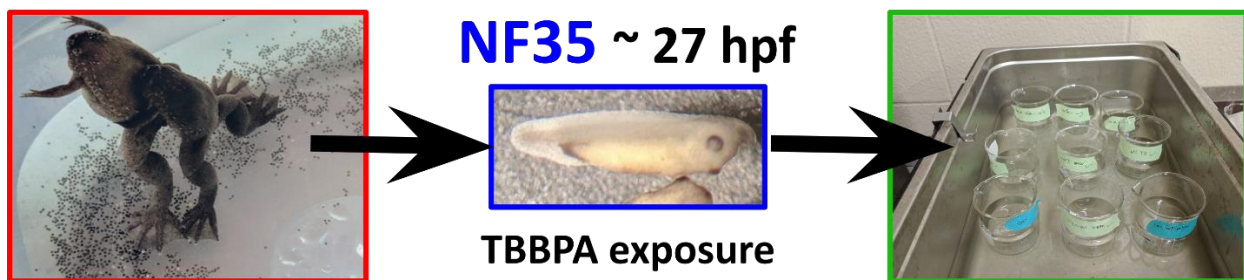


**Figure A2 | Experimental design of thyroid hormone inhibition experiment.** NF35 tadpoles (27 hpf) were exposed to varying concentrations of TBBPA for up to 30 hours.

## **Statistical analysis**

An independent samples t-test was used to determine if there was any significant difference between each experiment group and untreated samples. Alpha levels were set at  $\alpha = 0.05$ . Only the 1000 nM experimental groups were analyzed. From these datapoints, a line graph was generated with IBM SPSS Statistics (Build 1.0.0.1447).

### **A1.3 Preliminary results**

Exposing tadpoles to 1000 nM TBBPA produced a global delay in development, even if 1 nM  $T_3$  was added to counteract the effects of TBBPA (Fig. A3). By 30 hrs of exposure time, TBBPA-treated tadpoles had fallen up to three stages behind untreated tadpoles. According to a one sample t-test comparing experimental groups to untreated samples, differences were significant after 5 hrs (for the  $T_3$  group), 7 hrs ( $T_3$ ), 10 hrs (DMSO and TBBPA), 26 hrs (TBBPA and TBBPA+ $T_3$ ), and 30 hours (TBBPA and TBBPA+ $T_3$ ). There were no other obvious defects otherwise.

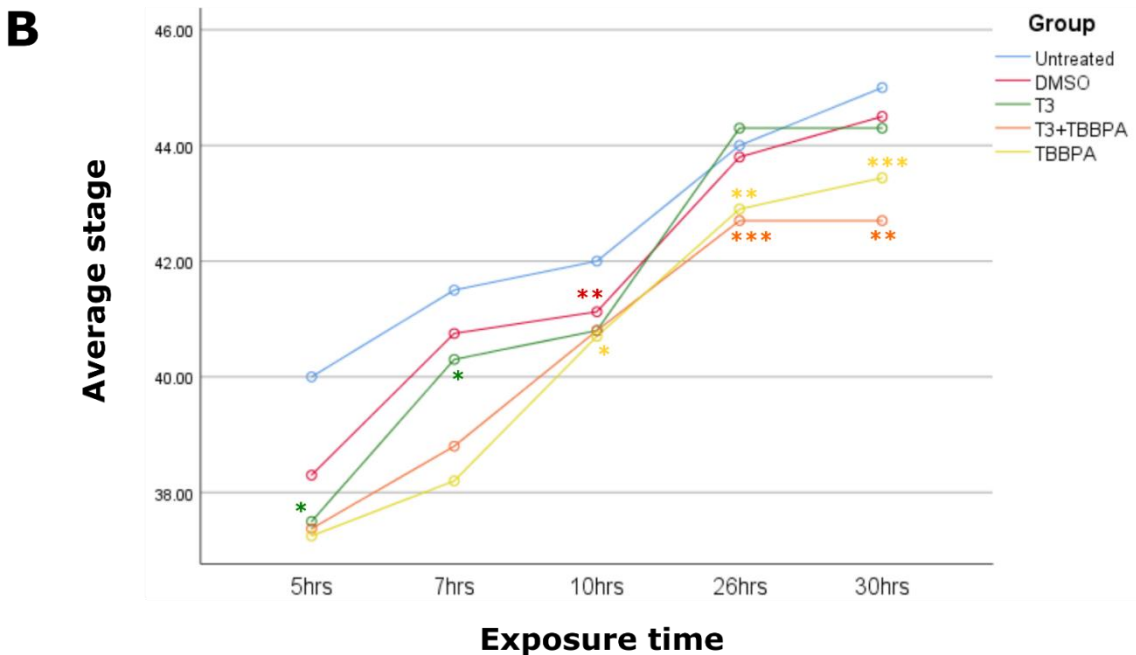
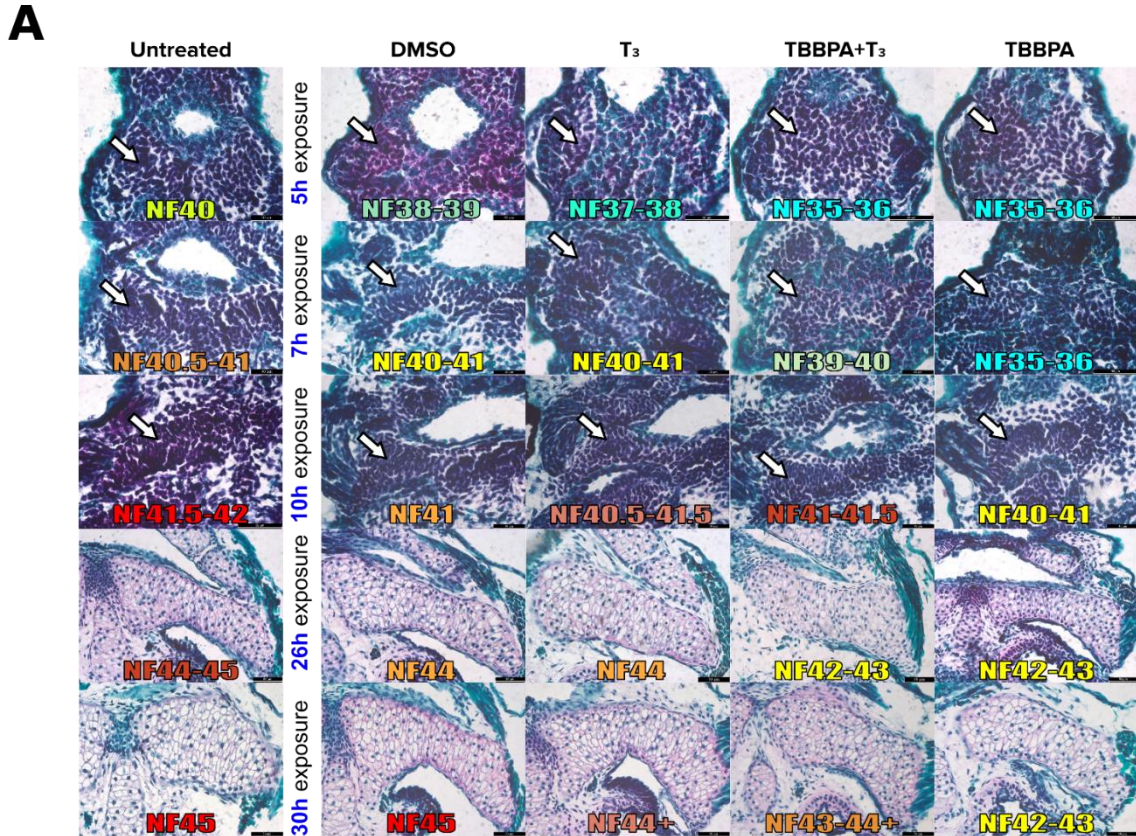


**Figure A3] Inhibiting thyroid hormone with TBBPA produced a global delay in development. [A]** Histological sections of all experimental groups stained with Safranin O. A representative sample was chosen for each group and time point. White arrows point at one half of the ceratohyal in experimental groups at 5h, 7h, and 10h after exposure. Samples at 26h and 30h after exposure show all groups have

undergone hypertrophy, but according to external staging, groups exposed to TBBPA are up to 2-3 stages behind in development. **[B]** A one sample t-test was performed for each group and plotted on a graph. Each experimental group at each time point consisted of at least  $n = 3$  up to  $n = 7$ . Asterisks indicate significance at  $*p < 0.05$ ,  $**p < 0.01$ , and  $***p < 0.001$ .

#### **A1.4 Discussion**

The experiment was stopped after 30 hours of exposure once untreated tadpoles had reached stage NF44-45 after the thyroid had already formed by NF43, but before production of new TH would have begun at NF48 (Fini et al., 2012). The p-values obtained from the one sample t-test were two-tailed, meaning there was no directionality to the test. Testing only signified there was a difference, not whether development was faster or slower.

A second attempt had been made to reproduce the results from the first TH inhibition experiment, this time by including NH-3 (a synthetic  $T_3$  competitor) and a higher concentration of  $T_3$  (5 nM). Unfortunately, due to technical difficulties those results were not included. Treatment had been initiated at stage NF32 (instead of NF35) and both TBBPA groups (with and without 1 nM  $T_3$ ) died approximately 10-15 hrs after exposure. The 5 nM  $T_3$  group may have experienced slightly accelerated growth, but significance testing was not performed to support this. Otherwise, no other groups exhibited any noticeable deviation from untreated samples.

## APPENDIX B

### MicroCT and K-Edge Subtraction images

*These images were taken by Dr. Arash Panahifar (CLS) and Oghenevwogaga (Joseph) Atake (microCT scanner). Scans searched for iodine levels and looked at mineralized head structures.*

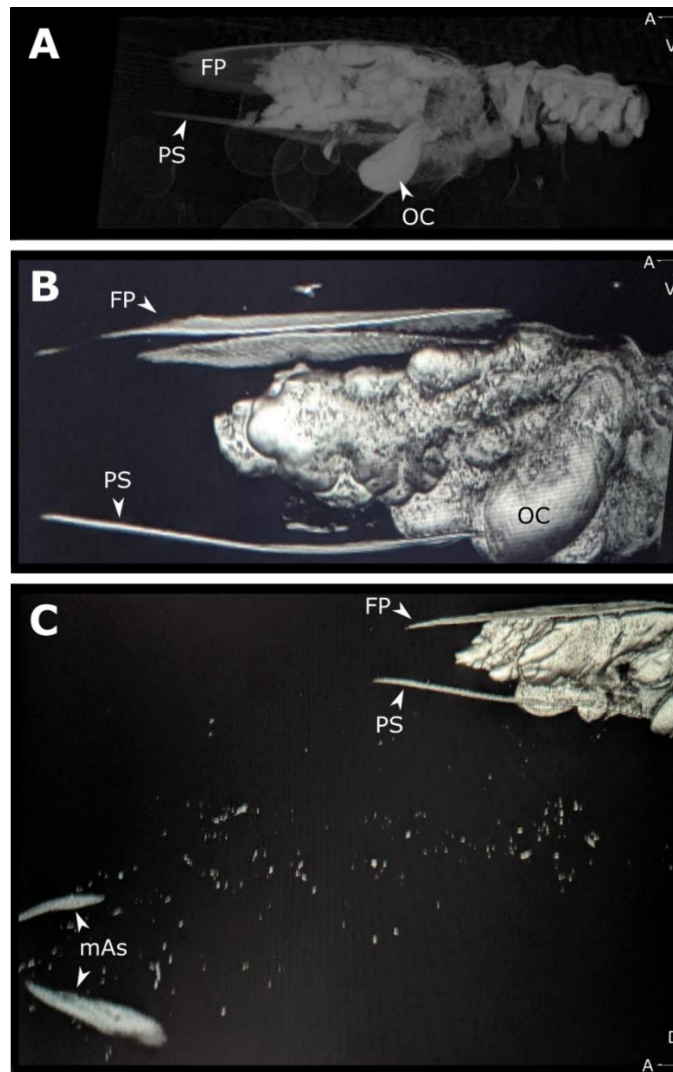


**Figure B1 | 3D images of stage NF57 and NF58 tadpoles during early metamorphosis. [A]** A stage NF58 tadpole scanned at the CLS using K-Edge Subtraction imaging (Panahifar et al., 2016). MicroCT scans of stages **[B]** NF57 and **[C]** NF58. Abbreviations: A=anterior; D=dorsal; FP=frontoparietal; mAs=medial angulosplenic; OC=optic capsule; PS=parasphenoid; V=ventral. (Fig. B1A credit: Dr. Arash Panahifar; Figs B1B,C credit: Oghenevwogaga Joseph Atake).

## REFERENCES

- Abzhanov, A. (2013). Von Baer's law for the ages: Lost and found principles of developmental evolution. In *Trends in Genetics* (Vol. 29, Issue 12, pp. 712–722).  
<https://doi.org/10.1016/j.tig.2013.09.004>
- Abzhanov, A., Rodda, S. J., McMahon, A. P., & Tabin, C. J. (2007). Regulation of skeletogenic differentiation in cranial dermal bone. *Development*, *134*(17), 3133–3144.  
<https://doi.org/10.1242/dev.002709>
- Aghajanian, P., & Mohan, S. (2018). The art of building bone: Emerging role of chondrocyte-to-osteoblast transdifferentiation in endochondral ossification. *Bone Research*, *6*(1), 19.  
<https://doi.org/10.1038/s41413-018-0021-z>
- Agüero, T. H., Fernández, J. P., Vega López, G. A., Tribulo, C., & Aybar, M. J. (2012). Indian hedgehog signaling is required for proper formation, maintenance and migration of *Xenopus* neural crest. *Developmental Biology*.  
<https://doi.org/10.1016/j.ydbio.2012.01.020>
- Akiyama, H., Chaboissier, M. C., Martin, J. F., Schedl, A., & De Crombrughe, B. (2002). The transcription factor Sox9 has essential roles in successive steps of the chondrocyte differentiation pathway and is required for expression of Sox5 and Sox6. *Genes and Development*, *16*(21), 2813–2828. <https://doi.org/10.1101/gad.1017802>
- Aldea, D., Hanna, P., Munoz, D., Espinoza, J., Torrejon, M., Sachs, L., Buisine, N., Oulion, S., Escriva, H., & Marcellini, S. (2013). Evolution of the vertebrate bone matrix: An expression analysis of the network forming collagen paralogues in amphibian osteoblasts. *Journal of Experimental Zoology Part B: Molecular and Developmental Evolution*.  
<https://doi.org/10.1002/jez.b.22511>
- Arendt, D. (2008). The evolution of cell types in animals: Emerging principles from molecular studies. In *Nature Reviews Genetics*. <https://doi.org/10.1038/nrg2416>
- Arendt, D., Musser, J. M., Baker, C. V. H., Bergman, A., Cepko, C., Erwin, D. H., Pavlicev, M., Schlosser, G., Widder, S., Laubichler, M. D., & Wagner, G. P. (2016). The origin and evolution of cell types. *Nature Reviews Genetics*. <https://doi.org/10.1038/nrg.2016.127>
- Atake, O. J., Cooper, D. M. L., & Eames, B. F. (2019). Bone-like features in skate suggest a novel elasmobranch synapomorphy and deep homology of trabecular mineralization patterns. *Acta Biomaterialia*, *84*, 424–436. <https://doi.org/10.1016/j.actbio.2018.11.047>
- Baer, K. E. von. (1828). *Über Entwicklungsgeschichte der Thiere. Beobachtung und Reflexion ... : Vol. Th.1. Bei den Gebrüdern Bornträger.*  
<https://www.biodiversitylibrary.org/item/28306>
- Bassett, J. H. D., & Williams, G. R. (2018). Analysis of physiological responses to thyroid hormones and their receptors in bone. In *Methods in Molecular Biology*.  
[https://doi.org/10.1007/978-1-4939-7902-8\\_12](https://doi.org/10.1007/978-1-4939-7902-8_12)

- Bassett, J H Duncan, & Williams, G. R. (2016). Role of Thyroid Hormones in Skeletal Development and Bone Maintenance. *Endocrine Reviews*, 37(2), 135–187. <https://doi.org/10.1210/er.2015-1106>
- Bates, G. P., Dorsey, R., Gusella, J. F., Hayden, M. R., Kay, C., Leavitt, B. R., Nance, M., Ross, C. A., Scahill, R. I., Wetzel, R., Wild, E. J., & Tabrizi, S. J. (2015). Huntington disease. *Nature Reviews Disease Primers*, 1(1), 15005. <https://doi.org/10.1038/nrdp.2015.5>
- Bayles, T. B. (1950). Hypertrophic Arthritis (Degenerative Joint Disease). *Medical Clinics of North America*, 34(5), 1435–1446. [https://doi.org/https://doi.org/10.1016/S0025-7125\(16\)35372-X](https://doi.org/https://doi.org/10.1016/S0025-7125(16)35372-X)
- Beck, C. W., & Slack, J. M. (2001). An amphibian with ambition: a new role for *Xenopus* in the 21st century. *Genome Biology*, 2(10), REVIEWS1029–REVIEWS1029. <https://doi.org/10.1186/gb-2001-2-10-reviews1029>
- Bedford, T., & Hartl, D. L. (2009). Optimization of gene expression by natural selection. In *PNAS* (Vol. 106, Issue 4).
- Bell, D. M., Leung, K. K. H., Wheatley, S. C., Ling Jim Ng, Zhou, S., Kam Wing Ling, Mai Har Sham, Koopman, P., Tam, P. P. L., & Cheah, K. S. E. (1997). SOX9 directly regulates the type-II collagen gene. *Nature Genetics*, 16(2). <https://doi.org/10.1038/ng0697-174>
- Benjamin, M. (1988). Mucochondroid (mucous connective) tissues in the heads of teleosts. *Anatomy and Embryology*, 178(5). <https://doi.org/10.1007/BF00306053>
- Benjamin, M. (1989). Hyaline-cell cartilage (chondroid) in the heads of teleosts. In *Anat Embryol* (Vol. 179).
- Benjamin, M., & Ralphs, J. R. (1991). Extracellular matrix of connective tissues in the heads of teleosts. In *J. Anat* (Vol. 179).
- Benton, M. J. (1990). Journal of Molecular Evolution Phylogeny of the Major Tetrapod Groups: Morphological Data and Divergence Dates. In *J Mol Evol* (Vol. 30).
- Berendsen, A. D., & Olsen, B. R. (2015). Bone development. In *Bone* (Vol. 80). <https://doi.org/10.1016/j.bone.2015.04.035>
- Bernstein, J. A., Khodursky, A. B., Lin, P.-H., Lin-Chao, S., & Cohen, S. N. (2002). Global analysis of mRNA decay and abundance in *Escherichia coli* at single-gene resolution using two-color fluorescent DNA microarrays. *Proceedings of the National Academy of Sciences*, 99(15), 9697 LP – 9702. <https://doi.org/10.1073/pnas.112318199>
- Bertin, A., Hanna, P., Otarola, G., Fritz, A., Henriquez, J. P., & Marcellini, S. (2014). Cellular and molecular characterization of a novel primary osteoblast culture from the vertebrate model organism *Xenopus tropicalis*. *Histochemistry and Cell Biology*. <https://doi.org/10.1007/s00418-014-1289-8>
- Bi, W., Deng, M., Zhang, Z., Behringer, R. R., & Benoit De Crombrughe, &. (1999). *Sox9 is required for cartilage formation*. <http://genetics.nature.com>

- Blackburn, D. G. (1992). Convergent evolution of viviparity, matrotrophy, and specializations for fetal nutrition in reptiles and other vertebrates. *Integrative and Comparative Biology*, 32(2). <https://doi.org/10.1093/icb/32.2.313>
- Blekhman, R., Oshlack, A., Chabot, A. E., Smyth, G. K., & Gilad, Y. (2008). Gene regulation in primates evolves under tissue-specific selection pressures. *PLoS Genetics*, 4(11). <https://doi.org/10.1371/journal.pgen.1000271>
- Blitz, E., Sharir, A., Akiyama, H., & Zelzer, E. (2013). Tendon-bone attachment unit is formed modularly by a distinct pool of  $\text{Scx}$ - and  $\text{Sox9}$ -positive progenitors. *Development*, 140(13), 2680 LP – 2690. <https://doi.org/10.1242/dev.093906>
- Block, W. M., Finch, D. M., & Brennan, L. A. (1999). Single-species versus multiple-species approaches for management. In *NCASI Technical Bulletin* (Issue 781 I).
- Blum, M., & Ott, T. (2019). *Xenopus*: An undervalued model organism to study and model human genetic disease. In *Cells Tissues Organs* (Vol. 205, Issues 5–6, pp. 303–312). S. Karger AG. <https://doi.org/10.1159/000490898>
- Bostrom, N. (2002). Existential Risks: Analyzing Human Extinction Scenarios. In *Journal of Evolution and Technology* (Vol. 9, Issue 1). <http://www.nickbostrom.com/existential/risks.html> <http://www.nickbostrom.com/existential/risks.pdf>
- Brown, D. D., & Cai, L. (2007). Amphibian metamorphosis. In *Developmental Biology*. <https://doi.org/10.1016/j.ydbio.2007.03.021>
- Brown, D. D., Cai, L., Das, B., Marsh-Armstrong, N., Schreiber, A. M., & Juste, R. (2005). *Thyroid hormone controls multiple independent programs required for limb development in Xenopus laevis metamorphosis*. [www.pnas.org/cgi/doi/10.1073/pnas.0505989102](http://www.pnas.org/cgi/doi/10.1073/pnas.0505989102)
- Brown, S. M. (1980). *Comparative ossification in tadpoles of the genus Xenopus (Anura, Pipidae)* (degree granting institution San Diego State University (Ed.)).
- Buchholz, D. R., Paul, B. D., Fu, L., & Shi, Y. B. (2006). Molecular and developmental analyses of thyroid hormone receptor function in *Xenopus laevis*, the African clawed frog. In *General and Comparative Endocrinology*. <https://doi.org/10.1016/j.ygcen.2005.07.009>
- Burns, A., & Iliffe, S. (2009). Alzheimer's disease. In *BMJ (Online)* (Vol. 338, Issue 7692, pp. 467–471). BMJ Publishing Group. <https://doi.org/10.1136/bmj.b158>
- Callery, E. M., & Elinson, R. P. (2000). Thyroid hormone-dependent metamorphosis in a direct developing frog. *Proceedings of the National Academy of Sciences of the United States of America*, 97(6). <https://doi.org/10.1073/pnas.050501097>
- Cardoso-Moreira, M., Halbert, J., Valloton, D., Velten, B., Chen, C., Shao, Y., Liechti, A., Ascenção, K., Rummel, C., Ovchinnikova, S., Mazin, P. V., Xenarios, I., Harshman, K., Mort, M., Cooper, D. N., Sandi, C., Soares, M. J., Ferreira, P. G., Afonso, S., ... Kaessmann, H.

- (2019). Gene expression across mammalian organ development. *Nature*, 571(7766), 505–509. <https://doi.org/10.1038/s41586-019-1338-5>
- Carroll, S. B. (2005). The origins of form. In *Natural History* (Vol. 114, Issue 9).
- Carroll, S. B. (2008). Evo-Devo and an Expanding Evolutionary Synthesis: A Genetic Theory of Morphological Evolution. In *Cell* (Vol. 134, Issue 1, pp. 25–36). <https://doi.org/10.1016/j.cell.2008.06.030>
- Carroll, S., Grenier, J., & Weatherbee, S. (2001). *From DNA to Diversity, Molecular Genetics and Evolution of Animal Design*.
- Cervantes-Diaz, F., Contreras, P., & Marcellini, S. (2017). Evolutionary origin of endochondral ossification: the transdifferentiation hypothesis. *Development Genes and Evolution*. <https://doi.org/10.1007/s00427-016-0567-y>
- Chiappe, L. M. (2009). Downsized Dinosaurs: The Evolutionary Transition to Modern Birds. *Evolution: Education and Outreach*, 2(2), 248–256. <https://doi.org/10.1007/s12052-009-0133-4>
- Chung, U. I., Lanske, B., Lee, K., Li, E., & Kronenberg, H. (1998). The parathyroid hormone/parathyroid hormone-related peptide receptor coordinates endochondral bone development by directly controlling chondrocyte differentiation. *Proceedings of the National Academy of Sciences of the United States of America*, 95(22), 13030–13035. <https://doi.org/10.1073/pnas.95.22.13030>
- Clack, J. A. (2007). Devonian climate change, breathing, and the origin of the tetrapod stem group. *Integrative and Comparative Biology*, 47(4), 510–523. <https://doi.org/10.1093/icb/icm055>
- Clack, J. A. (2009). The Fish–Tetrapod Transition: New Fossils and Interpretations. *Evolution: Education and Outreach*, 2(2), 213–223. <https://doi.org/10.1007/s12052-009-0119-2>
- Clack, J. A. (2012). *Gaining Ground, Second Edition* (2nd ed.). Indiana University Press. <http://www.jstor.org/stable/j.ctt16gz91r>
- Coady, K., Marino, T., Thomas, J., Currie, R., Hancock, G., Crofoot, J., Mcnalley, L., Mcfadden, L., Geter, D., & Klecka, G. (2010). Evaluation of the amphibian metamorphosis assay: exposure to the goitrogen methimazole and the endogenous thyroid hormone l-thyroxine. *Environmental Toxicology and Chemistry*, 29(4). <https://doi.org/10.1002/etc.74>
- Cole, A. G. (2011). A review of diversity in the evolution and development of cartilage: the search for the origin of the chondrocyte. In *European cells & materials*. <https://doi.org/10.22203/eCM.v021a10>
- Cooper, K. L., Oh, S., Sung, Y., Dasari, R. R., Kirschner, M. W., & Tabin, C. J. (2013). Multiple phases of chondrocyte enlargement underlie differences in skeletal proportions. *Nature*. <https://doi.org/10.1038/nature11940>
- Cordero, D., Tapadia, M., & Helms, J. A. (2007). *The Role of Sonic Hedgehog Signalling in*

- Craniofacial Development BT - Shh and Gli Signalling and Development* (C. E. Fisher & S. E. M. Howie (Eds.); pp. 44–57). Springer New York. [https://doi.org/10.1007/978-0-387-39957-7\\_5](https://doi.org/10.1007/978-0-387-39957-7_5)
- Currie, A. (2013). Convergence as Evidence. *The British Journal for the Philosophy of Science*, 64(4), 763–786. <https://doi.org/10.1093/bjps/axs027>
- Daniels, O., Frisch, J., Venkatesan, J. K., Rey-Rico, A., Schmitt, G., & Cucchiari, M. (2019). Effects of rAAV-Mediated sox9 Overexpression on the Biological Activities of Human Osteoarthritic Articular Chondrocytes in Their Intrinsic Three-Dimensional Environment. *Journal of Clinical Medicine*, 8(10), 1637. <https://doi.org/10.3390/jcm8101637>
- Darwin, C. (1859). On The Origin Of Species. In *October*.
- Dawson, M. N., & Hamner, W. M. (2008). A biophysical perspective on dispersal and the geography of evolution in marine and terrestrial systems. *Journal of the Royal Society Interface*, 5(19), 135–150.
- de Beer, G. (1930). *Embryology and evolution*. The Clarendon Press.
- De Sandre-Giovannoli, A., Bernard, R., Cau, P., Navarro, C., Amiel, J., Boccaccio, I., Lyonnet, S., Stewart, C. L., Munnich, A., Le Merrer, M., & Lévy, N. (2003). Lamin A truncation in Hutchinson-Gilford progeria. *Science*, 300(5628). <https://doi.org/10.1126/science.1084125>
- De Villiers, F. A., & Measey, J. (2017). Overland movement in African clawed frogs (*Xenopus laevis*): Empirical dispersal data from within their native range. *PeerJ*, 2017(11). <https://doi.org/10.7717/peerj.4039>
- Debiais-Thibaud, M., Simion, P., Ventéo, S., Muñoz, D., Marcellini, S., Mazan, S., & Haitina, T. (2019). Skeletal Mineralization in Association with Type X Collagen Expression Is an Ancestral Feature for Jawed Vertebrates. *Molecular Biology and Evolution*, 36(10), 2265–2276. <https://doi.org/10.1093/molbev/msz145>
- Decker, R. S., Koyama, E., & Pacifici, M. (2015). Articular Cartilage: Structural and Developmental Intricacies and Questions. In *Current Osteoporosis Reports* (Vol. 13, Issue 6). <https://doi.org/10.1007/s11914-015-0290-z>
- Degitz, S. J., Holcombe, G. W., Flynn, K. M., Kosian, P. A., Korte, J. J., & Tietge, J. E. (2005). Progress towards Development of an Amphibian-Based Thyroid Screening Assay Using *Xenopus laevis*. Organismal and Thyroidal Responses to the Model Compounds 6-Propylthiouracil, Methimazole, and Thyroxine. *Toxicological Sciences*, 87(2), 353–364. <https://doi.org/10.1093/toxsci/kfi246>
- Deniz, E., Jonas, S., Hooper, M., Griffin, J. N., Choma, M. A., & Khokha, M. K. (2017). Analysis of Craniocardiac Malformations in *Xenopus* using Optical Coherence Tomography. *Nature Publishing Group*. <https://doi.org/10.1038/srep42506>
- Denver, R. J. (2010). *Tadpole Behavior and Metamorphosis* (M. D. Breed & J. B. T.-E. of A. B. Moore (Eds.); pp. 375–378). Academic Press.

<https://doi.org/https://doi.org/10.1016/B978-0-08-045337-8.00255-2>

- Dietrich, M. R. (1998). Paradox and Persuasion: Negotiating the Place of Molecular Evolution within Evolutionary Biology. In *Journal of the History of Biology* (Vol. 31).
- Dobzhansky, T. (1937). *Genetics and the origin of species*. Columbia Univ. Press.
- Doolittle, R. F. (1994). Convergent evolution: the need to be explicit. *Trends in Biochemical Sciences*, 19(1). [https://doi.org/10.1016/0968-0004\(94\)90167-8](https://doi.org/10.1016/0968-0004(94)90167-8)
- Doyle, J. J. (1996). Homoplasy Connections and Disconnections: Genes and Species, Molecules and Morphology. In M. J. Sanderson & L. B. T.-H. Hufford (Eds.), *Homoplasy* (pp. 37–66). Academic Press. <https://doi.org/10.1016/b978-012618030-5/50004-6>
- Dreier, R. (2010). Hypertrophic differentiation of chondrocytes in osteoarthritis: The developmental aspect of degenerative joint disorders. In *Arthritis Research and Therapy* (Vol. 12, Issue 5). <https://doi.org/10.1186/ar3117>
- Ducy, P., & Zhang, R. (1997). Osf2/Cbfa1: A Transcriptional Activator of Osteoblast Differentiation. In *Cell* (Vol. 89).
- Dunn, C. W., Luo, X., & Wu, Z. (2013). Phylogenetic analysis of gene expression. *Integrative and Comparative Biology*, 53(5), 847–856. <https://doi.org/10.1093/icb/ict068>
- Eames, B. F., Allen, N., Young, J., Kaplan, A., Helms, J. A., & Schneider, R. A. (2007). Skeletogenesis in the swell shark *Cephaloscyllium ventriosum*. *Journal of Anatomy*, 210(5), 542–554. <https://doi.org/10.1111/j.1469-7580.2007.00723.x>
- Eames, B. F., Amores, A., Yan, Y.-L., & Postlethwait, J. H. (2012). *Evolution of the osteoblast: skeletogenesis in gar and zebrafish*.
- Eames, B. F., De la Fuente, L., & Helms, J. A. (2003). Molecular ontogeny of the skeleton. In *Birth Defects Research Part C - Embryo Today: Reviews*. <https://doi.org/10.1002/bdrc.10016>
- Eames, B. F., & Helms, J. A. (2004). Conserved molecular program regulating cranial and appendicular skeletogenesis. *Developmental Dynamics*, 231(1), 4–13. <https://doi.org/10.1002/dvdy.20134>
- Eames, B. F., Sharpe, P. T., & Helms, J. A. (2004). Hierarchy revealed in the specification of three skeletal fates by Sox9 and Runx2. *Developmental Biology*. <https://doi.org/10.1016/j.ydbio.2004.07.006>
- Eames, B. F., Singer, A., Smith, G. A., Wood, Z. A., Yan, Y.-L., He, X., Polizzi, S. J., Catchen, J. M., Rodriguez-Mari, A., Linbo, T., Raible, D. W., & Postlethwait, J. H. (2010). UDP xylose synthase 1 is required for morphogenesis and histogenesis of the craniofacial skeleton. *Developmental Biology*, 341(2), 400–415. <https://doi.org/10.1016/j.ydbio.2010.02.035>
- Eames, B. F., Yan, Y. L., Swartz, M. E., Levic, D. S., Knapik, E. W., Postlethwait, J. H., & Kimmel, C. B. (2011). Mutations in *fam20b* and *xylt1* reveal that cartilage matrix controls timing of endochondral ossification by inhibiting chondrocyte maturation. *PLoS Genetics*, 7(8).

<https://doi.org/10.1371/journal.pgen.1002246>

- Edwards, J. L. (1977). THE EVOLUTION OF TERRESTRIAL LOCOMOTION. *Major Patterns in Vertebrate Evolution*.
- Egawa, S., Miura, S., Yokoyama, H., Endo, T., & Tamura, K. (2014). Growth and differentiation of a long bone in limb development, repair and regeneration. *Development Growth and Differentiation*, 56(5), 410–424. <https://doi.org/10.1111/dgd.12136>
- Eliceiri, B. P., & Brown, D. D. (1994). Quantitation of endogenous thyroid hormone receptors alpha and beta during embryogenesis and metamorphosis in *Xenopus laevis*. *Journal of Biological Chemistry*, 269(39), 24459–24465. <http://www.jbc.org/content/269/39/24459.abstract>
- Enault, S., Muñoz, D. N., Silva, W. T. A. F., Borday-Birraux, V., Bonade, M., Oulion, S., Ventéo, S., Marcellini, S., & Debais-Thibaud, M. (2015). Molecular footprinting of skeletal tissues in the catshark *Scyliorhinus canicula* and the clawed frog *Xenopus tropicalis* identifies conserved and derived features of vertebrate calcification. *Frontiers in Genetics*, 6(SEP). <https://doi.org/10.3389/fgene.2015.00283>
- Enomoto, H., Enomoto-Iwamoto, M., Iwamoto, M., Nomura, S., Himeno, M., Kitamura, Y., Kishimoto, T., & Komori, T. (2000). Cbfa1 is a positive regulatory factor in chondrocyte maturation. *Journal of Biological Chemistry*, 275(12). <https://doi.org/10.1074/jbc.275.12.8695>
- Erlebacher, A., Filvaroff, E. H., Gitelman, S. E., & Derynck, R. (1995). Toward a Molecular Understanding of Skeletal Development Review. In *Cell* (Vol. 80).
- Espinoza, J., Sanchez, M., Sanchez, A., Hanna, P., Torrejon, M., Buisine, N., Sachs, L., & Marcellini, S. (2010). Two families of *Xenopus tropicalis* skeletal genes display well-conserved expression patterns with mammals in spite of their highly divergent regulatory regions. *Evolution and Development*, 12(6), 541–551. <https://doi.org/10.1111/j.1525-142X.2010.00440.x>
- Ferrandiz, C., & Sessions, A. (2008). Preparation and hydrolysis of digoxigenin-labeled probes for in situ hybridization of plant tissues. *Cold Spring Harbor Protocols*, 3(2). <https://doi.org/10.1101/pdb.prot4942>
- Fini, J. B., Le Mével, S., Palmier, K., Darras, V. M., Punzon, I., Richardson, S. J., Clerget-Froidevaux, M. S., & Demeneix, B. A. (2012). Thyroid hormone signaling in the *Xenopus laevis* embryo is functional and susceptible to endocrine disruption. *Endocrinology*. <https://doi.org/10.1210/en.2012-1463>
- Fleming, C. M., & Alexander, R. R. (2002). *Single Species versus Multiple Species Models: The Economic Implications*.
- Gearty, W., McClain, C. R., & Payne, J. L. (2018). Energetic tradeoffs control the size distribution of aquatic mammals. *Proceedings of the National Academy of Sciences*, 115(16), 4194 LP – 4199. <https://doi.org/10.1073/pnas.1712629115>

- Gentili, C., & Cancedda, R. (2009). Cartilage and Bone Extracellular Matrix. *Current Pharmaceutical Design*, 15(12), 1334–1348.  
<https://doi.org/10.2174/138161209787846739>
- Gerstenfeld, L. C., & Shapiro, F. D. (1996). Expression of bone-specific genes by hypertrophic chondrocytes: Implications of the complex functions of the hypertrophic chondrocyte during endochondral bone development. In *Journal of Cellular Biochemistry* (Vol. 62, Issue 1). [https://doi.org/10.1002/\(SICI\)1097-4644\(199607\)62:1<1::AID-JCB1>3.3.CO;2-O](https://doi.org/10.1002/(SICI)1097-4644(199607)62:1<1::AID-JCB1>3.3.CO;2-O)
- Gilbert, S. F., & Barresi, M. J. F. (2016). *Developmental biology*.
- Giovannone, D., Paul, S., Schindler, S., Arata, C., Farmer, J. T., Patel, P., Smeeton, J., & Gage Crump, J. (2019). *Programmed conversion of hypertrophic chondrocytes into osteoblasts and marrow adipocytes within zebrafish bones*. <https://doi.org/10.7554/eLife.42736.001>
- Glyn-Jones, S., Palmer, A. J. R., Agricola, R., Price, A. J., Vincent, T. L., Weinans, H., & Carr, A. J. (2015). Osteoarthritis. *The Lancet*, 386(9991), 376–387. [https://doi.org/10.1016/S0140-6736\(14\)60802-3](https://doi.org/10.1016/S0140-6736(14)60802-3)
- Gómez-Picos, P., & Eames, B. F. (2015). On the evolutionary relationship between chondrocytes and osteoblasts. *Frontiers in Genetics*. <https://doi.org/10.3389/fgene.2015.00297>
- Gould, S. J. (2002). *The Structure of Evolutionary Theory*. Harvard University Press.  
<http://www.jstor.org/stable/j.ctvjsf433>
- Gould, S. J., & Lewontin, R. C. (1979). The spandrels of San Marco and the Panglossian paradigm: a critique of the adaptationist programme. In *Proceedings of the Royal Society of London - Biological Sciences* (Vol. 205, Issue 1161).  
<https://doi.org/10.1098/rspb.1979.0086>
- Gould, Stephen J. (1977). Ontogeny and phylogeny. In *Ontogeny and phylogeny*. (pp. ix, 501–ix, 501). Harvard U Press.
- Grainger, R. M. (2012). *Xenopus tropicalis* as a model organism for genetics and genomics: past, present, and future. *Methods in Molecular Biology (Clifton, N.J.)*, 917, 3–15.  
[https://doi.org/10.1007/978-1-61779-992-1\\_1](https://doi.org/10.1007/978-1-61779-992-1_1)
- Gray, H., & Williams, P. L. (1989). *Gray's anatomy*. Edinburgh : Churchill Livingstone.
- Gray, J. (1968). *Animal Locomotion (The World Naturalist)*. Weidenfeld and Nicolson.
- Gross, J. B., & Hanken, J. (2005). Cranial neural crest contributes to the bony skull vault in adult *Xenopus laevis*: Insights from cell labeling studies. *Journal of Experimental Zoology Part B: Molecular and Developmental Evolution*. <https://doi.org/10.1002/jez.b.21028>
- Gross, J. B., & Hanken, J. (2008). Segmentation of the vertebrate skull: Neural-crest derivation of adult cartilages in the clawed frog, *Xenopus laevis*. *Integrative and Comparative Biology*. <https://doi.org/10.1093/icb/icn077>
- Grover, P. K., Cummins, A. G., Price, T. J., Roberts-Thomson, I. C., & Hardingham, J. E. (2012). A

- simple, cost-effective and flexible method for processing of snap-frozen tissue to prepare large amounts of intact RNA using laser microdissection. *Biochimie*, *94*, 2491–2497. <https://doi.org/10.1016/j.biochi.2012.06.031>
- Guntur, A. R., & Rosen, C. J. (2012). Bone as an endocrine organ. *Endocrine Practice : Official Journal of the American College of Endocrinology and the American Association of Clinical Endocrinologists*, *18*(5), 758–762. <https://doi.org/10.4158/EP12141.RA>
- Hadden, M. K. (2014). Hedgehog pathway agonism: Therapeutic potential and small-molecule development. *ChemMedChem*, *9*(1), 27–37. <https://doi.org/10.1002/cmdc.201300358>
- Haeckel, E. (1866). *Generelle Morphologie der organismen, Zweiter band*.
- Hall, B. K. (2003). Evo-Devo: Evolutionary developmental mechanisms. In *International Journal of Developmental Biology* (Vol. 47, Issues 7–8). <https://doi.org/10.1387/ijdb.14756324>
- Hammond, C. L., & Schulte-Merker, S. (2009). Two populations of endochondral osteoblasts with differential sensitivity to Hedgehog signalling. *Development*, *136*(23), 3991–4000. <https://doi.org/10.1242/dev.042150>
- Hanken, J., & Gross, J. B. (2005). Evolution of cranial development and the role of neural crest: insights from amphibians. *J. Anat*, *207*, 437–446.
- Hatori, M., Klatte, K. J., Teixeira, C. C., & Shapiro, I. M. (1995). End labeling studies of fragmented DNA in the Avian growth plate: Evidence of apoptosis in terminally differentiated chondrocytes. *Journal of Bone and Mineral Research*, *10*(12). <https://doi.org/10.1002/jbmr.5650101216>
- Hellsten, U., Harland, R. M., Gilchrist, M. J., Hendrix, D., Jurka, J., Kapitonov, V., Ovcharenko, I., Putnam, N. H., Shu, S., Taher, L., Blitz, I. L., Blumberg, B., Dichmann, D. S., Dubchak, I., Amaya, E., Detter, J. C., Fletcher, R., Gerhard, D. S., Goodstein, D., ... Rokhsar, D. S. (2010). The genome of the Western clawed frog *Xenopus tropicalis*. *Science (New York, N.Y.)*, *328*(5978), 633–636. <https://doi.org/10.1126/science.1183670>
- Hilton, M. J., Tu, X., & Long, F. (2007). Tamoxifen-inducible gene deletion reveals a distinct cell type associated with trabecular bone, and direct regulation of PTHrP expression and chondrocyte morphology by *Ihh* in growth region cartilage. *Developmental Biology*, *308*(1). <https://doi.org/10.1016/j.ydbio.2007.05.011>
- Hinton, R. J., Jing, Y., Jing, J., & Feng, J. Q. (2017). Roles of Chondrocytes in Endochondral Bone Formation and Fracture Repair. *Journal of Dental Research*, *96*(1). <https://doi.org/10.1177/0022034516668321>
- Hirasawa, T., & Kuratani, S. (2015). Evolution of the vertebrate skeleton: morphology, embryology, and development. *Zoological Letters*, *1*, 2. <https://doi.org/10.1186/s40851-014-0007-7>
- Hollowed, A. B., Bax, N., Beamish, R., Collie, J., Fogarty, M., Livingston, P., Pope, J., & Rice, J. C. (2000). Are multispecies models an improvement on single-species models for measuring

- fishing impacts on marine ecosystems? *ICES Journal of Marine Science*, 57(3), 707–719. <https://doi.org/10.1006/jmsc.2000.0734>
- Hu, X., & Lazar, M. A. (2000). Transcriptional repression by nuclear hormone receptors. In *Trends in Endocrinology and Metabolism* (Vol. 11, Issue 1). [https://doi.org/10.1016/S1043-2760\(99\)00215-5](https://doi.org/10.1016/S1043-2760(99)00215-5)
- Huycke, T., Eames, B., & Kimmel, C. (2012). *Hedgehog-dependent proliferation drives modular growth during morphogenesis of a dermal bone*. <https://doi.org/10.1242/dev.079806>
- Inada, M., Yasui, T., Nomura, S., Miyake, S., Deguchi, K., Himeno, M., Sato, M., Yamagiwa, H., Kimura, T., Yasui, N., Ochi, T., Endo, N., Kitamura, Y., Kishimoto, T., & Komori, T. (1999). Maturation disturbance of chondrocytes in Cbfa1-deficient mice. *Developmental Dynamics*, 214(4). [https://doi.org/10.1002/\(SICI\)1097-0177\(199904\)214:4<279::AID-AJA1>3.0.CO;2-W](https://doi.org/10.1002/(SICI)1097-0177(199904)214:4<279::AID-AJA1>3.0.CO;2-W)
- Janvier, P. (1996). Early Vertebrates. In *Oxford Monographs on Geology and Geophysics* (Oxford, Vol. 33). Clarendon Press.
- Jowett, T., & Yan, Y.-L. (1996). Double fluorescent in situ hybridization to zebrafish embryos. *Trends in Genetics*, 12(10), 387–389. [https://doi.org/https://doi.org/10.1016/S0168-9525\(96\)90091-8](https://doi.org/https://doi.org/10.1016/S0168-9525(96)90091-8)
- Jupp, S., Burdett, T., Malone, J., Leroy, C., Pearce, M., McMurry, J., & Parkinson, H. (2015). A new ontology lookup service at EMBL-EBI. *CEUR Workshop Proceedings*, 1546, 118–119.
- Kague, E., Roy, P., Asselin, G., Hu, G., Simonet, J., Stanley, A., Albertson, C., & Fisher, S. (2016). Osterix/Sp7 limits cranial bone initiation sites and is required for formation of sutures. *Developmental Biology*, 413(2), 160–172. <https://doi.org/https://doi.org/10.1016/j.ydbio.2016.03.011>
- Karp, S. J., Schipani, E., St-Jacques, B., Hunzelman, J., Kronenberg, H., & McMahon, A. P. (2000). Indian hedgehog coordinates endochondral bone growth and morphogenesis via parathyroid hormone related-protein-dependent and -independent pathways. *Development*, 127(3), 543 LP – 548. <http://dev.biologists.org/content/127/3/543.abstract>
- Karsenty, G., & Oury, F. (2012). Biology Without Walls: The Novel Endocrinology of Bone. *Annual Review of Physiology*, 74(1), 87–105. <https://doi.org/10.1146/annurev-physiol-020911-153233>
- Karsenty, G., & Park, R. W. (1995). Regulation of type I collagen genes expression. *International Reviews of Immunology*, 12(2–4). <https://doi.org/10.3109/08830189509056711>
- Karsenty, G., & Wagner, E. F. (2002). Review Reaching a Genetic and Molecular Understanding of Skeletal Development patterning were not really involved in the control of cell differentiation. Thus, the development of the skeleton encompasses. In *Developmental Cell* (Vol. 2).
- Kawahara, A., Baker, B. S., & Tataf, J. R. (1991). Developmental and regional expression of

- thyroid hormone receptor genes during *Xenopus* metamorphosis. In *Development* (Vol. 112).
- Kerney, R., Gross, J. B., & Hanken, J. (2007). Runx2 is essential for larval hyobranchial cartilage formation in *Xenopus laevis*. *Developmental Dynamics*.  
<https://doi.org/10.1002/dvdy.21175>
- Kerney, R., Hall, B. K., & Hanken, J. (2010). Regulatory elements of *Xenopus col2a1* drive cartilaginous gene expression in transgenic frogs. *International Journal of Developmental Biology*. <https://doi.org/10.1387/ijdb.092848rk>
- Kerney, R. R., Brittain, A. L., Hall, B. K., & Buchholz, D. R. (2012). Cartilage on the move: Cartilage lineage tracing during tadpole metamorphosis. *Development Growth and Differentiation*.  
<https://doi.org/10.1111/dgd.12002>
- Kerney, R., Wassersug, R., & Hall, B. K. (2010). Skeletal advance and arrest in giant non-metamorphosing African clawed frog tadpoles (*Xenopus laevis*: Daudin). *Journal of Anatomy*. <https://doi.org/10.1111/j.1469-7580.2009.01176.x>
- Khaitovich, P., Enard, W., Lachmann, M., & Pääbo, S. (2006). Evolution of primate gene expression. In *Nature Reviews Genetics* (Vol. 7, Issue 9). <https://doi.org/10.1038/nrg1940>
- Khokha, M. K., Chung, C., Bustamante, E. L., Gaw, L. W. K., Trott, K. A., Yeh, J., Lim, N., Lin, J. C. Y., Taverner, N., Amaya, E., Papalopulu, N., Smith, J. C., Zorn, A. M., Harland, R. M., & Grammer, T. C. (2002). Techniques and probes for the study of *Xenopus tropicalis* development. *Developmental Dynamics*. <https://doi.org/10.1002/dvdy.10184>
- Khoury, M. J. (2014). *Geography, Genetics, and Leading Causes of Death*. Office of Public Health Genomics, Centers for Disease Control and Prevention (U. S.).  
<https://blogs.cdc.gov/genomics/2014/05/15/geography/>
- Kim, H.-Y., & Mohan, S. (2013). Role and Mechanisms of Actions of Thyroid Hormone on the Skeletal Development. *Bone Research*, 1(2), 146–161.  
<https://doi.org/10.4248/BR201302004>
- Kim, I. S., Otto, F., Zabel, B., & Mundlos, S. (1999). Regulation of chondrocyte differentiation by Cbfa1. *Mechanisms of Development*. [https://doi.org/10.1016/S0925-4773\(98\)00210-X](https://doi.org/10.1016/S0925-4773(98)00210-X)
- Komori, T, Yagi, H., & Nomura, S. (1997). Targeted Disruption of Cbfa1 Results in a Complete Lack of Bone Formation owing to Maturational Arrest of Osteoblasts. In *Cell* (Vol. 89).
- Komori, Toshihisa. (2010). Regulation of bone development and extracellular matrix protein genes by RUNX2. *Cell and Tissue Research*, 339(1), 189–195.  
<https://doi.org/10.1007/s00441-009-0832-8>
- Koyama, E., Leatherman, J. L., Noji, S., & Pacifici, M. (1996). Early chick limb cartilaginous elements possess polarizing activity and express Hedgehog-related morphogenetic factors. *Developmental Dynamics*, 207(3). [https://doi.org/10.1002/\(SICI\)1097-0177\(199611\)207:3<344::AID-AJA11>3.0.CO;2-4](https://doi.org/10.1002/(SICI)1097-0177(199611)207:3<344::AID-AJA11>3.0.CO;2-4)

- Kozhemyakina, E., Lassar, A. B., & Zelzer, E. (2015). A pathway to bone: signaling molecules and transcription factors involved in chondrocyte development and maturation. *Development*, *142*(5). <https://doi.org/10.1242/dev.105536>
- Kozmik, Z., Ruzickova, J., Jonasova, K., Matsumoto, Y., Vopalensky, P., Kozmikova, I., Strnad, H., Kawamura, S., Piatigorsky, J., Paces, V., & Vlcek, C. (2008). Assembly of the cnidarian camera-type eye from vertebrate-like components. *Proceedings of the National Academy of Sciences of the United States of America*, *105*(26), 8989–8993. <https://doi.org/10.1073/pnas.0800388105>
- Kronenberg, H. M. (2003). Developmental regulation of the growth plate. *Nature*, *423*(6937), 332–336. <https://doi.org/10.1038/nature01657>
- Kulyk, W. M., & Zalik, S. E. (1982). *Differentiation Synthesis of Sulfated Glycosaminoglycan in Newt Iris during Lens Regeneration*.
- Kwan, K. M., Pang, M. K., Zhou, S., Cowan, S. K., Kong, R. Y., Pfordte, T., Olsen, B. R., Sillence, D. O., Tam, P. P., & Cheah, K. S. (1997). Abnormal compartmentalization of cartilage matrix components in mice lacking collagen X: implications for function. *The Journal of Cell Biology*, *136*(2), 459–471. <https://doi.org/10.1083/jcb.136.2.459>
- Laudet, V. (2011). The Origins and Evolution of Vertebrate Metamorphosis. *Current Biology*, *21*(18), R726–R737. <https://doi.org/https://doi.org/10.1016/j.cub.2011.07.030>
- Leboy, P. S., Shapiro, I. M., Uschmann, B. D., Oshima, O., & Lin, D. (1988). Gene expression in mineralizing chick epiphyseal cartilage. *Journal of Biological Chemistry*, *263*(17).
- Lefebvre, V., Huang, W., Harley, V. R., Goodfellow, P. N., & de Crombrughe, B. (1997). SOX9 is a potent activator of the chondrocyte-specific enhancer of the pro alpha1(II) collagen gene. *Molecular and Cellular Biology*, *17*(4). <https://doi.org/10.1128/mcb.17.4.2336>
- Lefebvre, Véronique, & de Crombrughe, B. (1998). Toward understanding SOX9 function in chondrocyte differentiation. *Matrix Biology*, *16*(9). [https://doi.org/10.1016/s0945-053x\(98\)90065-8](https://doi.org/10.1016/s0945-053x(98)90065-8)
- Lefebvre, Véronique, Garofalo, S., & De Crombrughe, B. (1995). Type X collagen gene expression in mouse chondrocytes immortalized by a temperature-sensitive simian virus 40 large tumor antigen. *Journal of Cell Biology*, *128*(1–2). <https://doi.org/10.1083/jcb.128.1.239>
- Li, F., Lu, Y., Ding, M., Napierala, D., Abbassi, S., Chen, Y., Duan, X., Wang, S., Lee, B., & Zheng, Q. (2011). Runx2 contributes to murine Col10a1 gene regulation through direct interaction with its cis-enhancer. *Journal of Bone and Mineral Research : The Official Journal of the American Society for Bone and Mineral Research*, *26*(12), 2899–2910. <https://doi.org/10.1002/jbmr.504>
- Li, W. H., & Graur, D. (1991). Fundamentals of molecular evolution. *Trends in Ecology & Evolution*, *6*(10). [https://doi.org/10.1016/0169-5347\(91\)90046-z](https://doi.org/10.1016/0169-5347(91)90046-z)

- Lim, W., Nguyen, N.-H., Yang, H. Y., Scanlan, T. S., & Furlow, J. D. (2002). *A Thyroid Hormone Antagonist That Inhibits Thyroid Hormone Action in Vivo\**. <https://doi.org/10.1074/jbc.M205608200>
- Linsenmayer, T. F., Chen, Q., Gibney, E., Gordon, M. K., Marchant, J. K., Mayne, R., & Schmid, T. M. (1991). Collagen types IX and X in the developing chick tibiotarsus: analyses of mRNAs and proteins. In *Development* (Vol. 111).
- Long, F., Chung, U. Il, Ohba, S., McMahon, J., Kronenberg, H. M., & McMahon, A. P. (2004). Ihh signaling is directly required for the osteoblast lineage in the endochondral skeleton. *Development*, *131*(6). <https://doi.org/10.1242/dev.01006>
- Long, F., & Ornitz, D. M. (2013). Development of the endochondral skeleton. In *Cold Spring Harbor Perspectives in Biology*. <https://doi.org/10.1101/cshperspect.a008334>
- Loveridge, J. P. (1976). Strategies of Water Conservation in Southern African Frogs. *Zoologica Africana*, *11*(2), 319–333. <https://doi.org/10.1080/00445096.1976.11447538>
- Lui, J. C., Yue, S., Lee, A., Kikani, B., Temnycky, A., Barnes, K. M., & Baron, J. (2019). Persistent Sox9 expression in hypertrophic chondrocytes suppresses transdifferentiation into osteoblasts. *Bone*, *125*, 169–177. <https://doi.org/10.1016/j.bone.2019.05.027>
- Lukas, P., & Olsson, L. (2017). Sequence and timing of early cranial skeletal development in *Xenopus laevis*. *Journal of Morphology*. <https://doi.org/10.1002/jmor.20754>
- Mackie, E. J., Ahmed, Y. A., Tatarczuch, L., Chen, K. S., & Mirams, M. (2008). Endochondral ossification: How cartilage is converted into bone in the developing skeleton. In *International Journal of Biochemistry and Cell Biology* (Vol. 40, Issue 1, pp. 46–62). <https://doi.org/10.1016/j.biocel.2007.06.009>
- Magrun, W. M. (2011). *Normal and abnormal development : a comparative analysis*. Clinician's View. <http://www.aspresolver.com/aspresolver.asp?RTIV>
- Mak, K. K., Kronenberg, H. M., Chuang, P. T., Mackem, S., & Yang, Y. (2008). Indian hedgehog signals independently of PTHrP to promote chondrocyte hypertrophy. *Development*, *135*(11). <https://doi.org/10.1242/dev.018044>
- Mallatt, J., & Chen, J. Y. (2003). Fossil Sister Group of Craniates: Predicted and Found. *Journal of Morphology*, *258*(1). <https://doi.org/10.1002/jmor.10081>
- Marconi, A., Hancock-Ronemus, A., & Gillis, J. A. (2020). Adult chondrogenesis and spontaneous cartilage repair in the skate, *Leucoraja erinacea*. *ELife*, *9*, e53414. <https://doi.org/10.7554/eLife.53414>
- Marks, S. C., Lundmark, C., Christersson, C., Wurtz, T., Odgren, P. R., Seifert, M. F., Mackay, C. A., Mason-Savas, A., & Popoff, S. N. (2000). Chondrocytes, collagen X and mineralization Endochondral bone formation in toothless (osteopetrotic) rats: failures of chondrocyte patterning and type X collagen expression. In *Int. J. Dev. Biol* (Vol. 44). [www.ehu.es/ijdb](http://www.ehu.es/ijdb)
- McGhee, G. R. (2011). *Convergent Evolution*. The MIT Press.

<https://doi.org/10.2307/j.ctt5hhhwt>

- McKee, M. D., Glimcher, M. J., & Nanci, A. (1992). High-resolution immunolocalization of osteopontin and osteocalcin in bone and cartilage during endochondral ossification in the chicken tibia. *The Anatomical Record*, 234(4). <https://doi.org/10.1002/ar.1092340404>
- McManus, J. F. A., & Mowry, R. W. (1960). *Staining Methods, Histologic and Histochemical [by] J.F.A. McManus [and] Robert W. Mowry*. Hoeber.  
<https://books.google.ca/books?id=PWY3swEACAAJ>
- McMenamin, S. K., & Parichy, D. M. (2013). Metamorphosis in teleosts. *Current Topics in Developmental Biology*, 103, 127–165. <https://doi.org/10.1016/B978-0-12-385979-2.00005-8>
- McNamara, K. J. (1986). A guide to the nomenclature of heterochrony. *Journal of Paleontology*, 60(1). <https://doi.org/10.1017/s0022336000021454>
- Mengeling, B. J., Wei, Y., Dobrawa, L. N., Streekstra, M., Lousse, J., Singh, V., Singh, L., Lein, P. J., Wulff, H., Murk, A. J., Furlow, J. D., & Author, A. T. (2017). A multi-tiered, in vivo, quantitative assay suite for environmental disruptors of thyroid hormone signaling HHS Public Access Author manuscript. *Aquat Toxicol*, 190, 1–10.  
<https://doi.org/10.1016/j.aquatox.2017.06.019>
- Mitogawa, K., Makanae, A., & Satoh, A. (2018). Hyperinnervation improves *Xenopus laevis* limb regeneration. *Developmental Biology*, 433(2), 276–286.  
<https://doi.org/https://doi.org/10.1016/j.ydbio.2017.10.007>
- Miura, S., Hanaoka, K., & Togashi, S. (2008). Skeletogenesis in *Xenopus tropicalis*: Characteristic bone development in an anuran amphibian. *Bone*.  
<https://doi.org/10.1016/j.bone.2008.07.005>
- Mori-Akiyama, Y., Akiyama, H., Rowitch, D. H., & De Crombrughe, B. (2003). Sox9 is required for determination of the chondrogenic cell lineage in the cranial neural crest. In *Proceedings of the National Academy of Sciences of the United States of America* (Vol. 100, Issue 16). <https://doi.org/10.1073/pnas.1631288100>
- Moriishi, T., Shibata, Y., Tsukazaki, T., & Yamaguchi, A. (2005). Expression profile of *Xenopus* banded hedgehog, a homolog of mouse Indian hedgehog, is related to the late development of endochondral ossification in *Xenopus laevis*. *Biochemical and Biophysical Research Communications*. <https://doi.org/10.1016/j.bbrc.2005.01.032>
- Morvan-Dubois, G., Demeneix, B. A., & Sachs, L. M. (2008). *Xenopus laevis* as a model for studying thyroid hormone signalling: From development to metamorphosis. *Molecular and Cellular Endocrinology*, 293, 71–79. <https://doi.org/10.1016/j.mce.2008.06.012>
- Moskalewski, S., & Malejczyk, J. (1989). Bone formation following intrarenal transplantation of isolated murine chondrocytes: chondrocyte-bone cell transdifferentiation? In *Development* (Vol. 107).

- Mullur, R., Liu, Y.-Y., & Brent, G. A. (2014). Thyroid hormone regulation of metabolism. *Physiological Reviews*, *94*(2), 355–382. <https://doi.org/10.1152/physrev.00030.2013>
- Muñoz, D., Castillo, H., Henríquez, J. P., & Marcellini, S. (2018). Bone regeneration after traumatic skull injury in *Xenopus tropicalis*. *Mechanisms of Development*, *154*, 153–161. <https://doi.org/https://doi.org/10.1016/j.mod.2018.06.007>
- Nagalakshmi, U., Waern, K., & Snyder, M. (2010). RNA-seq: A method for comprehensive transcriptome analysis. In *Current Protocols in Molecular Biology* (Issue SUPPL. 89). <https://doi.org/10.1002/0471142727.mb0411s89>
- Nah, H.-D., Swoboda, B., Birk, D. E., & Kirsch, T. (2001). *Type IIA Procollagen: Expression in Developing Chicken Limb Cartilage and Human Osteoarthritic Articular Cartilage*.
- Nakahara, H., Bruder, S. P., Goldberg, V. M., & Caplan, A. I. (1990). In vivo osteochondrogenic potential of cultured cells derived from the periosteum. *Clinical Orthopaedics and Related Research*, *259*. <https://doi.org/10.1097/00003086-199010000-00032>
- Nakahara, J., Maeda, M., Aiso, S., & Suzuki, N. (2012). Current concepts in multiple sclerosis: Autoimmunity versus oligodendrogliaopathy. *Clinical Reviews in Allergy and Immunology*, *42*(1). <https://doi.org/10.1007/s12016-011-8287-6>
- Nakase, T., Takaoka, K., Hirakawa, K., Hirota, S., Takemura, T., Onoue, H., Takebayashi, K., Kitamura, Y., & Nomura, S. (1994). Alterations in the expression of osteonectin, osteopontin and osteocalcin mRNAs during the development of skeletal tissues in vivo. *Bone and Mineral*, *26*(2). [https://doi.org/10.1016/S0169-6009\(08\)80056-6](https://doi.org/10.1016/S0169-6009(08)80056-6)
- Nakashima, K., Zhou, X., Kunkel, G., Zhang, Z., Deng, M., Behringer, R. R., & De Crombrughe, B. (2002). The Novel Zinc Finger-Containing Transcription Factor Osterix Is Required for Osteoblast Differentiation and Bone Formation blasts derive from a common precursor (Fang and Hall, 1997). Chondrocytes deposit a cartilage-specific extracellular matrix, proliferate, and, in most cases, hypertrophy and die. At the same time, some of the mesenchymal Cloning of cDNA for Osterix When C2C12 skeletal muscle progenitor cells become. In *Cell* (Vol. 108). <http://www.cell.com/cgi/content/full/108/1/17/>
- Nanci, A. B. T.-T. C. O. H. (Eighth E. (Ed.). (2013). *Chapter 8 - Dentin-Pulp Complex* (pp. 165–204). Mosby. <https://doi.org/https://doi.org/10.1016/B978-0-323-07846-7.00008-2>
- Neuhold, L. A., Killar, L., Zhao, W., Sung, M. L. A., Warner, L., Kulik, J., Turner, J., Wu, W., Billingham, C., Meijers, T., Poole, A. R., Babij, P., & DeGennaro, L. J. (2001). Postnatal expression in hyaline cartilage of constitutively active human collagenase-3 (MMP-13) induces osteoarthritis in mice. *Journal of Clinical Investigation*, *107*(1). <https://doi.org/10.1172/JCI10564>
- Ng, L. J., Wheatley, S., Muscat, G. E. O., Conway-Campbell, J., Bowles, J., Wright, E., Bell, D. M., Tam, P. P. L., Cheah, K. S. E., & Koopman, P. (1997). SOX9 binds DNA, activates transcription, and coexpresses with type II collagen during chondrogenesis in the mouse. *Developmental Biology*, *183*(1). <https://doi.org/10.1006/dbio.1996.8487>

- Nguyen, J. K. B., & Eames, B. F. (2020). Evolutionary repression of chondrogenic genes in the vertebrate osteoblast. In *FEBS Journal*. Blackwell Publishing Ltd.  
<https://doi.org/10.1111/febs.15228>
- Nguyen, N. H., Apriletti, J. W., Cunha Lima, S. T., Webb, P., Baxter, J. D., & Scanlan, T. S. (2002). Rational design and synthesis of a novel thyroid hormone antagonist that blocks coactivator recruitment. *Journal of Medicinal Chemistry*.  
<https://doi.org/10.1021/jm0201013>
- Nielsen, F. C., Van Overeem Hansen, T., & Sørensen, C. S. (2016). Hereditary breast and ovarian cancer: New genes in confined pathways. In *Nature Reviews Cancer* (Vol. 16, Issue 9).  
<https://doi.org/10.1038/nrc.2016.72>
- Nieuwkoop, P. D., & Faber, J. (1994). *Normal table of Xenopus laevis (Daudin) : a systematical and chronological survey of the development from the fertilized egg till the end of metamorphosis*. Garland Pub.
- Nishimura, R., Hata, K., Ono, K., Takashima, R., Yoshida, M., & Yoneda, T. (2012). *Regulation of endochondral ossification by transcription factors*.  
<https://doi.org/10.1016/j.job.2012.09.001>
- Olubamiji, A. D., Izadifar, Z., Zhu, N., Chang, T., Chen, X., & Eames, B. F. (2016). Using synchrotron radiation inline phase-contrast imaging computed tomography to visualize three-dimensional printed hybrid constructs for cartilage tissue engineering. *Journal of Synchrotron Radiation*, 23(3), 802–812. <https://doi.org/10.1107/S1600577516002344>
- Olubamiji, A. D., Zhu, N., Chang, T., Nwankwo, C. K., Izadifar, Z., Honaramooz, A., Chen, X., & Eames, B. F. (2017). Traditional Invasive and Synchrotron-Based Noninvasive Assessments of Three-Dimensional-Printed Hybrid Cartilage Constructs in Situ. *Tissue Engineering - Part C: Methods*, 23(3), 156–168. <https://doi.org/10.1089/ten.tec.2016.0368>
- Ono, N., Ono, W., Nagasawa, T., & Kronenberg, H. M. (2014). A subset of chondrogenic cells provides early mesenchymal progenitors in growing bones. *Nature Cell Biology*, 16(12), 1157–1167. <https://doi.org/10.1038/ncb3067>
- Otto, F., Thornell, A. P., Crompton, T., Denzel, A., Gilmour, K. C., & Rosewell, I. R. (1997). Cbfa1, a Candidate Gene for Cleidocranial Dysplasia Syndrome, Is Essential for Osteoblast Differentiation and Bone Development. In *Cell* (Vol. 89).
- Panahifar, A., Swanston, T. M., Jake Pushie, M., Belev, G., Chapman, D., Weber, L., & Cooper, D. M. L. (2016). Three-dimensional labeling of newly formed bone using synchrotron radiation barium K-edge subtraction imaging. *Physics in Medicine and Biology*, 61(13), 5077–5088. <https://doi.org/10.1088/0031-9155/61/13/5077>
- Pascal, L. E., True, L. D., Campbell, D. S., Deutsch, E. W., Risk, M., Coleman, I. M., Eichner, L. J., Nelson, P. S., & Liu, A. Y. (2008). Correlation of mRNA and protein levels: Cell type-specific gene expression of cluster designation antigens in the prostate. *BMC Genomics*, 9(1), 246. <https://doi.org/10.1186/1471-2164-9-246>

- Pechak, D. G., Kujawa, M. J., & Caplan, A. I. (1986). Morphology of bone development and bone remodeling in embryonic chick limbs. *Bone*, 7(6), 459–472.  
[https://doi.org/https://doi.org/10.1016/8756-3282\(86\)90005-0](https://doi.org/https://doi.org/10.1016/8756-3282(86)90005-0)
- Poole, A. R. (1991). The growth plate: cellular physiology, cartilage assembly and mineralization. *Cartilage: Molecular Aspects*, 179–211.
- Porro, L. B., & Richards, C. T. (2017). Digital dissection of the model organism *Xenopus laevis* using contrast-enhanced computed tomography. *Journal of Anatomy*.  
<https://doi.org/10.1111/joa.12625>
- Porter, K. R., & Vial, J. L. (1974). Evolutionary Biology of the Anurans. Contemporary Research on Major Problems. In *Copeia* (Vol. 1974, Issue 4). <https://doi.org/10.2307/1442618>
- Rasys, A. M., Park, S., Ball, R. E., Alcalá, A. J., Lauderdale, J. D., & Menke, D. B. (2019). CRISPR-Cas9 Gene Editing in Lizards through Microinjection of Unfertilized Oocytes. *Cell Reports*, 28(9), 2288–2292.e3. <https://doi.org/https://doi.org/10.1016/j.celrep.2019.07.089>
- Ratjen, F., & Döring, G. (2003). Cystic fibrosis. *Lancet*, 361(9358), 681–689.  
[https://doi.org/10.1016/S0140-6736\(03\)12567-6](https://doi.org/10.1016/S0140-6736(03)12567-6)
- Riddle, R. D., Johnson, R. L., Laufer, E., & Tabin, C. (1993). Sonic hedgehog mediates the polarizing activity of the ZPA. *Cell*, 75(7). [https://doi.org/10.1016/0092-8674\(93\)90626-2](https://doi.org/10.1016/0092-8674(93)90626-2)
- Roach, H. I. (1994). Why does bone matrix contain non-collagenous proteins? The possible roles of osteocalcin, osteonectin, osteopontin and bone sialoprotein in bone mineralisation and resorption. *Cell Biology International*, 18(6). <https://doi.org/10.1006/cbir.1994.1088>
- Rosati, R., Horan, G. S. B., Pinero, G. J., Garofalo, S., Keene, D. R., Horton, W. A., Vuorio, E., de Crombrughe, B., & Behringer, R. R. (1994). Normal long bone growth and development in type X collagen-null mice. In *Nature Genetics* (Vol. 8, Issue 2).  
<https://doi.org/10.1038/ng1094-129>
- Rose, C. (2009). Generating, growing and transforming skeletal shape: Insights from amphibian pharyngeal arch cartilages. In *BioEssays* (Vol. 31, Issue 3, pp. 287–299).  
<https://doi.org/10.1002/bies.200800059>
- Rose, C S. (2014). The importance of cartilage to amphibian development and evolution. *International Journal of Developmental Biology*. <https://doi.org/10.1387/ijdb.150053cr>
- Rose, C S, & Cahill, J. W. (2019). How thyroid hormones and their inhibitors affect cartilage growth and shape in the frog *Xenopus laevis*. *Journal of Anatomy*, 234(1), 89–105.  
<https://doi.org/10.1111/joa.12897>
- Rose, Christopher S., Murawinski, D., & Horne, V. (2015). Deconstructing cartilage shape and size into contributions from embryogenesis, metamorphosis, and tadpole and frog growth. *Journal of Anatomy*. <https://doi.org/10.1111/joa.12303>
- Rowe, T., & Beard, S. (2018). *Probabilities, methodologies and the evidence base in existential risk assessments Working paper Probabilities, Methodologies and the Evidence Base in*

*Existential Risk Assessments CSER Working Paper.*

- Rychel, A. L., Smith, S. E., Shimamoto, H. T., & Swalla, B. J. (2006). *Evolution and Development of the Chordates: Collagen and Pharyngeal Cartilage*.  
<https://doi.org/10.1093/molbev/msj055>
- Sachs, L. M., & Campinho, M. A. (2019). Editorial: The Role of Thyroid Hormones in Vertebrate Development. *Frontiers in Endocrinology*, *10*, 863.  
<https://doi.org/10.3389/fendo.2019.00863>
- Sandell, L. J., Nalin, A. M., & Reife, R. A. (1994). Alternative splice form of type II procollagen mRNA (IIA) is predominant in skeletal precursors and non-cartilaginous tissues during early mouse development. *Developmental Dynamics*, *199*(2), 129–140.  
<https://doi.org/https://doi.org/10.1002/aja.1001990206>
- Schaeffer, B. (1941). The morphological and functional evolution of the tarsus in amphibians and reptiles. *Bull Amer Mus Nat Hist*, *78*.
- Schmid, T. M., & Linsenmayer, T. F. (1985). Developmental acquisition of type  $\times$  collagen in the embryonic chick tibiotarsus. *Developmental Biology*, *107*(2), 373–381.  
[https://doi.org/https://doi.org/10.1016/0012-1606\(85\)90319-7](https://doi.org/https://doi.org/10.1016/0012-1606(85)90319-7)
- Schultze, H.-P., & Trueb, L. (Eds.). (1991). *Origins of the Higher Groups of Tetrapods*. Cornell University Press. <http://www.jstor.org/stable/10.7591/j.ctv75d32t>
- Schwanhäusser, B., Busse, D., Li, N., Dittmar, G., Schuchhardt, J., Wolf, J., Chen, W., & Selbach, M. (2011). Global quantification of mammalian gene expression control. *Nature*, *473*(7347), 337–342. <https://doi.org/10.1038/nature10098>
- Sedra, S. N., & Michael, M. I. (1957). *The development of the skull, visceral arches, larynx and visceral muscles of the South African Clawed Toad, "Xenopus Laevis" (Daudin) during the process of metamorphosis (from stage 55 to stage 66)*. N.V. Noord-Hollandsche Uitgevers Maatschappij.
- Segerdell, E., Ponferrada, V. G., James-Zorn, C., Burns, K. A., Fortriede, J. D., Dahdul, W. M., Vize, P. D., & Zorn, A. M. (2013). Enhanced XAO: The ontology of Xenopus anatomy and development underpins more accurate annotation of gene expression and queries on Xenbase. *Journal of Biomedical Semantics*. <https://doi.org/10.1186/2041-1480-4-31>
- Showell, C., & Conlon, F. L. (2009). Natural mating and tadpole husbandry in the western clawed frog xenopus tropicalis. *Cold Spring Harbor Protocols*.  
<https://doi.org/10.1101/pdb.prot5292>
- Shriver, E. K. (2001). *Developmental Biology - Understanding Normal and Abnormal Development*.
- Shubin, N. H. (2002). Origin of evolutionary novelty: Examples from limbs. *Journal of Morphology*, *252*(1), 15–28. <https://doi.org/10.1002/jmor.10017>
- Shubin, N. H., Daeschler, E. B., & Coates, M. I. (2004). The Early Evolution of the Tetrapod

- Humerus. *Science*, 304(5667), 90 LP – 93. <https://doi.org/10.1126/science.1094295>
- Signor, S. A., & Nuzhdin, S. V. (2018). The Evolution of Gene Expression in cis and trans. *Trends in Genetics : TIG*, 34(7), 532–544. <https://doi.org/10.1016/j.tig.2018.03.007>
- Sive, H. L., Grainger, R. M., & Harland, R. M. (2000). *Early Development of Xenopus Laevis: A Laboratory Manual*. Cold Spring Harbor Laboratory Press. <https://books.google.ca/books?id=DyandJfspJ8C>
- Slater, B. J., Liu, K. J., Kwan, M. D., Quarto, N., & Longaker, M. T. (2009). Cranial osteogenesis and suture morphology in *Xenopus laevis*: A unique model system for studying craniofacial development. *PLoS ONE*. <https://doi.org/10.1371/journal.pone.0003914>
- Smits, P., Li, P., Mandel, J., Zhang, Z., Deng, J. M., Behringer, R. R., De Crombrugghe, B., & Lefebvre, V. (2001). The Transcription Factors L-Sox5 and Sox6 Are Essential for Cartilage Formation. *Developmental Cell*, 1(2). [https://doi.org/10.1016/S1534-5807\(01\)00003-X](https://doi.org/10.1016/S1534-5807(01)00003-X)
- Sophia Fox, A. J., Bedi, A., & Rodeo, S. A. (2009). The basic science of articular cartilage: Structure, composition, and function. *Sports Health*, 1(6). <https://doi.org/10.1177/1941738109350438>
- Spokony, R. F. (2002). Sox9 and neural crest formation. *Dev.Biologists.Org*. <https://dev.biologists.org/content/129/2/421.short>
- St-Jacques, B., Hammerschmidt, M., & McMahon, A. P. (1999). *Indian hedgehog signaling regulates proliferation and differentiation of chondrocytes and is essential for bone formation*.
- Stearns, S. C. (1992). *The Evolution of Life Histories*. OUP Oxford. <https://books.google.ca/books?id=-NcNAZ06nNoC>
- Steel, M., & Penny, D. (2010). Common ancestry put to the test. *Nature*, 465(7295), 168–169. <https://doi.org/10.1038/465168a>
- Stone, J. R., & Wray, G. A. (2001). Rapid Evolution of cis-Regulatory Sequences via Local Point Mutations. *Mol. Biol. Evol*, 18(9), 1764–1770. <http://www.zoo>.
- Strähle, U., Blader, P., Adam, J., & Ingham, P. W. (1994). A simple and efficient procedure for non-isotopic in situ hybridization to sectioned material. *Trends in Genetics*, 10(3), 75–76. [https://doi.org/https://doi.org/10.1016/0168-9525\(94\)90221-6](https://doi.org/https://doi.org/10.1016/0168-9525(94)90221-6)
- Suzuki, M., Yakushiji, N., Nakada, Y., Satoh, A., Ide, H., & Tamura, K. (2006). Limb regeneration in *Xenopus laevis* froglet. *TheScientificWorldJournal*, 6 Suppl 1, 26–37. <https://doi.org/10.1100/tsw.2006.325>
- Tchetina, E. V., Mwale, F., & Poole, A. R. (2014). Changes in gene expression associated with matrix turnover, chondrocyte proliferation and hypertrophy in the bovine growth plate. *Acta Naturae*, 6(22). <https://doi.org/10.32607/20758251-2014-6-3-89-97>
- Tew, S. R., Murdoch, A. D., Rauchenberg, R. P., & Hardingham, T. E. (2008). Cellular methods in

- cartilage research: Primary human chondrocytes in culture and chondrogenesis in human bone marrow stem cells. *Methods*, 45(1), 2–9.  
<https://doi.org/https://doi.org/10.1016/j.ymeth.2008.01.006>
- Theobald, D. L. (2010). A formal test of the theory of universal common ancestry. *Nature*, 465(7295), 219–222. <https://doi.org/10.1038/nature09014>
- Thesingh, C. W., Groot, C. G., & Wassenaar, A. M. (1991). Transdifferentiation of hypertrophic chondrocytes into osteoblasts in murine fetal metatarsal bones, induced by co-cultured cerebrum. *Bone and Mineral*, 12(1), 25–40. [https://doi.org/10.1016/0169-6009\(91\)90119-K](https://doi.org/10.1016/0169-6009(91)90119-K)
- Thomson, D. A. R. (1986). Meckel's cartilage in *Xenopus laevis* during metamorphosis: a light and electron microscope study. *J. Anat*, 149, 77–87.
- Thomson, D. A. R. (1987). A quantitative analysis of cellular and matrix changes in Meckel's cartilage in *Xenopus laevis*. *J. Anat*, 151, 249–254.
- Tietge, J. E., Butterworth, B. C., Haselman, J. T., Holcombe, G. W., Hornung, M. W., Korte, J. J., Kosian, P. A., Wolfe, M., & Degitz, S. J. (2010). Early temporal effects of three thyroid hormone synthesis inhibitors in *Xenopus laevis*. *Aquatic Toxicology*, 98, 44–50.  
<https://doi.org/10.1016/j.aquatox.2010.01.014>
- Trueb, L., & Hanken, J. (1992). Skeletal development in *Xenopus laevis* (Anura: Pipidae). *Journal of Morphology*, 214(1), 1–41. <https://doi.org/https://doi.org/10.1002/jmor.1052140102>
- Trümpy, R., & Bernasconi, A. F. (1951). *Der Lias der Glarner Alpen. Ueber den Ossifikationsmodus bei Xenopus laevis Daud.* Birkhäuser Basel.  
<https://books.google.ca/books?id=zNi4PQAACAAJ>
- Tussellino, M., Ronca, R., Carotenuto, R., Pallotta, M. M., Furia, M., & Capriglione, T. (2016). Chlorpyrifos exposure affects fgf8, sox9, and bmp4 expression required for cranial neural crest morphogenesis and chondrogenesis in *Xenopus laevis* embryos. *Environmental and Molecular Mutagenesis*, 57(8), 630–640. <https://doi.org/10.1002/em.22057>
- Van Eeden, F. J. M., Granato, M., Schach, U., Brand, M., Furutani-Seiki, M., Haffter, P., Hammerschmidt, M., Heisenberg, C. P., Jiang, Y. J., Kane, D. A., Kelsh, R. N., Mullins, M. C., Odenthal, J., Warga, R. M., Allende, M. L., Weinberg, E. S., & Nüsslein-Volhard, C. (1996). Mutations affecting somite formation and patterning in the zebrafish, *Danio rerio*. *Development*, 123.
- Vaškaninová, V. (2020). Bone of contention. In *Nature Ecology and Evolution* (Vol. 4, Issue 11, pp. 1447–1448). Nature Research. <https://doi.org/10.1038/s41559-020-01300-3>
- Verkerk, A. J. M. H., Pieretti, M., Sutcliffe, J. S., Fu, Y. H., Kuhl, D. P. A., Pizzuti, A., Reiner, O., Richards, S., Victoria, M. F., Zhang, F., Eussen, B. E., van Ommen, G. J. B., Blonden, L. A. J., Riggins, G. J., Chastain, J. L., Kunst, C. B., Galjaard, H., Thomas Caskey, C., Nelson, D. L., ... Warran, S. T. (1991). Identification of a gene (FMR-1) containing a CGG repeat coincident with a breakpoint cluster region exhibiting length variation in fragile X syndrome. *Cell*,

- 65(5). [https://doi.org/10.1016/0092-8674\(91\)90397-H](https://doi.org/10.1016/0092-8674(91)90397-H)
- Volkman, D., & Baluška, F. (2006). Gravity: One of the driving forces for evolution. *Protoplasma*. <https://doi.org/10.1007/s00709-006-0200-4>
- Von Der Mark, H., Von Der Mark, K., & Gay, S. (1976). Study of Differential Collagen Synthesis during Development of the Chick Embryo by Immunofluorescence I. Preparation of Collagen Type I and Type II Specific Antibodies and Their Application to Early Stages of the Chick Embryo. In *DEVELOPMENTAL BIOLOGY* (Vol. 48).
- Vortkamp, A., Lee, K., Lanske, B., Segre, G. V, Kronenberg, H. M., & Tabint, C. J. (1996). *Regulation of Rate of Cartilage Differentiation by Indian Hedgehog-and elat elated protein*.
- Wagner, G. P., & Lynch, V. J. (2010). Evolutionary novelties. In *Current Biology* (Vol. 20, Issue 2). <https://doi.org/10.1016/j.cub.2009.11.010>
- Wake, D. B., Wake, M. H., & Specht, C. D. (2011). Homoplasy: From Detecting Pattern to Determining Process and Mechanism of Evolution. *Science*, 331(6020), 1032 LP – 1035. <https://doi.org/10.1126/science.1188545>
- Walker, & Kimmel. (2006). *A two-color acid-free cartilage and bone stain for zebrafish larvae*. <https://www.ncbi.nlm.nih.gov/m/pubmed/17510811/>
- Wang, L., Jie, Q., & Yang, L. (2017). Chondrocytes-osteoblast transition in endochondral ossification. *Annals of Joint*, 2, 4–4. <https://doi.org/10.21037/aoj.2017.01.06>
- Wang, Yao, Li, Y., Qin, Z., & Wei, W. (2017). Re-evaluation of thyroid hormone signaling antagonism of tetrabromobisphenol A for validating the T3-induced *Xenopus* metamorphosis assay. *Journal of Environmental Sciences (China)*. <https://doi.org/10.1016/j.jes.2016.09.021>
- Wang, Yulei, Liu, C. L., Storey, J. D., Tibshirani, R. J., Herschlag, D., & Brown, P. O. (2002). Precision and functional specificity in mRNA decay. *Proceedings of the National Academy of Sciences*, 99(9), 5860 LP – 5865. <https://doi.org/10.1073/pnas.092538799>
- Wang, Z., Gerstein, M., & Snyder, M. (2009). RNA-Seq: A revolutionary tool for transcriptomics. In *Nature Reviews Genetics* (Vol. 10, Issue 1, pp. 57–63). <https://doi.org/10.1038/nrg2484>
- Webb, T. J. (2012). Marine and terrestrial ecology: unifying concepts, revealing differences. *Trends in Ecology & Evolution*, 27(10), 535–541.
- Weinstein, B. S., & Cizek, D. (2002). The reserve-capacity hypothesis: evolutionary origins and modern implications of the trade-off between tumor-suppression and tissue-repair. *Experimental Gerontology*, 37(5), 615–627. [https://doi.org/https://doi.org/10.1016/S0531-5565\(02\)00012-8](https://doi.org/https://doi.org/10.1016/S0531-5565(02)00012-8)
- Wen, L., & Shi, Y.-B. (2015). Unliganded thyroid hormone receptor  $\alpha$  controls developmental timing in *Xenopus tropicalis*. *Endocrinology*, 156(2), 721–734. <https://doi.org/10.1210/en.2014-1439>

- Wen, L., & Shi, Y. B. (2016). Regulation of growth rate and developmental timing by Xenopus thyroid hormone receptor  $\alpha$ . In *Development Growth and Differentiation*. <https://doi.org/10.1111/dgd.12231>
- Weng, J. J., & Su, Y. (2013). Nuclear matrix-targeting of the osteogenic factor Runx2 is essential for its recognition and activation of the alkaline phosphatase gene. *Biochimica et Biophysica Acta - General Subjects*, 1830(3). <https://doi.org/10.1016/j.bbagen.2012.12.021>
- Wheeler, G. N., & Brändli, A. W. (2009). Simple vertebrate models for chemical genetics and drug discovery screens: Lessons from zebrafish and Xenopus. In *Developmental Dynamics* (Vol. 238, Issue 6, pp. 1287–1308). <https://doi.org/10.1002/dvdy.21967>
- Willaert, B., Bossuyt, F., Janssenswillen, S., Adriaens, D., Baggerman, G., Matthijs, S., Pauwels, E., Proost, P., Raepsaet, A., Schoofs, L., Stegen, G., Treer, D., Van Hoorebeke, L., Vandeborgh, W., & Van Bocxlaer, I. (2013). Frog nuptial pads secrete mating season-specific proteins related to salamander pheromones. *The Journal of Experimental Biology*, 216(22), 4139 LP – 4143. <https://doi.org/10.1242/jeb.086363>
- Wittkopp, P. J., & Kalay, G. (2012). Cis-regulatory elements: Molecular mechanisms and evolutionary processes underlying divergence. In *Nature Reviews Genetics* (Vol. 13, Issue 1, pp. 59–69). <https://doi.org/10.1038/nrg3095>
- Woese, C. R., & Fox, G. E. (1977). *Phylogenetic structure of the prokaryotic domain: The primary kingdoms (archaeobacteria/eubacteria/urkaryote/16S ribosomal RNA/molecular phylogeny)* (Vol. 74, Issue 11).
- Wood, T. W. P., & Nakamura, T. (2018). Problems in fish-to-tetrapod transition: Genetic expeditions into old specimens. In *Frontiers in Cell and Developmental Biology* (Vol. 6, Issue JUL). Frontiers Media S.A. <https://doi.org/10.3389/fcell.2018.00070>
- Yanai, I., Peshkin, L., Jorgensen, P., & Kirschner, M. W. (2011). Mapping Gene Expression in Two Xenopus Species: Evolutionary Constraints and Developmental Flexibility. *Developmental Cell*, 20(4). <https://doi.org/10.1016/j.devcel.2011.03.015>
- Yang, H., Wanner, I. B., Roper, S. D., & Chaudhari, N. (1999). An Optimized Method for In Situ Hybridization with Signal Amplification That Allows the Detection of Rare mRNAs. *Journal of Histochemistry & Cytochemistry*, 47(4), 431–445. <https://doi.org/10.1177/002215549904700402>
- Yang, L., Tsang, K. Y., Tang, H. C., Chan, D., & Cheah, K. S. E. (2014). Hypertrophic chondrocytes can become osteoblasts and osteocytes in endochondral bone formation. *Proceedings of the National Academy of Sciences of the United States of America*, 111(33), 12097–12102. <https://doi.org/10.1073/pnas.1302703111>
- Yaoita, Y., & Brown, D. D. (1990). A correlation of thyroid hormone receptor gene expression with amphibian metamorphosis. *Genes and Development*, 4(11). <https://doi.org/10.1101/gad.4.11.1917>
- Yoshida, C. A., Yamamoto, H., Fujita, T., Furuichi, T., Ito, K., Inoue, K. I., Yamana, K., Zanma, A.,

- Takada, K., Ito, Y., & Komori, T. (2004). Runx2 and Runx3 are essential for chondrocyte maturation, and Runx2 regulates limb growth through induction of Indian hedgehog. *Genes and Development*, *18*(8), 952–963. <https://doi.org/10.1101/gad.1174704>
- Yu, T., Graf, M., Renn, J., Scharl, M., Larionova, D., Huysseune, A., Witten, P. E., & Winkler, C. (2017). A vertebrate-specific and essential role for *osterix* in osteogenesis revealed by gene knockout in the teleost medaka. *Development*. <https://doi.org/10.1242/dev.139550>
- Zahn, N., Levin, M., & Adams, D. S. (2017). The Zahn drawings: new illustrations of *Xenopus* embryo and tadpole stages for studies of craniofacial development. *Development*. <https://doi.org/10.1242/dev.151308>
- Zaragoza, C., López-Rivera, E., García-Rama, C., Saura, M., Martínez-Ruíz, A., Lizarbe, T. R., Martín-de-Lara, F., & Lamas, S. (2006). Cbfa-1 mediates nitric oxide regulation of MMP-13 in osteoblasts. *Journal of Cell Science*, *119*(9). <https://doi.org/10.1242/jcs.02895>
- Zhang, Y. F., Xu, W., Lou, Q. Q., Li, Y. Y., Zhao, Y. X., Wei, W. J., Qin, Z. F., Wang, H. L., & Li, J. Z. (2014). Tetrabromobisphenol a disrupts vertebrate development via thyroid hormone signaling pathway in a developmental stage-dependent manner. *Environmental Science and Technology*. <https://doi.org/10.1021/es502366g>
- Zheng, Q., Zhou, G., Morello, R., Chen, Y., Garcia-Rojas, X., & Lee, B. (2003). Type X collagen gene regulation by Runx2 contributes directly to its hypertrophic chondrocyte-specific expression in vivo. *Journal of Cell Biology*, *162*(5). <https://doi.org/10.1083/jcb.200211089>
- Zhou, G., Zheng, Q., Engin, F., Munivez, E., Chen, Y., Sebald, E., Krakow, D., & Lee, B. (2006). Dominance of SOX9 function over RUNX2 during skeletogenesis. *Proceedings of the National Academy of Sciences of the United States of America*, *103*(50). <https://doi.org/10.1073/pnas.0605170103>
- Zhou, X., von der Mark, K., Henry, S., Norton, W., Adams, H., & de Crombrughe, B. (2014). Chondrocytes Transdifferentiate into Osteoblasts in Endochondral Bone during Development, Postnatal Growth and Fracture Healing in Mice. *PLoS Genetics*. <https://doi.org/10.1371/journal.pgen.1004820>
- Ziermann, J. M., & Olsson, L. (2007). A New Staging table for *Xenopus laevis* (Anura, Pipidae). *Journal of Morphology*, *268*(electronic supplement), 1– 42.